CHEMICAL ENGINEERING SCIENCE
GENIE CHIMIQUE

VOL. 12 1960 No. 4

Two-phase (gas/liquid) flow phenomena—II

Liquid entrainment

G. H. Anderson and B. G. Mantzouranis
Department of Chemical Engineering, Imperial College, Prince Consort Road, London, S.W.7

(*Received* 28 *January* 1960)

VOL. 12 1960

Abstract—Measurements have been made of the entrainment of water droplets in an air-stream when air and water flow concurrently up a vertical glass tube of 0·5in. diameter. It was found that the mass flow of entrained liquid varied with the air rate to the power 2·6 and the liquid rate to the power 1·5 when annular flow conditions prevailed. The effect of entrainment on the calculation of the thickness of the annular liquid film by the method given in Part I is discussed.

Résumé—Les auteurs ont fait des mesures sur l'entrainement de gouttelettes d'eau par un écoulement d'air quand l'eau et l'air se déplacent dans le même sens et vers le haut dans un tube de verre vertical de 0,5 in. de diamètre. Ils ont trouvé que l'écoulement massique du liquide entraîné varie avec la vitesse de l'air à la puissance 2,6 et la vitesse du liquide à la puissance 1,5 quand les conditions d'écoulement annulaire prevalent. L'effet de l'entrainment sur le calcul de l'épaisseur du film liquide annulaire par la méthode donnée partie I est discuté.

Zusammenfassung—Es wurden Messungen durchgeführt über die Mitnahme von Wassertropfen durch einen Luftstrom, wobei Luft und Wasser im Gleichstrom aufwärts durch ein senkrechtes Glasrohr mit 0,5″ Durchmesser strömten. Dabei wurde gefunden, dass der Mengendurchsatz der eingegebenen Flüssigkeit sich mit der 2,6ten Potenz der Luftgeschwindigkeit und dass sich die Flüssigkeitsgeschwindigkeit mit der 1,5ten Potenz ändert, wenn die Bedingungen einer Ringströmung herrschen. Der Einfluss der Mitnahme auf die Berechnung der Dicke des Ring-Flüssigkeits-Films mit Hilfe der in Teil I angegebenen Methode wird diskutiert.

Introduction

In a previous paper [1] on the pressure gradient and hold-up in a vertical tube carrying both liquid and gas, attention was drawn to the fact that a proportion of the liquid travels as droplets within the gas phase. Although this phenomenon has been observed by many workers, little quantitative work has been reported. This paper describes a method of measuring quantitatively the local mass flow density of the liquid drops and their velocity as a function of the flow variables, in a glass tube of approximately 0·5in. diameter. The influence of this liquid entrainment on the calculation of the liquid holdup is also discussed.

Experimental Technique

In order to separate the drop-laden gas core from the liquid flowing in the annular film, the arrangement 1, Fig. 1 was used. A short brass tube T fits closely round the glass tube GT in which air and water are flowing cocurrently upwards. Tube T carries a copper dome D fitted with a circular knife edge KE 0·8 times the inside diameter of the glass tube and 1 in. long. The central core of fluid leaves uninterrupted through KE and the rest including the liquid film leaves through E and returns to the feed tank. The probe PL is used to sample the gas core; it is connected via tube MC to a differential manometer which indicates the impact pressure on the probe when valve V_1 is closed. To determine the mass flow of liquid drops in the cross-sectional area of the probe tip, the connection MC is blocked, V_1 fully opened and the water discharged through this valve collected and measured. To measure

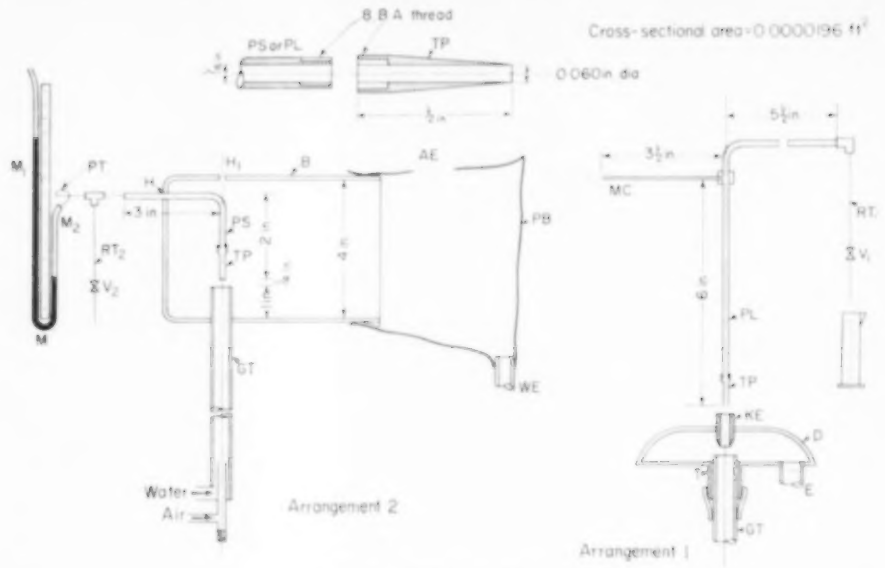

Fig. 1. Sampling devices.

the impact head, the 6 in. length of the probe between the end of the tip and the horizontal connection MC must be filled with a single fluid by purging with either air or water through RT_1 and V_1.

In arrangement 2, Fig. 1, the whole stream emerging from the glass tube GT is confined in a polythene beaker B followed by a polythene bag PG: the liquid drains through WE to the feed tank and the air escapes through the hole AE. The long probe PL can be used as before through hole H_1 or a shorter probe PS 4 in. long inserted through hole H.

The manometer M is a U-tube 3 ft. long filled with bromoform (s.g. = 2·9). The leg M_1 is open to atmosphere and M_2 is connected to the probe via a plastic tube PT kept in a horizontal plane. The bromoform in M_2 is kept under water which also fills tube PT; the capacity of the horizontal portion of PT is such that it acts as a constant liquid reservoir (effective s.g. = 2·4).

Measurements of entrainment and impact pressure were made on air and water flowing cocurrently upwards through a 0·427 in. i.d. tube for three different tube lengths. Continuous lengths of glass tube were used 10·25 in., 34·5 in. and 72 in. long. Most of the experiments were carried out with the probe in the centre of the core but some radial profiles were also explored.

Limitations and accuracy of the experimental technique

To obtain a truly quantitative sample of a discontinuous phase (water drops) flowing in a continuous phase (gas or vapour) it is necessary to sample isokinetically; only then are the streamlines of the continuous phase directly in front of the probe undistorted by the presence of the probe. Sampling is isokinetic when the impact pressure registered by the probe is zero, since then both phases flow through the probe with the same velocity as they flow outside and upstream of it.

In these experiments, since the path through the probe offers considerably higher resistance than the alternative one, sampling is not isokinetic. The smaller the probe resistance, the closer the sampling approaches isokinetic conditions; this is why the shorter probe PS was also used.

As the hydraulic resistance of the probe path increases – by closing valve V_1 – progressively less air flows through it until at the limit, when the probe exit is sealed off, the gas streamlines

VOL 12 1960

suffer the greatest deviation. Under these extreme conditions the water drops, because of their high momentum, tend to cross the gas streamlines and hit the probe (see Fig. 2).

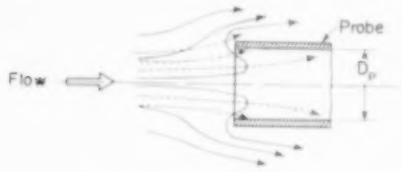

FIG. 2. Air purged probe.
—— Gas streamlines
– – – Liquid drop paths

The proportion of drops hitting the probe to those crossing the same area in the absence of the probe is termed the capture efficiency, e; it has been related to the liquid, gas and probe dimensions by DUSSOURD and SHAPIRO [2] (Fig. 3). Applying this plot to the present experimental set-up, for a gas flow of 30 lb/hr and drop sizes of 100 and 50 μ the capture efficiency is 99·8 per cent and 99·4 per cent respectively when the probe exit is shut. Hence, under the conditions used for measuring the entrainment, capture efficiencies should be better than 99 per cent, despite the non-isokinetic conditions. From a study of the volume–time plots of the water collected the mass flow density of the entrained liquid (G_e') is estimated to be accurate to ± 2 per cent. The impact pressure measurements are far less accurate.

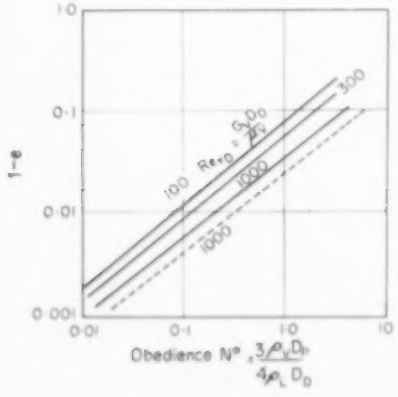

FIG. 3. —— Solid probe (or liquid purged)
– – – Thin walled probe (air purged)
D_p = probe diameter
D_D = drop diameter
e = collection efficiency

EXPERIMENTAL RESULTS AND REPRODUCIBILITY

When arrangement 1 was used, the gas core was distinctly visible on discharge because of the drops it contained. It was quantitatively observed that the number of drops in the gas core increased with increasing gas or water rate and the size of the drops increased with increasing water rate but decreased with increasing gas rate; the diameter of the drops was estimated to range between 50 and 1,000 μ. This arrangement was unsatisfactory for impact pressure measurements since the amount of air leaving the system via E rather than KE was unknown.

The entrainment results for the top of the tube using three different set-ups are shown in Fig. 4. Values of the mass flow density of the entrained liquid in the centre of the gas core, i.e. the liquid sampling rate divided by the sampling area, are plotted against the mass flow rate of gas, with the liquid feed rate as a parameter. Despite the good control of the liquid and gas flow rates and of the liquid temperature – mainly 19–21 °C and always between 18 and 22 °C – the reproducibility is on the whole 20 per cent, no particular set-up showing a consistent bias. The corresponding values of the impact pressures are shown in Fig. 5, where the reproducibility is of the same order. The log-linear plot is used because it can conveniently combine a thousand-fold range of variation of the independent variable with clarity of presentation. Results for the bottom and the middle of the tube are shown in Figs. 6 and 7 and radial profiles in Fig. 8. Fig. 8 provides the justification for taking the radial distribution of entrainment within the gas core to be uniform within 20 per cent of the axial value.

VELOCITY OF THE ENTRAINED PHASE

It is possible to calculate the velocity of the drops in the following way.

The differential equation for the conservation of linear momentum flow is

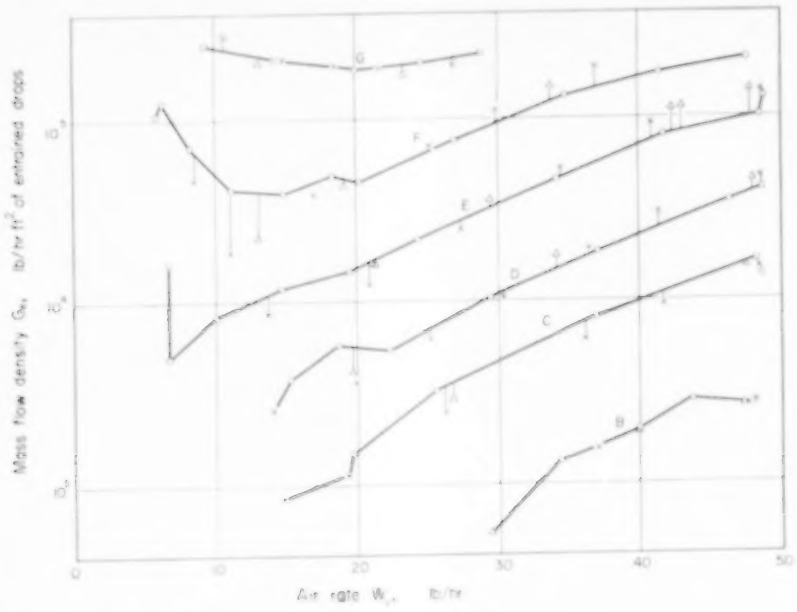

Fig. 4. Air–water flow. Entrainment rates at the tube axis 72in. above inlet.

Series	W_L lb/hr.
B	22
C	50
D	100
E	220
F	500
G	1000

○ Top, short probe, beaker
△ Top, long probe, beaker
× Top, long probe, knife edge

Fig. 5. Air–water flow. Impact pressures at the tube axis 72in. above inlet.

△ Top, long probe, water purged, beaker
× Top, long probe, air purged, beaker
○ Top, short probe, air purged, beaker

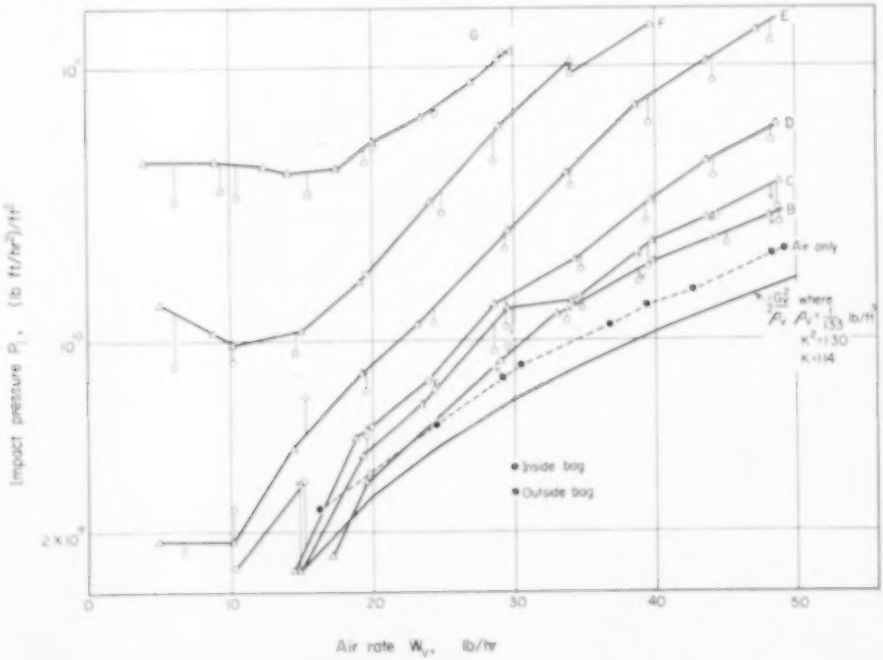

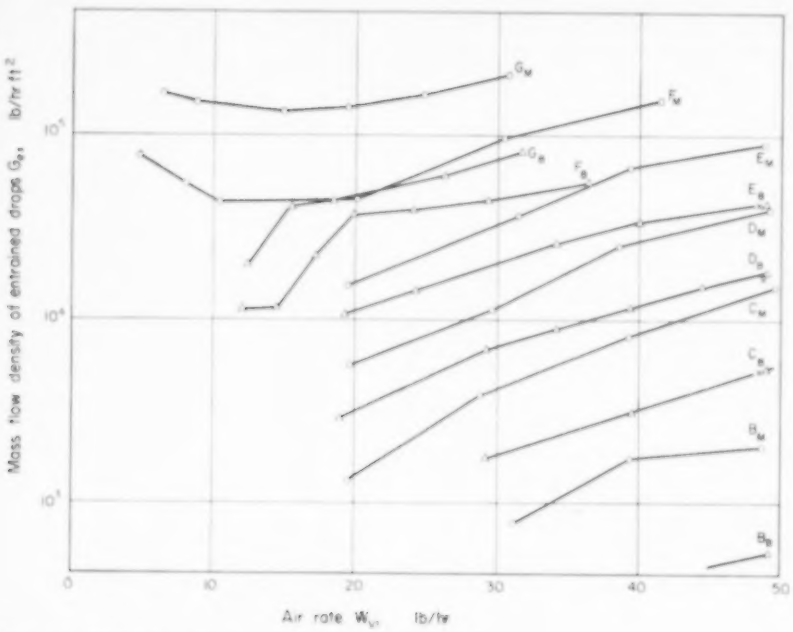

FIG. 6. Air–water flow. Entrainment rates at the tube axis 32·5in. and 10·25in. above inlet.

- ○ Middle, short probe, beaker
- △ Bottom, long probe, beaker
- × Bottom, short probe, beaker

Series	W_L lb/hr.
B	22
C	50
D	100
E	220
F	500
G	1000

FIG. 7. Air–water flow. Impact pressures at the tube axis 32·5in. and 10·25in. above inlet.

- ○ Middle, short probe, air purged, beaker
- △ Bottom, long probe, air purged, beaker
- × Bottom, short probe, air purged, beaker

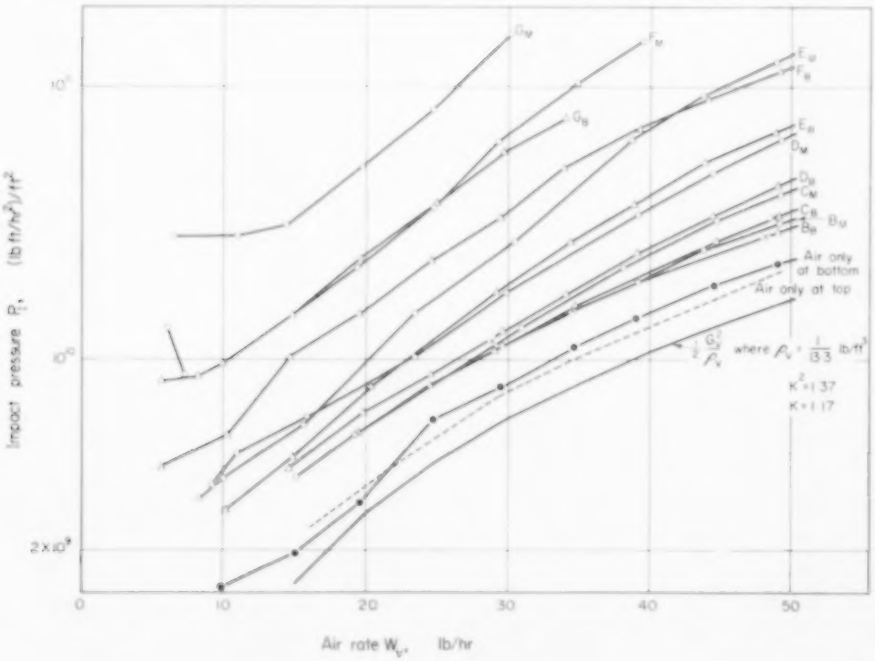

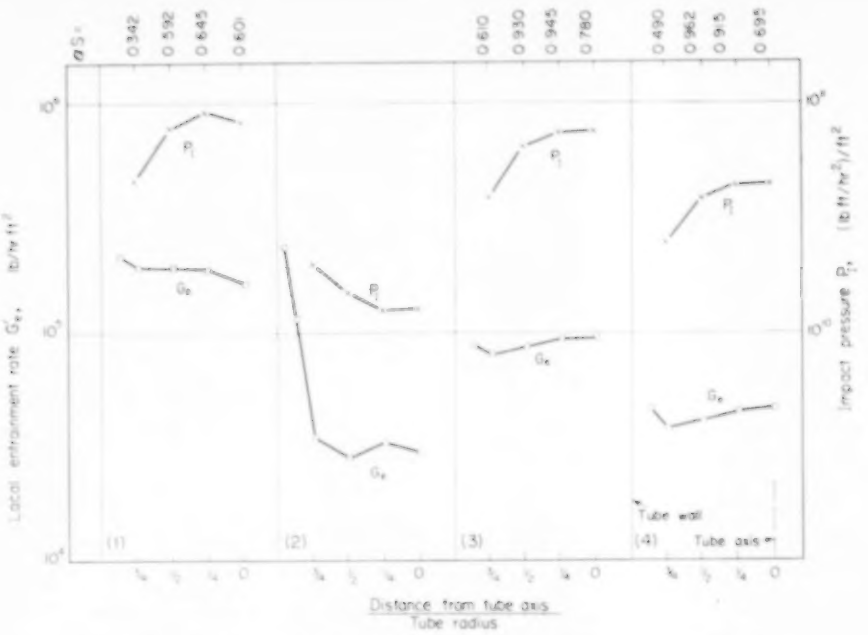

Fig. 8. Air–water flow. Radial traverses at 72in. from inlet.

	(1)	(2)	(3)	(4)
W_L	500 lb/hr.	500 lb/hr.	220 lb/hr.	100 lb/hr.
W_V	36·0 lb/hr.	18·5 lb/hr.	40·6 lb/hr.	45·5 lb/hr.

$$d\,(\text{Force}) = (\text{mass rate})\,d\,(\text{velocity})$$

or considering unit cross-sectional area in the direction of flow,

$$d\,(\text{Pressure, } P) = (\text{mass flow density, } G')\,d\,(\text{velocity, } u) \qquad (1)$$

For the continuous phase, the mass flow density is a function of the velocity, ($G' = \rho u$) and (1) integrated between upstream conditions, $u = u$, and the probe, $u = 0$, yields:

$$\text{impact pressure of gas} = \tfrac{1}{2}\rho u^2 = \tfrac{1}{2}\frac{G_V^2}{R_V^2\,\rho_V}K^2 \qquad (2)$$

where K = local gas velocity/mean bulk gas velocity

Strictly, this impact pressure should be multiplied by the factor $R_V/R_V + R_e$, but this is virtually unity since $R_V > R_e$ (see below).

For the discontinuous phase, (1) integrated over the same limits yields:

$$\text{impact pressure of liquid drops} = \alpha G_e' u_e \qquad (3)$$

where α is a constant depending on the behaviour of the drops on reaching the probe: if the drops follow the gas streamlines $\alpha = 1/2$; if when they hit the probe they are brought to rest and then escape along the probe face in a direction normal to their original path, G_e' is independent of the velocity and $\alpha = 1$; if they bounce backwards, their velocity changing sign but not magnitude, $\alpha = 2$. Shapiro allows for the first two possibilities but does not consider the third.

Writing the ratio of the mass flow of entrained liquid to the mass flow of vapour

as $x_V = \dfrac{G_e'}{G_V}R_V$ and

$$S = \frac{\text{drop velocity}}{\text{local gas velocity}} = \frac{u_e}{u_V K}$$

(3) becomes

$$\text{impact pressure of liquid drops} = \alpha x_V S K \frac{G_V^2}{R_V^2 \rho_V} \qquad (4)$$

Table 1. Calculations on interpolated entrainment and impact pressure values at the centre of the tube during cocurrent upward air–water flow

					Top						*Middle*				*Bottom*				
Code letter	G_L (lb/hr. ft^2) $\times 10^{-3}$	W_L (lb/hr)	R_L	$\frac{G_L^2}{R_L^2 \rho_V}$ $\times 10^{-8}$	P_I $\times 10^{-8}$	G_e' (lb/hr. ft^2) $\times 10^{-3}$	$\frac{x_V}{G_e'/G_V} R_V$	$\frac{P_I}{G_L^2/R_L^2 \rho_V}$	$x_V \alpha S K$	αS	P_I $\times 10^{-8}$	G_e' (lb/hr.ft^2) $\times 10^{-3}$	x_V	αS	P_I $\times 10^{-8}$	G_e' (lb/hr.ft^2) $\times 10^{-3}$	x_V	αS	
B	22·1	48	0·035	336	232	3·1	0·0621	0·691	0·041	0·58	276	2·60	0·0521	2·90					
	22·1	44	0·038	286	209	2·6	0·0566	0·731	0·081	1·26	252	2·55	0·0555	3·66					$r_W = 0·0178$ ft
	22·1	38	0·042	214	152	1·75	0·0439	0·710	0·060	1·20	188	1·65	0·0432	4·66					Glass tube
	22·1	32	0·047	153	112	1·09	0·0323	0·732	0·082	2·23	115	1·00	0·0296	3·50					
C	50·2	48	0·041	341	305	16·0	0·318	0·895	0·245	0·676	365	14·0	0·2875	1·32	325	5·0	0·0994	2·32	P_I is in
	50·2	44	0·044	289	259	13·0	0·281	0·897	0·247	0·772	315	11·0	0·2425	1·59	265	4·0	0·0865	2·36	(lb ft/hr^2)/ft^2
	50·2	38	0·050	218	175	9·0	0·224	0·802	0·152	0·596	220	7·7	0·1915	1·65	192	2·2	0·0696	2·45	
	50·2	32	0·056	156·5	115	5·7	0·167	0·735	0·085	0·446	145	4·8	0·1408	1·73	136	2·0	0·0586	2·77	$\frac{1}{\rho_V} = 13·45$ ft^3/lb
	50·2	25	0·067	97·2	70	3·0	0·1115	0·720	0·070	0·551	87	2·55	0·0948	2·73	86	1·3	0·0484	3·46	for wet air
	50·2	20	0·077	64·0	46	1·55	0·0711	0·719	0·069	0·851	57	1·40	0·0643	3·30					
D	100·5	48	0·052	349	560	40·0	0·786	1·605	0·955	1·07	690	37	0·728	1·29	410	18	0·345	1·21	
	100·5	44	0·056	296	405	31·0	0·662	1·37	0·72	1·02	480	28	0·598	1·42	345	15	0·320	1·28	
	100·5	38	0·062	223	240	20·5	0·503	1·076	0·426	0·742	305	19	0·466	1·35	225	11	0·270	1·36	
	100·5	32	0·072	162	145	13·5	0·389	0·90	0·250	0·564	198	12·5	0·360	1·39	158	8·1	0·234	1·06	TOP
	100·5	25	0·085	101	80	6·8	0·244	0·792	0·142	0·511	116	8·0	0·292	1·50	90	5·1	0·186	0·965	72in. above inlet
	100·5	20	0·098	67	49	4·6	0·206	0·731	0·081	0·344	82	5·7	0·256	1·96	63	3·25	0·146	1·52	$K = 1·14$
E	221	48	0·073	365	1210	105	2·06	3·315	2·665	1·13	1210	93	1·788	1·31	680	41·5	0·799	1·26	
	221	44	0·078	310	900	92	1·92	2·90	2·25	1·03	960	83	1·733	1·24	550	38	0·793	1·17	
	221	38	0·088	236	540	64	1·53	2·29	1·54	0·92	640	64	1·530	1·18	365	31·5	0·753	0·99	
	221	32	0·100	172	300	40	1·118	1·745	1·095	0·86	355	44	1·232	1·01	280	23	0·643	1·26	
	221	25	0·117	109	141	24	0·844	1·295	0·645	0·671	161	26	0·914	0·796	132	14·5	0·510	0·89	MIDDLE
	221	20	0·133	72·5	81	17	0·733	1·118	0·468	0·561	94	16	0·690	0·824	81	12	0·519	0·727	34·5in. above inlet
	221	15	0·155	42·7	47	12	0·671	1·100	0·450	0·589	55	9·0	0·504	1·11	47	9·9	0·554	0·65	$K = 1·14$
F	502	37	0·141	251	1220	155	3·58	4·86	4·21	1·03	1220	135	3·12	1·18	590	57·5	1·33	1·08	
	502	34	0·150	218	930	130	3·23	4·26	3·61	0·981	930	120	2·18	1·45	475	51	1·27	1·01	
	502	31	0·157	184	700	110	2·97	3·80	3·15	0·931	700	105	2·84	0·974	380	46	1·241	0·95	
	502	28	0·165	153	500	86	2·545	3·27	2·62	0·904	500	82	2·42	0·946	305	41·5	1·23	0·995	
	502	25	0·173	124	350	69	2·27	2·82	2·17	0·839	350	64	2·11	0·904	240	39·5	1·301	0·83	
	502	22	0·185	99	250	56	2·06	2·525	1·875	0·799	250	52·5	1·93	0·855	190	37·5	1·39	0·76	BOTTOM
	502	20	0·200	85	200	49	1·95	2·355	1·705	0·767	200	46	1·83	0·815	160	35	1·392	0·735	10·25in. above inlet
	502	15	0·240	53	100	39	1·96	1·888	1·238	0·555	100	38	1·915	0·569	100	15·5	0·78	1·32	$K = 1·17$
	502	11	0·325	36	84	40·5	2·47	2·335	1·685	0·599	84	38·5	2·35	0·627					
	502	8	0·352	20·8	84	71	5·71	4·04	3·39	0·521	84	58	4·04	0·637					
G	1005	30	0·233	208	1250	245	6·22	6·01	5·35	0·756	1500	205	5·21	1·111	600	71	1·889	1·00	
	1005	27	0·245	174	880	220	6·10	5·06	4·41	0·634	1100	185	5·14	0·970	465	61	1·70	0·965	
	1005	23	0·260	131	600	200	6·51	4·38	3·73	0·503	720	160	5·13	0·787	330	50·5	1·616	0·915	
	1005	18	0·280	85	410	195	7·75	4·82	4·17	0·472	420	140	5·68	0·662	210	42·5	1·69	0·905	
	1005	14	0·302	54·8	350	220	10·58	6·40	5·75	0·477	310	140	6·95	0·635	140	29	1·44	1·110	
	1005	10·5	0·330	33·4	340	240	15·25	14·50	13·85	0·798	280	150	9·53	1·06					

VOL
12
196

Thus the resultant impact pressure P_I is given by

$$P_I = \frac{G_V}{R_V^2 \rho_V} \{\tfrac{1}{2}K^2 + x_V \cdot \alpha SK\} \qquad (5)$$

The value of K can be obtained for fully developed flow in tubes from the universal velocity profile [3].

Calculations using entrainment and impact pressure values interpolated from Figs. 4 to 7 and hold-up values from experiments previously reported [1] are shown in Table 1. The resulting values of αS range mainly between 0·4 and 1·3 but in extreme cases of very low values of x_V values as high as 4·0 or more are obtained. Since it is the gas that entrains the liquid, S has an upper limit of 1·0 and therefore αS cannot be greater than 2·0. The abnormally high values of αS may be partially accounted for by the estimated experimental error ($\pm 15 \times 10^8$ lb/ft hr^2 in the measurement of impact pressure). Since no concrete indication of the value of α is furnished by these calculations, its most probable value, $\alpha = 1{\cdot}0$, is adopted.

Some Characteristics of the Entrained Phase

A study of Table 1 indicates that the amount of liquid dispersed in the gas core is perhaps an exponential function of the distance from the inlet, first increasing quickly from a value of zero at inlet and then more slowly to a steady equilibrium value. However, if entrainment is primarily caused by the interaction of the gas core and the liquid interface due to the velocity difference between them, no true equilibrium is ever possible because the gas velocity continuously increases due to the unavoidable pressure gradient.

The available data seem to indicate that for a given run, the process of entrainment starts by the detachment of a few drops which accelerate to a high speed and then, as the mass flow of liquid in the core increases, the mean velocity of the drops is reduced.

From the radial traverses it seems that the mass flow rate of the drops and their velocity is reasonably constant near the axis of the gas core. As soon as the probe approaches the gas–liquid interface, the ripples interfere with the drops. Since the diameter of the probe is about 20 per cent of the gas core diameter, the accuracy of the traverse is limited, but the use of a smaller probe would lead to inaccuracy on account of its diameter being comparable with that of the drops.

No quantitative measurements were made on the size distribution of the drops, but it is possible to calculate the maximum diameter D_D of stable drops given the physical properties of the system and the relative velocity by the use of the relation originally proposed by Hinze.

Critical Weber number =

$$= \frac{(u_{V_i}' - u_D)^2 \rho_V D_D}{\sigma} = \text{constant.}$$

Values of this constant have been proposed as 20 and 18·2 for the higher limit and 11·2, 10 and 8 for the lower limit [4].

For the air–water system, taking a value of $(u_V - u_D) = 30 \times 10^4$ ft/hr to represent conditions during the formation of the drop, the maximum drop size is 400 μ.

Effect of Entrainment on the Predicted and Calculated Values of Liquid Film Thickness

A previous paper [1] shows how the liquid film thickness, expressed in dimensionless form $y_i^+ = \rho u^* y/\mu$ can be predicted. This prediction depends on the liquid flow in the film and so, when allowance is made for the proportion of liquid travelling in the vapour core, the predicted value of y_i^+ is reduced.

The value of y_i^+ calculated from experimental results is essentially the product of the liquid hold-up R_L and $\sqrt{\tau_w}$. The value of R_L measured is the sum of the liquid hold-up in the annulus, R_A, and that in the vapour core, R_e.

$$\text{i.e. } R_L = R_A + R_e$$

Since the liquid in the core travels faster than that in the annulus, its residence time in the test section is lower. If x_L is the fraction of liquid travelling in the vapour core, then

$$\frac{R_e}{R_A} = \frac{x_L}{1 - x_L} \cdot \frac{u_A}{Su_V}$$

$$\text{Now } \frac{u_A}{u_V} = \frac{W_A}{\rho_L R_A} \cdot \frac{\rho_V R_V}{W_V} = \frac{W_L(1-x_L)\,\rho_V\,(1-R_L)}{\rho_L R_A W_V}$$

$$\therefore R_e = \frac{x_L(1-R_L)}{S} \cdot \frac{W_L}{W_V} \cdot \frac{\rho_V}{\rho_L} \qquad (6)$$

It is hence possible to derive the value of R_e from the data of Alves [5], assuming that in his experiments $S = 1$, $\rho_L = 62{\cdot}2$ lb/ft³ and $1/\rho_v = 13$ ft³/lb, and that the entrainment is given as a percentage of the total liquid flow.

W_L lb/hr	W_V lb/hr	x_L	R_L	R_e
146	102	0·051	0·045	0·000087
146	141	0·179	0·038	0·00022
146	166	0·369	0·029	0·00037
452	122	0·254	0·060	0·00109

It is seen that, even at quite high entrainment rates, $R_e \ll R_L$ and so R_A can be taken as equal to R_L generally with little error, and $R_V = 1 - R_A$.

In the presence of entrainment part of the total pressure gradient is accounted for by the acceleration of liquid droplets, and so the calculated value of τ_w will be reduced, resulting in a lower calculated value of y_i^+. Thus, when account is taken of the presence of entrained liquid both the predicted and calculated values of y_i^+ are reduced.

By a momentum balance, it has been shown [1] that in the absence of entrainment

$$\frac{dP_{aV}}{dz} = \frac{dP_T}{dz} - \frac{dP_f}{dz} + g\rho_V - \frac{u_i}{A_{XV}}\frac{dW_V}{dz}$$

When entrained droplets are present this equation is modified to

$$\frac{dP_{aV}}{dz} + \frac{dP_{ae}}{dz} = \frac{dP_T}{dz} - \frac{dP_f}{dz} + g\rho_V - \frac{u_i}{A_{XV}}\left(\frac{dW_V}{dz} + \frac{dW_e}{dz}\right)$$

if any forces due to droplets leaving the vapour core at a higher velocity than u_i are neglected. This can be written as

$$\frac{dP_{aV}}{dz} + \frac{dP_{ae}}{dz} = \frac{dP_T}{dz} - \frac{dP_f}{dz} + g\rho_V - \frac{u_i}{R_V}\frac{d}{dz}\{G_V(1+x_V)\}$$

$$\text{i.e. } \frac{dP_{aV}}{dz} + \frac{dP_{ae}}{dz} = \frac{dP_T}{dz} - \frac{dP_f}{dz} + g\rho_V - \frac{u_i}{u_V}\frac{G_V{}^2(1+x_V)}{R_V{}^2\rho_V}\frac{d}{dz}\{\ln G_V(1+x_V)\} \qquad (7)$$

$$\text{Now } \frac{dP_{ae}}{dz} = -\frac{1}{A_{XV}}\frac{d}{dz}(W_e u_e);$$

$$\text{putting } \frac{W_e}{W_V} \equiv x_V \text{ and } \frac{u_e}{u_V} \equiv S$$

$$\text{we have } \frac{dP_{ae}}{dz} = -\frac{1}{A_{XV}}\frac{d}{dz}\left(G_V A_{XT} x_V \frac{G_V}{\rho_V R_V} S\right)$$

$$\text{i.e. } \frac{dP_{ae}}{dz} = -\frac{x_V S G_V{}^2}{\rho_V R_V{}^2}\frac{d}{dz}\left\{\ln \frac{G_V{}^2 x_V S}{\rho_V R_V}\right\} \qquad (8)$$

Evaluation of (7) and (8) from interpolated data as shown in Table 1 shows that there is considerable improvement in the agreement between the predicted and calculated values of y_i^+ when entrainment is allowed for (Fig. 9). In carrying out this computation the following assumptions were made:

(1) The mass flow density of entrained liquid at any cross-section within the limits of the gas core is equal to the axial value. This has experimental support (Fig. 8).

(2) Top and bottom values of x_V and of αS are used to evaluate the acceleration pressure gradient, assuming α to be constant along the tube.

(3) When $\alpha S > 1$, S is taken as unity.

Although the ambiguity in the corrections to y_i^+ is large (of the order of 20 per cent) the ambiguity in the corrected values of y_i^+ is small (generally less that 3 per cent). The points corresponding to both low liquid and low gas rates (Fig. 9) are left unchanged because no entrainment values could be measured (mainly due to the resulting impact pressure being too small to drive the fluids through the sampling probe).

Conclusions

(1) The proportion of the total liquid flow travelling as drops in the core during annular flow can be very considerable at high gas rates; figures of 40 per cent

VOL 12 1960

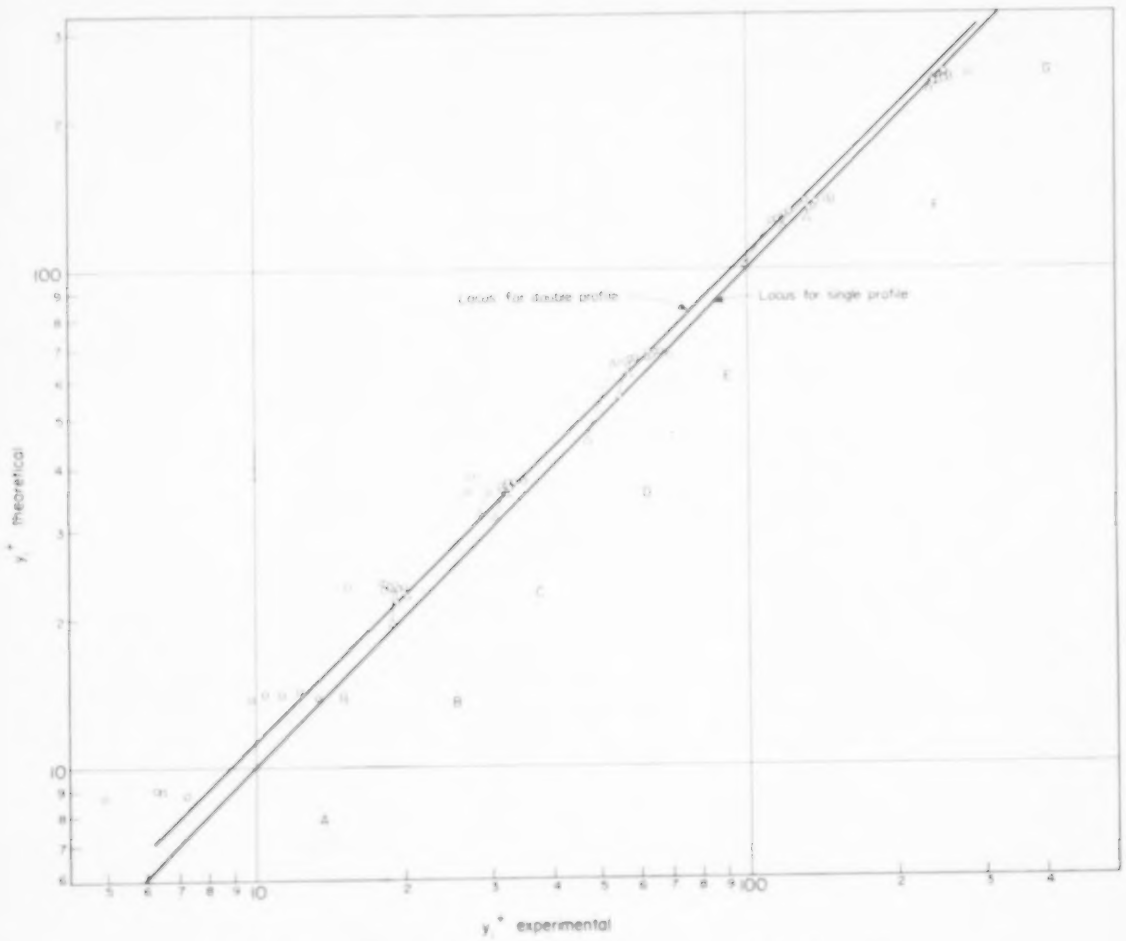

FIG. 9. Comparison of theoretical and experimental values of y_i^+ [1]
○ original points △ corrected for entrainment.

entrainment (see Table 1, Series E) have been recorded with indications that they further increase with increasing gas flow until virtually all the liquid flows as a dispersed phase.

(2) The minimum obtained by the entrainment values in the case of the two highest liquid rates might be attributed to the transition from slug flow to mist flow; nevertheless, the theory based on annular flow is obeyed.

(3) After the correction for entrainment is made, the experimental values of y_i^+ do not deviate in general from the values predicted from the theory discussed in detail elsewhere [1], to an extent greater than is attributable to experimental error [3].

(4) Due to the absence of any guiding principles for the prediction of the extent, quality and distribution of entrainment, no correlation is attempted of the available data; by inspection of Figs. 4 and 6 it is possible to say that for a given position in the tube the following is approximately true for annular flow conditions; G_e' is proportional to $W_V^{2\cdot6}$ for constant W_L, and proportional to $W_L^{1\cdot5}$ for constant W_V.

Acknowledgements—The authors wish to thank Professor D. M. Newitt, in whose Department this work was carried out, and Dr. G. G. Haselden for his helpful guidance of the work, and to acknowledge the generous financial assistance of Shell Internationale Research Mij N.V.

Notation

Symbols

D = diameter
e = capture efficiency, i.e. ratio of entrained liquid collected to that in the same cross-section in the absence of the collecting device.
G = superficial mass flow density
G' = actual mass flow density
K = ratio of local gas velocity to mean bulk gas velocity
P = pressure
R = fraction of cross-section occupied by one phase
S = ratio of entrained drop velocity to the gas velocity
u = velocity
u^* = friction velocity at the wall = $(\tau_W/\rho_L)^{1/2}$
W = mass flow
x = ratio of mass flow of entrained drops to the flow of liquid or gas
y = distance from tube wall
α = constant depending on the behaviour of drops on reaching an obstruction
μ = dynamic viscosity
ρ = density
σ = surface tension
τ = shear stress

Subscripts

a = acceleration
A = liquid flowing in annulus
D = entrained drop
e = entrained liquid in vapour stream
i = vapour–liquid interface
I = impact
L = liquid
V = vapour or gas
w = wall

References

[1] Anderson G. H. and Mantzouranis B. G. *Chem. Engng. Sci.* To be published.
[2] Dussourd J. L. and Shapiro A. H., DIC 5–6985 Massachusetts Institute of Technology May 1955.
[3] Mantzouranis B. G., Ph.D. Thesis, University of London 1959.
[4] Knelman F. H., Ph.D. Thesis, University of London 1953
[5] Alves, G. E. *Chem. Engng. Progr.* 1954 **50** 449.

Chemical Engineering Science, 1960, Vol. 12, pp. 243 to 252. Pergamon Press Ltd., London. Printed in Great Britain

Studies in optimization—I

The optimum design of adiabatic reactors with several beds

R. Aris

Department of Chemical Engineering, University of Minnesota, Minneapolis 14, Minnesota

(*Received* 1 *December* 1959)

Abstract—The optimum design of an adiabatic reactor involves the choice of the size of each bed and the amount of interstage cooling between beds. These decisions can be made in an orderly way by applying the notion of dynamic programming, and in the case of a single reaction allow of a simple graphical presentation. The principal subject of this paper is case of a single reaction with costs proportional to the bed volume and the amount of heat removed. It is shown that this simple model suffices to solve a number of more general problems.

Résumé—Le projet optimum d'un réacteur adiabatique met en jeu le choix de la dimension de chaque lit et la valeur, à des stades intermédiaires, de la réfrigération entre les lits. Ces conclusions peuvent être tirées méthodiquement par l'application de la programmation dynamique et dans le cas où une réaction unique permet une représentation graphique simple. Le sujet principal de ce mémoire traite le cas d'une réaction simple dont le coût est proportionnel au volume du lit et à la quantité de chaleur éliminée. On voit que ce simple modèle suffit pour résoudre un certain nombre de problèmes les plus généraux.

Zusammenfassung—Die optimale Gestatlung eines adiabatischen Reaktors läuft hinaus auf die Wahl der Abmessungen jeder Kontakt-schicht und den Umfang der Kühlung zwischen den Kontakt-schichten. Diese Entscheidungen können durch Anwendung der dynamischen Programmierung getroffen werden. Im Falle einer einfachen Reaktion ist eine einfache graphische Darstellung möglich. Hauptgegenstand dieser Arbeit ist der Fall einer einfachen Reaktion, bei dem die Kosten proportional dem Kontaktvolumen und der abgeführten Reaktionswärme sind. Es wird gezeigt, dass dieses einfache Modell genügt, um eine Reihe allgemeiner Probleme zu lösen.

1. Introduction

The type of reactor to be considered consists of one or more adiabatic beds of catalyst in which a single reaction is taking place. Before entering the first bed and between each bed the reaction mixture is heated or cooled to the most suitable temperature. Such a reactor is commonly used, as, for example, in the oxidation of sulphur dioxide or the production of methanol. The cooling between stages is needed to keep away from equilibrium conditions and is accomplished either by an interchanger or by adding a cold shot of reactants to the reaction mixture; in this paper we shall be concerned only with interchanger cooling.

When a single reaction is considered the design of such a reactor is susceptible to a simple graphical procedure. Since the beds are adiabatic the composition and temperature variations are related, for, if the reaction is exothermic, the heat of reaction is entirely used in heating up the reaction mixture. For a fixed reference composition, from which the reaction mixture is obtained by letting the reaction proceed to a certain point, the composition at all times can be specified in terms of the concentration of one reactant. Thus, for example, if the reference composition of the reacting mixture were $O_2 : SO_2 : SO_3 = 34 : 65 : 1$ (per cent volume or mole fraction) then when the concentration of SO_3 is c, the stoicheiometry of the reaction gives concentrations of $(0{\cdot}345 - 0{\cdot}33\,c)/1{\cdot}005$ and $(0{\cdot}66 - 0{\cdot}67\,c)/1{\cdot}005$ for O_2 and SO_2 respectively. We shall use the concentration c of the product to define the composition of the mixture so that, if T is its temperature, the state of the reactants

at any instant can be represented by a point in a c–T diagram such as is shown in Fig. 1. Let the rate of reaction be a function of composition and temperature $R(c, T)$, then if v is the linear velocity of flow and x the distance along the bed, a mass balance gives

$$v\frac{dc}{dx} = R(c, T) \tag{1}$$

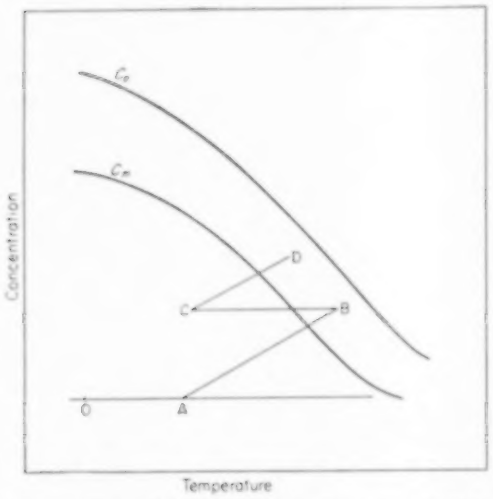

FIG. 1. The adiabatic paths in the concentration–temperature plane.

Since there is no heat loss a heat balance over an element of the bed gives

$$v\,c_p\,\rho\frac{dT}{dx} = H\,R(c, T) \tag{2}$$

where c_p is the specific heat and ρ the density of the reaction mixture and H is the heat of reaction. Writing $H/c_p\,\rho = h$ and dividing (2) by (1) we have

$$\frac{dT}{dc} = h. \tag{3}$$

h will generally be a function of c and T so that (3) is a first order differential equation which has to be solved for the relation between c and T in any adiabatic bed. For simplicity we will assume h is constant (though the analysis is equally valid for varying h) and the adiabatic paths are then straight lines with slope $1/h$, as shown on Fig. 1. Thus if c_0, T_0 is the state of the reactants at the inlet to a bed (the point A in Fig. 1) the composition and temperature at any other point are related by

$$T = T_0 + h(c - c_0) \tag{4}$$

It follows that at any point in the bed the rate of reaction is a function of c only, namely $R(c, T_0 + h(c - c_0)) = \phi(c\,;\, c_0, T_0)$. Equation (1) can now be integrated immediately, for, setting $t = x/v$, the variables separate to give

$$t - t_0 = \int_{c_0}^{c}\frac{dc}{\phi(c)} \tag{5}$$

where $(t - t_0)$ is the holding time of a bed that suffices to raise the concentration of the product from c_0 to c. The adiabatic paths can thus be graduated in the variable t and the bed size required to get from a state $A(c_0, T_0)$ to another state $B(c_1, T_1)$ is the difference of the graduations $(t_1 - t_0)$.

The reactions for which this type of reactor is used are generally limited by equilibrium and at a given temperature T the reaction cannot yield a greater concentration than $c_e(T)$. If this function is plotted in the c–T diagram it gives a curve, C_e, along which $R \equiv R(c_e(T), T) = 0$, and we are limited to the left hand side of this curve. Since the reaction velocity is small for low temperatures and vanishes on the equilibrium curve, C_e, there must be a point on each adiabatic line at which R is greatest. Let such a point be (c_m, T_m), at which

$$\frac{\partial R}{\partial c} + h\frac{\partial R}{\partial T} = 0, \tag{6}$$

and denote the locus of these points by C_m. Then the intersection of this curve with an adiabatic line gives us a suitable origin for the integration in (5), and we can graduate the adiabatic lines with

$$t(c) = \int_{c_m}^{c}\frac{dc}{\phi(c)} = \int_{c_m}^{c}\frac{dc}{R\left[c, T_m + h(c - c_m)\right]} \tag{7}$$

Fig. 2 shows some typical curves for the reversible reaction $A \rightleftharpoons B$ first order in the concentrations of A and B. The curves C_e, C_m and some of the

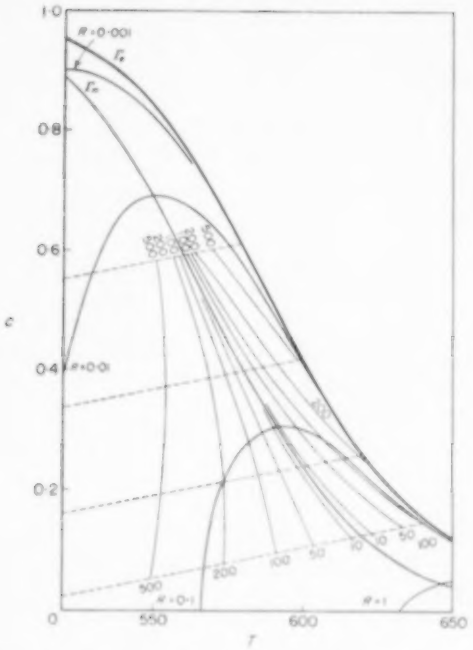

Fig. 2. Concentration–temperature plane for first order reversible reaction.

contours of constant t and R are shown; C_m is by definition the curve $t = 0$, whilst C_e is $R = 0$ or $t = \infty$.

The interstage cooling that is required to bring the reactants away from equilibrium can also be represented on the c–T diagram. Supposing the reaction mixture enters the first bed in a state corresponding to the point A (Fig. 1) and the bed is of such a length that it leaves it in state B. In the interchanger it is cooled down to a lower temperature but does not change in composition. This is represented by a horizontal line BC, where the abcissa of C is the temperature to which the reactants are cooled. In the next bed the reaction will follow the adiabatic path through C, reaching the state D, for example. Finally we may observe that as originally available to the reactor the reaction mixture will be of a certain composition but probably not at the best temperature; the point O represents such a state. It is therefore necessary to heat, or cool, the reactants to the inlet temperature most suitable for the first bed. The decisions that have to be taken in seeking the optimum policy for an original state O are thus connected with the points A, B, C etc. and we might expect that in a good design the line segments AB, CD, etc. would lie over the curve of maximum reaction velocity. To formulate the optimum problem precisely we must first construct a suitable profit function.

2. The Profit Function and Method of Maximizing it

The beds of an N-stage adiabatic reactor will be numbered backwards, N being the first bed the reactants enter and 1 the last. Primed quantities will denote exit values and unprimed inlet values. Thus c'_1 is the exit concentration from the last bed (and T'_1 the corresponding temperature); c_1 is the inlet concentration to the last bed and equals c'_2, the exit concentration at the penultimate. We may consistently write the feed condition as c'_{N+1}, T'_{N+1} and $c'_{n+1} = c_n$, $n = 1, 2, \ldots N$. Thus the total increase in concentration is

$$c'_1 - c'_{N+1} = \sum_1^N (c'_n - c_n).$$

If q is the flow rate and α the value of a unit quantity of the product, the rate of increase in value of the product stream is $\alpha q (c'_1 - c'_{N+1})$. This is the simplest expression for the rate at which money is made by the reaction process; more sophisticated profit functions will be discussed in the last section.

The cost associated with the process are those of providing and maintaining the catalyst beds and heat interchanges. We will again consider these as simple proportionalities, reserving generalizations until later. The cost associated with the bed will be taken to be proportional to the total volume $q \sum_1^N t_n$. This includes the cost of the catalyst, of maintainance and of construction amortized in the conventional way. The cost of heating or cooling will be taken to be proportional to the total heat added or removed, namely $q c_p \rho \sum_1^N |T_n - T'_{n+1}|$. If β and γ are the two unit costs the net profit from the reaction is

$$\alpha q (c'_1 - c'_{N+1}) - \beta q \sum_1^N t_n - \gamma q c_p \rho \sum_1^N |T_n - T'_{n+1}|$$

$$= q \sum_1^N \{\alpha (c'_n - c_n) - \beta t_n - \gamma c_p \rho |T_n - T'_{n+1}|\}$$

If we write $\lambda = \beta/\alpha$, $\mu = \gamma c_p \rho/\alpha$ then the total profit is $q \alpha P_N$, where

$$P_N = \sum_1^N p_n = \sum_1^N \{c'_n - c_n - \lambda t_n - \mu |T_n - T'_{n-1}|\} \quad (8)$$

The optimum problem may now be stated in precise terms: Given the initial state c'_{N+1}, T'_{N+1} and the constants λ and μ, the bed sizes $t_1, t_2, \ldots t_N$ and inlet temperatures $T_1, T_2, \ldots T_N$ are to be chosen so that the greatest value of P_N is attained. Although this may seem a somewhat restricted problem it will be shown later that it can be extended to cope with more complicated situations. When the choice of policy (t_n, T_n, $n = 1, 2, \ldots N$) has been made, the resulting maximum of P_N will be a function only of c'_{N+1} and T'_{N+1},

$$f_N (c'_{N+1}, T'_{N+1}) = \text{Max } P_N \quad (9)$$

It is thus necessary to make a choice of $2N$ variables and if these have to be found simultaneously the problem is formidable. However, by using the methods of dynamic programming the problem can be reduced to a sequence of problems each of which requires the simultaneous choice of only two variables.

To show this we first observe that the N-stage process and the profit function can be broken into two parts, the first stage (labelled N) and an $(N-1)$-stage process. The exit conditions c'_N, T'_N of the first stage are the feed conditions for the subsequent $(N-1)$-stage process. The optimum from the N-stage process with respect to its feed c'_{N+1}, T'_{N+1} will certainly not be achieved unless the $(N-1)$-stage process is giving its best with respect to its feed c'_N, T'_N. If we know the optimum $(N-1)$-stage policy we can get the optimum N-stage policy by varying the operating conditions t_N, T_N of the first stage only, always using the optimum $(N-1)$-stage policy for the subsequent stages. By selecting the t_N, T_N for which P_N is greatest we shall have the optimum policy for N-stages. In our notation this may be written

$$f_N (c'_{N+1}, T'_{N+1}) = \text{Max} \{P_N + f_{N-1} (c'_N, T'_N)\} \quad (10)$$

where the maximum is over variations of t_1 and T_1,

$$\left.\begin{aligned} p_N &= c'_N - c_N - \lambda t_N - \mu |T_N - T'_{N+1}| \\ \text{and} \\ t_N &= \int_{c_N}^{c'_N} \frac{dc}{R[c, T_N + h(c - c_N)]}, \; c_N = c'_{N+1} \end{aligned}\right\} \quad (11)$$

Equation (10) gives a simple method of successively calculating $f_1, f_2, \ldots f_N$; f_0 is, of course, zero.

We are thus led to consider the optimum design of a one-stage reactor first afterwards making it the second stage of a two-stage reactor, and so on. The so-called principle of optimality, on which dynamic programming rests [1], has been invoked to establish the basic equation (10).

3. The Optimum Performance of a Single Bed

For a single bed we have

$$f_1 (c'_2, T'_2) = \text{Max } p_1 = \text{Max} \{c'_1 - c_1 - \lambda t_1 - \mu |T_1 - T'_2|\} \quad (12)$$

where the maximization is by correct choice of t_1 and T_1. Suppose that T_1 has already been chosen, then since $c_1 = c'_2$ we are already committed to the adiabatic path through (c_1, T_1) and have to choose t_1 to maximize p_1. However from (12) and (7),

$$\frac{\partial p_1}{\partial t_1} = \frac{dc'_1}{dt_1} - \lambda = R (c'_1, T'_1) - \lambda$$

the derivative being taken along the adiabatic path. If p_1 is to be maximum the end point (c'_1, T'_1) must therefore lie on the curve $R (c, T) = \lambda$, which we denote by Γ'_1. Moreover only the part of the curve $R = \lambda$ which lies to the right of C_m is of interest since otherwise $\partial p_1/\partial t_1$ would be negative during the reaction, which is uneconomic unprofitable. Analytically the condition for the end point is

$$R'_1 = R (c'_1, T'_1) = R (c'_1, T_1 + h (c'_1 - c_1)) = \lambda \quad (13)$$

Consider now the choice of the best T_1, that is the point A on the horizontal line $c = c'_2 = c_1$. Denote by I_1 the integral

$$I_1 = \int_{c_1}^{c'_1} \left(1 - \frac{\lambda}{R}\right) dc \qquad (14)$$

where c'_1 is always chosen to satisfy the condition (13), so that I_1 is a function of T_1 only. If A is at C in Fig. 3 the intersection of $c = c'_2$ and Γ'_1 then $c'_1 = c_1$ and $I_1 = 0$. As T_1 decreases (A moves to the left) I_1 will increase at first and then decrease for in the position $A'B'$, where B' is the intersection of c_m and Γ'_1, I_1 is certainly negative. It follows that I_1 as a function of T_1 must be a curve such as is shown in the lower part of Fig. 3. But

$$p_1 = I_1 - \mu\,|T_1 - T'_2|,$$

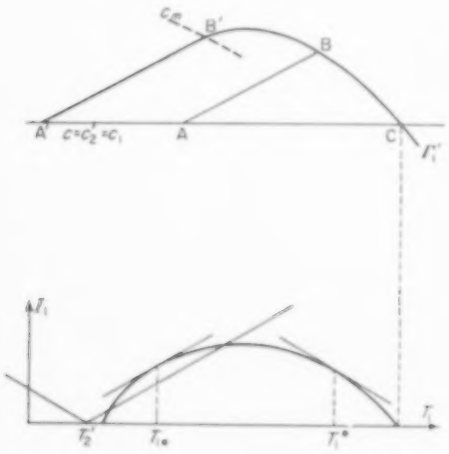

FIG. 3. The construction of the integral I_1.

the difference between the humped curve of I_1 just constructed and the V-shaped curve $\mu\,|T_1 - T'_2|$. The maximum difference will occur when T_1 has a value of either $T_{1\bullet}$ or T^*_1 the point at which $\partial I_1/\partial T_1 = +\mu$ or $-\mu$.

For given $c'_2 = c_1$ the optimum policy for the choice of T_1 and the resulting maximum profit f_1 is now seen to have a very simple structure. In Fig. 4 S_* and S^* are the points where the tangents at $T_{1\bullet}$ and T^*_1 meet the axis $I_1 = 0$. Then if:

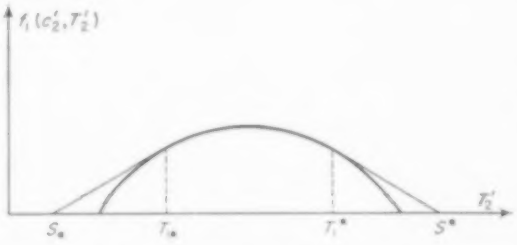

FIG. 4. $f_1(c'_2, T'_2)$ for a given c'_2.

(i) $T'_2 < S_*$, p_1 is always negative and it is unprofitable to react (i.e. the reactants are so cold that it is not worth heating them up at the cost of heating μ).

(ii) $S_* \leqslant T'_2 \leqslant T_{1\bullet}$, p_1 is maximum when $T_1 = T_{1\bullet}$ (i.e. the reactants should be heated to $T_{1\bullet}$ before entering the reaction bed). $f_1 = I_1(T_{1\bullet}) - \mu\,(T_1^* - T'_2)$.

(iii) $T_{1\bullet} \leqslant T'_2 \leqslant T^*_1$, p_1 is maximum when $T_1 = T'_0$ (i.e. the reactants should be introduced into the reaction bed immeddiately). $f_1 = I_1(T'_2)$.

(iv) $T_1^* \leqslant T'_2 \leqslant S^*$, p_1 is maximum when $T_1 = T^*_1$ (i.e. the reactants should be cooled to T^*_1 before entering the reaction bed). $f_1 = I_1(T^*_1) - \mu\,(T'_2 - T^*_1)$.

(v) $S^* < T'_2$, p_1 is always negative (i.e. the reactants are too hot to be worth cooling).

Moreover the maximum profit function

$$f_1(c'_2, T'_2) = \begin{cases} I_1(c'_2, T_{1\bullet}) - \mu\,(T_{1\bullet} - T'_2), & S_\bullet \leqslant T'_2 \leqslant T_{1\bullet} \\ I_1(c'_2, T'_2), & T_{1\bullet} \leqslant T'_2 \leqslant T_1^* \\ I_1(c'_2, T_1^*) - \mu\,(T'_2 - T^*_1), & T^*_1 \leqslant T'_2 \leqslant S^* \end{cases} \qquad (15)$$

is precisely the curve $I_1(c'_2, T'_2)$ bevelled off with its two tangents of slope $\pm\mu$.

In the last paragraph $c'_2 = c_1$ has been held constant and the values of T^*_1 and T_{1*} determined. If this is done for various c'_2 we obtain T^*_1 and T_{1*} as functions of c'_2. These may be plotted in the C, T plane as a curve Γ_1 having two branches, Γ^*_1 and Γ_{1*}. The optimum policy for a single bed is completely given by the curves Γ_1 and Γ'_1 as in Fig. 5. If the feed point c'_2, T'_2 lies to the left of Γ_{1*} (as A in Fig. 5)

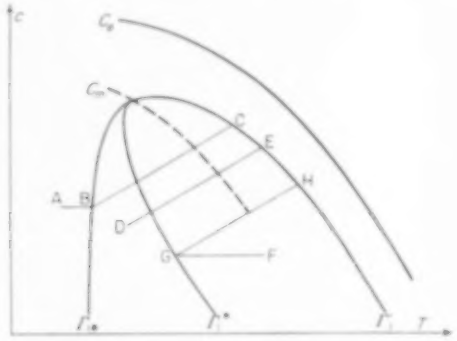

Fig. 5. Typical optimum policies with one bed.

the policy is to heat the reactants to $T_{1*}(c'_2)$ (point B) and then react until $R(c'_1, T'_1) = \lambda$ (point C). If the feed point lies between the two branches of Γ_1 the policy is just to react (the line DE). If the feed point lies to the right of Γ^*_1 the reactants are cooled to $T_1{}^*(c'_2)$ and reacted (the line FGH). Since the single bed will next be regarded as the second of two stages it is the last situation that is important. The surface $f_1(c'_2, T'_2)$ is shown in Fig. 6.

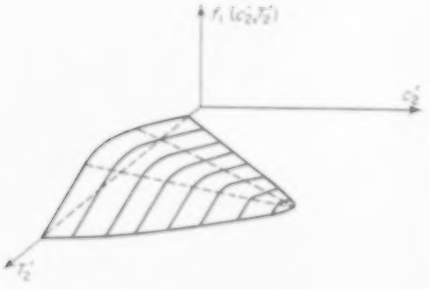

Fig. 6. The optimum yield surface.

The foregoing construction has been given to show the structure of the policy but to calculate the curve Γ_1 it is best to proceed analytically. Thus (14) is actually

$$I_1(c'_2, T'_2) = \int_{c'_2}^{c'_1} \left\{1 - \frac{\lambda}{R[c, T_1 + h(c - c'_2)]}\right\} dc \quad (16)$$

so

$$\frac{\partial I_1}{\partial T_1} = \lambda \int_{c'_2}^{c'_1} \left(\frac{1}{R^2}\frac{\partial R}{\partial T}\right) dc = \lambda J_1 \quad (17)$$

In both the integrals I_1 and J_1 the upper limit lies on the curve Γ'_1 so that on any adiabatic path J_1 can be calculated as a function of the lower limit by integrating back from the upper limit. Now

$$\frac{\partial p_1}{\partial T_1} = \frac{\partial}{\partial T_1}(I_1 - \mu|T_1 - T'_2|) =$$
$$\lambda J_1 \mp \mu \text{ according as } T_1 \gtrless T'_2.$$

Then on any adiabatic path we can find the points at which $J_1 = \pm\mu/\lambda$ and these are the intersections of the curves Γ_{1*} and Γ^*_1 with the adiabatic path.

For the next step it is necessary to have the partial derivatives of f_1. These will only be stated here; the proof of them is given in the appendix. In these formulae it is understood that J_1 is calculated using the optimum policy for its end points and $R_1 = R(c_1, T_1)$, T_1 being chosen optimally. Then

$$\frac{\partial f_1}{\partial c'_2} = -\left(1 - \frac{\lambda}{R_1}\right) - h\lambda J_1 \quad (18)$$

$$\frac{\partial f_1}{\partial T'_2} = \lambda J_1 \quad (19)$$

$$\frac{\partial f_1}{\partial c'_2} + h\frac{\partial f_1}{\partial T_2'} = -\left(1 - \frac{\lambda}{R_1}\right). \quad (20)$$

If c'_2, T'_2 lies outside the branches of the curve Γ_1 then $\lambda J_1 = \mu$ or $-\mu$. In the important case $T'_2 > T^*_1(c'_2)$ $\lambda J_1 = -\mu$.

4. The Optimum Performance of Several Beds

In the case of two adiabatic beds with feed conditions c'_3, T'_3 we have

$$f_2(c'_3, T'_3) = \text{Max}\{p_2 + f_1(c'_2, T'_2)\} \quad (21)$$

where

$$p_2 = \int_{c_2}^{c'_2} \left(1 - \frac{\lambda}{R}\right) - \mu\,|T_2 - T'_3|$$

$$= I_2 - \mu\,|T_2 - T'_3| \quad (22)$$

We again assume T_2 the inlet temperature to the first bed to have been fixed and ask at what concentration c'_2 the reaction in the first bed be stopped to give the greatest value of $p_2 + f_1$. T'_2 is linearly related to c'_2 by

$$T'_2 = T_2 + h\,(c'_2 - c_2)$$

so differentiating along the adiabatic path

$$\frac{d}{dc'_2}\{p_2 + f_1(c'_2, T'_2)\} = \frac{\partial p_2}{\partial c'_2} + \frac{\partial f_1}{\partial c'_2} + h\,\frac{\partial f_1}{\partial T'_2}.$$

Setting this derivative equal to zero for the maximum and using (20) and (22) we have

$$\left(1 - \frac{\lambda}{k'_2}\right) - \left(1 - \frac{\lambda}{R_1}\right) = 0$$

where $R'_2 = R(c'_2, T'_2)$. Thus

$$R'_2 = R(c'_2, T'_2) = R(c_1, T_1) = R_1 \quad (23)$$

and the reaction in the first bed should continue to such a point that on cooling to the optimum inlet temperature for the second bed the reaction will continue at the same rate. This is a remarkably simple criterion and allows a curve Γ'_2 to be drawn on which the exit conditions of the first bed must lie. To construct Γ'_2 we have only to take a point c_1, T_1 on the curve Γ^*_1 and draw through it the line of constant reaction rate R until it again meets the horizontal line $c = c_1$.

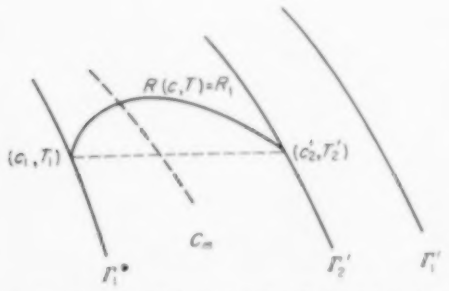

Fig. 7. Exit conditions for the first of two beds.

It is evident that Γ'_2 must lie between C_m and Γ'_1. This is shown in Fig. 7. Analytically we find T'_2 as a function of c'_2 by solving

$$R[c'_2, T'_2(c'_2)] = R[c'_2, T^*_1(c'_2)].$$

To find the best value of the inlet temperature T_2 we proceed as before. The quantity

$$I_2 + f_1(c'_2, T'_2)$$

as a function of T_2 for fixed c_2 gives a humped distortion of the curve of Fig. 4 to which we can draw the tangents with slope $\pm\mu$ and obtain f_2 precisely as before. This will yield two temperatures T_{2*} and T^*_2 to which the reactants should be heated or cooled according as T'_3 is less than T^*_2 or greater than T^*_2. Again a curve Γ_2 with two branches can be drawn in the c, T plane and the policy for a two-stage reactor is found immediately in the same way as before.

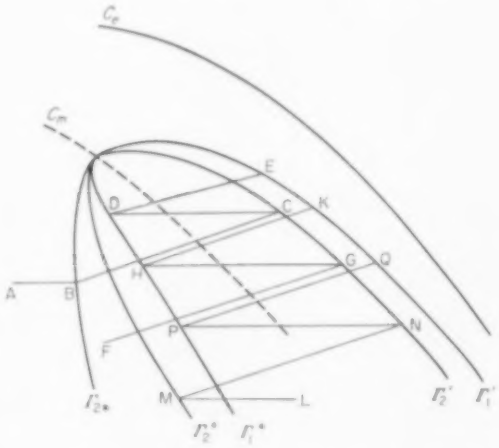

Fig. 8. Typical optimum policies with two beds.

Fig. 8 shows the three different kinds of reaction path given by a reaction mixture initially too cold ($ABCDE$), at a suitable temperature ($FGHK$) and initially too hot ($LMNPQ$). This process will generate an optimum policy surface $f_2(c'_3, T'_3)$ lying wholly above the surface f_1 and therefore extends to some degree the limits S_*, S^*, without which it is unprofitable to operate.

Analytically the condition for the optimum T_2 simplifies in a remarkable way and if $T'_3 > T_2$

$$\frac{\partial}{\partial T_2}\{I_2 - \mu\,|T_2 - T'_3| + f_1\} = \lambda J_2 \qquad (24)$$

whilst if $T_2 < T'_3$ the same derivative is $\lambda J_2 - 2\mu$. Thus Γ^*_2 and Γ_{2*} can be determined by integrating back from Γ'_2 along the adiabatic until $J_2 = 0$ to give Γ^*_2 and on until $J_2 = 2\lambda/\lambda$ to give Γ^*_2. The detailed manipulations are given in the Appendix. Even more remarkable is the fact that the partial derivatives of $f_2(c'_3, T'_3)$ have the same structure as before and in particular the derivative in an adiabatic direction is

$$\frac{\partial f_2}{\partial c'_3} + h\,\frac{\partial f_2}{\partial T'_3} = -\left(1 - \frac{\lambda}{R_2}\right)$$

where R_2 is the reaction rate at the optimum inlet conditions (c_2, T_2) for the feed (c'_3, T'_3).

Because of this we can proceed to the three bed optimum with equal ease. Γ'_2 the curve on which exit conditions of the first of three beds should lie is constructed from Γ^*_2 in the same way as Γ'_2 was constructed from Γ^*_1 (see Fig. 7). When Γ'_2 is known, Γ^*_2 and Γ_{2*} can be found as the curves for which $J_2 = 0$ and $2\mu/\lambda$ respectively.

5. Generalizations

Although the profit function P_N may appear to be too simple to be realistic it can be adapted to meet a variety of practical problems. Until now the parameters λ and μ have been regarded as constants, but it is clear that the optimum policy is a function of λ and μ. The maximum profit function is thus $f_N(c'_{N+1}, T'_{N+1};\ \lambda, \mu)$. In particular if μ is fixed the total bed volume $V_N = q\sum_1^N t_n$ will depend upon λ. By repeating the calculation for various λ the function $V_N(\lambda)$ may be found; it is a monotonic decreasing one for λ is the relative cost of bed volume and the higher this is the smaller will be the optimum volume. If then a design were asked for to give a certain total volume V it would be the solution of the optimum problem outlined above with $\lambda = \lambda_N$ so chosen that $V_N(\lambda_N) = V$. This might be a consideration of overriding importance as, for example, when the reactor is required to fit into some existing high pressure forging, which is too valuable to waste. Programmed for a modern computer such a problem as this would be very rapidly solved. If the interchangers between stages had also to be accommodated within a given volume it would be necessary to vary both λ and μ and to use data on the volume required by an interchanger removing a given amount of heat according to best design practice. In this case for each μ there would be a value of $\lambda = \Lambda(\mu)$ satisfying the volume requirement and the final choice of μ would be the one that made $f_N(c'_{N+1}, T'_{N+1};\ \Lambda(\mu), \mu)$ the greatest.

Again supposing λ and μ are known we might ask for a design with a given output $Q = q(c'_1 - c'_{N+1})$. Here we may take into account the cost of pumping the reactants at a rate q. For any q the exit concentration $c'_1 = c'_{N+1} + Q/q$. We can design the last bed first for its exit conditions must lie on Γ'_1. Taking the adiabatic back from the point $c = c'_1$ on Γ'_1 to Γ^*_1 we have the inlet conditions to the last bed c_1, T_1. Moving to the right along the line $c = c_1$ to the curve Γ'_2 gives the exit conditions of the penultimate bed. Again moving down an adiabatic we find c_2, T_2 on Γ^*_2 and so on. Some adiabatic line will cross the horizontal line through the feed $c = c_F$ and this intersection will give the feed conditions to the first bed. Thus the number of beds to give the required output has been found and the volume of each may be calculated. Using the accepted design practice the pressure drop through the reactor may be found and hence the cost $g(q)$ of pumping the reactants through at a rate q is found. Finally q is chosen to maximize $f_N(c'_{N+1}, T'_{N+1}) - g(q)$.

If the value of the product is not proportional to c'_1 but is a more complicated function, say $q\{v(c'_1) - v(c'_{N+1})\} = q\sum_1^N \{v(c'_n) - v(c_n)\}$ precisely the same technique may be applied as above save that we redefine the integral I as

$$I_n = v(c'_n) - v(c_n) - \lambda\int_{c_n}^{c'_n}\frac{dc}{R} = \int_{c_n}^{c'_n}\{v'(c) - \lambda/R\}\,dc$$

if $v(c)$ is differentiable. The curve Γ'_1 is now given by $v'(c)\,R(c, T) = \lambda$. A specification restriction could be included in $v(c)$, for in case c must lie between c_* and c^* we could set

$v(c) \equiv 0$ outside this interval. More interestingly $v(c)$ might take account of subsequent operations on the product stream such as the separation of the valuable product. If the optimum policy of operating the separating unit is studied so that $v(c)$ is maximized with respect to this operation then the principle of optimality shows that we would find the optimum overall policy for both reactor and separating unit.

If the cost of bed volume and heat interchange is not proportional to the volume or the heat removed the optimum problem can still be solved by solving the sequence of equations (10), using the appropriate non-linear expressions in p_N. In this case, however, the simple structure of the policy will be lost and it will no longer be possible to draw the sequence of curves Γ'_n and Γ_n. The solution, however, is still within the powers of a modern digital computer.

It thus appears that the method of dynamic programming is well suited to a number of significant problems in the design of adiabatic reactors. It may be extended to the design of cold-shot reactors and to the case of more than one reaction, as will be shown in later publications.

Appendix

To calculate the partial derivatives of f_1 we consider the three regions defined by (15). Take first the region $T_{1*} \leqslant T'_2 \leqslant T^*_1$ in which

$$f_1(c'_2, T'_2) = \int_{c}^{c'_1} \left\{1 - \frac{\lambda}{R[c, T'_2 + h(c - c_1)]}\right\} dc$$

and $R'_1 = R[c'_1, T'_2 + h(c'_1 - c'_2)] = \lambda$ and $c_1 = c'_2$. In the expression on the right side of c'_1 is a function of c'_2 and T'_2. Thus differentiating the limits and under the integral

$$\frac{\partial f_1}{\partial c'_2} = \left\{1 - \frac{\lambda}{R'_1}\right\} \frac{\partial c'_1}{\partial c'_2} - \left\{1 - \frac{\lambda}{R_1}\right\} - \lambda h J_1$$

But since $R_1' = \lambda$ the first term vanishes and

$$\frac{\partial f_1}{\partial c_2} = -\left\{1 - \frac{\lambda}{R_1}\right\} - \lambda h J_1 \tag{25}$$

Similarly

$$\frac{\partial f_1}{\partial T'_2} = \left\{1 - \frac{\lambda}{R'_1}\right\} \frac{\partial c'_1}{\partial T'_2} + \lambda J_1 = \lambda J_1 \tag{26}$$

and

$$\frac{\partial f_1}{\partial c'_2} + h \frac{\partial f_1}{\partial T'_2} = -\left\{1 - \frac{\lambda}{R_1}\right\}. \tag{27}$$

In the region $S_* \leqslant T'_2 \leqslant T_{1*}$

$$f_1(c'_2, T'_2) \int_{c'_2}^{c'_1} \left\{1 - \frac{\lambda}{R[c, T_{1*}(c'_2) + h(c - c'_2)]}\right\} dc + \mu(T'_2 - T_{1*})$$

Here

$$\frac{\partial f_1}{\partial c'_2} = \left\{1 - \frac{\lambda}{R'_1}\right\} \frac{\partial c'_1}{\partial c_2} - \left\{1 - \frac{\lambda}{R_1}\right\} + \lambda J_1 \left\{\frac{dT_{1*}}{dc'_2} - h\right\} - \mu \frac{dT_{1*}}{dc'_2},$$

but $R'_1 = \lambda$ and $\lambda J_1 = \mu$ so that

$$\frac{\partial f_1}{\partial c'_2} = -\left\{1 - \frac{\lambda}{R_1}\right\} - \lambda h J_1$$

Clearly $\partial f_1 / \partial T'_2 = \mu = \lambda J_1$, so that the same formulae apply, it being understood that the path for J_1 is chosen optimally. A similar calculation for the region $T_1^* \leqslant T'_2 \leqslant S^*$ gives the same formulae.

To establish the formula (24), let $T'_3 > T^*_2$ and

$$F_2 = \int_{c_2}^{c'_2} \left\{1 - \frac{\lambda}{R[c, T_2 + h(c - c_2)]}\right\} dc - \mu(T'_3 - T_2) + f_1(c'_2, T'_2)$$

and observe that c'_2 and T'_2 are both functions of T_2. However since $T'_2 = T_2 + h(c'_2 - c_2)$ we have

$$\frac{\partial T'_2}{\partial T_2} = 1 + h \frac{\partial c'_2}{\partial T_2}. \tag{28}$$

Then

$$\begin{aligned}\frac{\partial F_2}{\partial T_2} &= \left\{1 - \frac{\lambda}{R'_2}\right\} \frac{\partial c'_2}{\partial T_2} + \lambda J_2 + \mu + \frac{\partial f_1}{\partial c'_2} \frac{\partial c'_2}{\partial T_2} + \frac{\partial f_1}{\partial T'_2} \frac{\partial T'_2}{\partial T_2} \\ &= \left[\left\{1 - \frac{\lambda}{R'_2}\right\} - \left\{1 - \frac{\lambda}{R_1}\right\} - h\lambda J_1 + h\lambda J_1\right] \frac{\partial c'_2}{\partial T_2} \\ &\quad + \lambda J_2 + \mu + \lambda J_1 \\ &= \lambda J_2; \end{aligned} \tag{29}$$

to get the second line we use (25), (26) and (28) and the final reduction depends on the fact that $R_1 = R'_2$ and $\lambda J_1 = -\mu$. In case $T_2 > T'_3$ the sign of the term $\mu(T'_3 - T_2)$ in F_2 must be changed, this gives a $-\mu$ in the penultimate line of (29) and so $\partial F_2 / \partial T_2 = \lambda J_2 - 2\mu$.

To show how the derivative of f_2 simplifies so dramatically we will consider the case $T'_3 > T^*_2(c'_3)$. Here

$$f_2(c'_3, T'_3) = I_2 - \mu(T'_3 - T^*_2) + f_1(c'_2, T'_2) \tag{30}$$

and the R in I_2 is $R[c, T_2^*(c'_3) + h(c - c'_3)]$. c'_2 and T'_2 both depend on c'_3 and T'_3 but since

$$T'_2 = T^*_2(c'_3) + h(c'_2 - c'_3)$$

we have

$$\frac{\partial T'_2}{\partial c'_3} = \left(\frac{dT^*_2}{dc'_3} - h\right) + h\frac{\partial c'_2}{\partial c'_3}. \tag{31}$$

Hence

$$\frac{\partial f_2}{\partial c'_3} = \left\{1 - \frac{\lambda}{R'_2}\right\}\frac{\partial c'_2}{\partial c'_3} - \left\{1 - \frac{\lambda}{R_2}\right\} + \lambda J_2\left\{\frac{dT^*_2}{dc'_3} - h\right\}$$
$$+ \mu\frac{dT^*_2}{dc'_3} + \frac{\partial f_1}{\partial c'_2}\frac{\partial c'_2}{\partial c'_3} + \frac{\partial f_1}{\partial T'_2}\frac{\partial T'_2}{\partial c'_2}$$

in which the first line is the derivative of I_2. Making use of (31), (25) and (26) and collecting terms together

$$\frac{\partial f_2}{\partial c'_3} = -\left\{1 - \frac{\lambda}{R_2}\right\} - \lambda h(J_2 + J_1) +$$
$$+ \frac{dT^*_2}{dc'_3}[\lambda J_2 + \mu + \lambda J_1]$$
$$+ \frac{\partial c'_2}{\partial c'_3}\left[\left\{1 - \frac{\lambda}{R'_2}\right\} - \left\{1 - \frac{\lambda}{R_1}\right\} - \lambda h J_1 + \lambda h J_1\right]$$
$$= -\left\{1 - \frac{\lambda}{R_2}\right\} - h(\lambda J_2 - \mu) \tag{32}$$

since the square brackets vanish. Of course $J_2 = 0$ so the second term is really $h\mu$. However a little more work shows that in the form (32) the expression is valid when $T'_3 < T^*_2$, it being understood that J_2 is on an optimal path. Clearly

$$\frac{\partial f_2}{\partial T'_3} = -\mu = (\lambda J_2 - \mu) \tag{33}$$

in this region this formula can again be extended.

Finally

$$\frac{\partial f_2}{\partial c'_3} + h\frac{\partial f_2}{\partial T'_3} = -\left\{1 - \frac{\lambda}{R_2}\right\} \tag{34}$$

is everywhere valid, so that the derivative along an adiabatic path of the optimum f_2 is related to R_2 just as the derivative of f_1 was related to R_1.

Notation

c = concentration of product
c_p = specific heat of reactants
c_m = concentration for maximum reaction range
f_N = maximum profit from N beds
H = heat of reaction
h = $H/c_p\rho$
I = integral defined by equation (16)
J = integral defined by equation (17)
N = number of beds
P_N = total profit from N beds
p_n = profit from n^{th} bed
q = flow rate of reactants
R = $R(c, T)$, reaction rate
T = temperature
t = holding time, x/v
V_N = total volume of N beds
v = linear velocity of reactants
$v(c)$ = value function of product
x = distance from inlet of bed
α = unit value of product
β = unit cost of bed volume
γ = unit cost of heat interchange
λ = β/α
μ = $\gamma c_p \rho/\alpha$
ρ = density of reactants

Suffix n denotes value in the n^{th} bed from the exit. A prime denotes conditions at exit of any bed.

Reference

[1] Bellman R. *Dynamic Programming.* Princeton University Press. Princeton 1957.

Chemical Engineering Science, 1960, Vol. 12, pp. 253 to 259. Pergamon Press Ltd., London. Printed in Great Britain

The frequency response of rotameters

G. S. Harrison
African Explosives and Chemical Industries, Modderfontein, Transvaal, S. Africa.

and W. D. Armstrong
Department of Chemical Engineering, Pembroke Street, Cambridge.

(*Received* 21 *December* 1959 ; *in revised form* 30 *December* 1959)

Abstract—The dynamic characteristics of a rotameter type flowmeter has been investigated experimentally by making frequency response measurements using floats of various shapes and materials in two different liquids. The experimental results are compared with calculations based on a simplified theory which is derived.

Résume—La caractéristique dynamique d'un débitmètre type rotamètre a été étudiée expérimentalement dans deux liquides différents en faisant des mesures de réponse de fréquence, et en utilisant des flotteurs de formes et matières variées. Les résultats expérimentaux sont comparés avec des calculs basés sur une théorie simplifiée qui a été établie.

Zusammenfassung—Die dynamische Charakteristik von Rotamessern wurde durch Frequenzgangmessungen experimentell untersucht in zwei verschiedenen Flüssigkeiten unter Benutzung von Schwimmern verschiedener Gestalt und Materialien. Die experimentellen Ergebnisse werden mit Berechnungen verglichen, die auf einer eigens abgeleiteten vereinfachten Theorie beruhen.

Introduction

Previously published studies of rotameters have been confined almost entirely to considerations of their operation under conditions of constant liquid flow-rate and the relationship between the flow-rate and the height of the float in the tube.

Whitwell and Plumb [1] derived a correlation between the flow-rate and the rotameter scale reading, using a modified form of Bernoulli's equation. This method involved the graphical determination of two functions, whereas the now generally accepted correlation, first proposed by Schoenborn and Colburn [2], requires the graphical evaluation of only the rotameter coefficient K_R, in the expression :

$$Q = K_R A \sqrt{\left[\frac{2gv\,(\rho_f - \rho_w)}{A_f\,\rho_w}\right]} \qquad (1)$$

where Q = the volume flow-rate,
K_R = the rotameter coefficient.
A = the miminum annular area between the float and tube wall,
g = the acceleration due to gravity,
v = the volume of the float,
ρ_f = the density of the float,
ρ_w = the density of the metered liquid.

This expression was derived by assuming that the flow between the float and tube was equivalent to that through an annular orifice.

Using the same basic assumptions, Martin [3] derived a slightly modified version of the above equation by substituting a function of the Reynolds number for K_R.

The work of Fischer *et. al.* [4] was concerned with the design of a rotameter float which would have a calibration independent of the viscosity of the metered liquid.

Using equation (1), Fritsche [5] found that K_R was very nearly constant for different values of a so-called "viscous influence number." This method was suggested as a means of correlating the calibrations of rotameters metering different liquids.

Vitovec and Režábek, [6] by dimensional analysis, obtained an expression similar to that derived by Martin [3].

These authors all concerned themselves only with the steady-state operation of the rotameter. MacMillan [7], on the other hand, suggested an expression for the transient response of a rotameter but this would be applicable only in cases of laminar flow through the annulus between the float and the tube wall.

The Differential Equation of the Unsteady Operation of a Rotameter

The forces acting on a rotameter float, displaced from its equilibrium position, are:

(1) The upward forces due to the drag of the fluid in the annulus, the pressure difference across the float and the buoyancy of the liquid.

(2) The downward force due to the weight of the float.

The forces due to the drag and the pressure drop will be some function of the fluid velocity in the annulus and the vertical velocity of the float. Thus a force balance across the float may be written:

$$M\frac{d^2h}{dt^2} = f\left(V, \frac{dh}{dt}\right) - g_v(\rho_f - \rho_w) \qquad (2)$$

where M = the mass of the float,
V = the linear velocity of the liquid in the annulus.
h = the height in the rotameter tube,
t = time,

and the other symbols have the same significance as before.

The force, F, acting on a body due to form drag is usually expressed by an equation of the form:

$$F_{\text{drag}} = \frac{K_1 A_f \rho_w V^2}{2} \qquad (3)$$

Assuming that the pressure drop across the annulus may be expressed in the same form as pressure drop across an annular orifice, the force acting on the float, due to the pressure difference across it, may be written:

$$F_{\text{press.}} = A_f \Delta p = \frac{K_2 A_f \rho_w V^2}{2} \qquad (4)$$

Thus it is to be expected that the function $f(V, dh/dt)$ in equation (2) would be of the same form as equations (3) and (4).

By analogy with a body falling through an infinite fluid, the obvious choice for a first attempt would be the substitution of the difference between the float velocity and the mean velocity of the fluid in the annulus, for V in equation (2). This substitution gave results which are not in agreement with experimental results, so that it was necessary to devise a means of investigating the nature of the function f.

An experimental study was made of the terminal velocities of steel and duralumin floats and steel and bronze spheres (up to 1in. diameter) in cylindrical tubes through which liquids flowed at various rates (see Table 1). It was found that the experimental results could be expressed in the form:

$$u = B\frac{\Delta d}{d_f}V + u_0$$

where V = volume flow-rate/minimum annular area between the float (or sphere) and the tube,
u = velocity of float or sphere in the tube,
u_0 = value of u when $V = 0$.

Table 1

Shape of float	*Float material*	*Float diameter* (ft)	*Tube diameter* (ft)	*Liquid*
Rotameter	Steel	0·0625	0·0690	Water
Rotameter	Steel	0·0625	0·0717	Water
Rotameter	Steel	0·0625	0·0753	Water
Rotameter	Steel	0·0625	0·0690	Glycerol
Rotameter	Steel	·00625	0·0717	Glycerol
Rotameter	Steel	0·0625	0·0753	Glycerol
Rotameter	Duralumin	0·0625	0·0690	Water
Rotameter	Duralumin	0·0625	0·0717	Water
Rotameter	Duralumin	0·0625	0·0753	Water
Rotameter	Duralumin	0·0625	0·0690	Glycerol
Rotameter	Duralumin	0·0625	0·0717	Glycerol
Rotameter	Duralumin	0·0625	0·0753	Glycerol
Rotameter	Steel	0·0831	0·0852	Water
Rotameter	Steel	0·0328	0·0392	Water
Rotameter	Steel	0·0328	0·0428	Water
Rotameter	Steel	0·0328	0·0418	Water
Rotameter	Steel	0·0466	0·0540	Water
Rotameter	Steel	0·0466	0·0592	Water
Sphere	Steel	0·0313	0·0392	Water
Sphere	Steel	0·0313	0·0428	Water
Sphere	Steel	0·0313	0·0418	Water
Sphere	Steel	0·0469	0·0540	Water
Sphere	Steel	0·0469	0·0592	Water
Sphere	Steel	0·0833	0·0852	Water
Sphere	Steel	0·0833	0·0916	Water
Sphere	Steel	0·0625	0·0690	Water
Sphere	Steel	0·0625	0·0717	Water
Sphere	Bronze	0·0625	0·0690	Water
Sphere	Bronze	0·0625	0·0717	Water

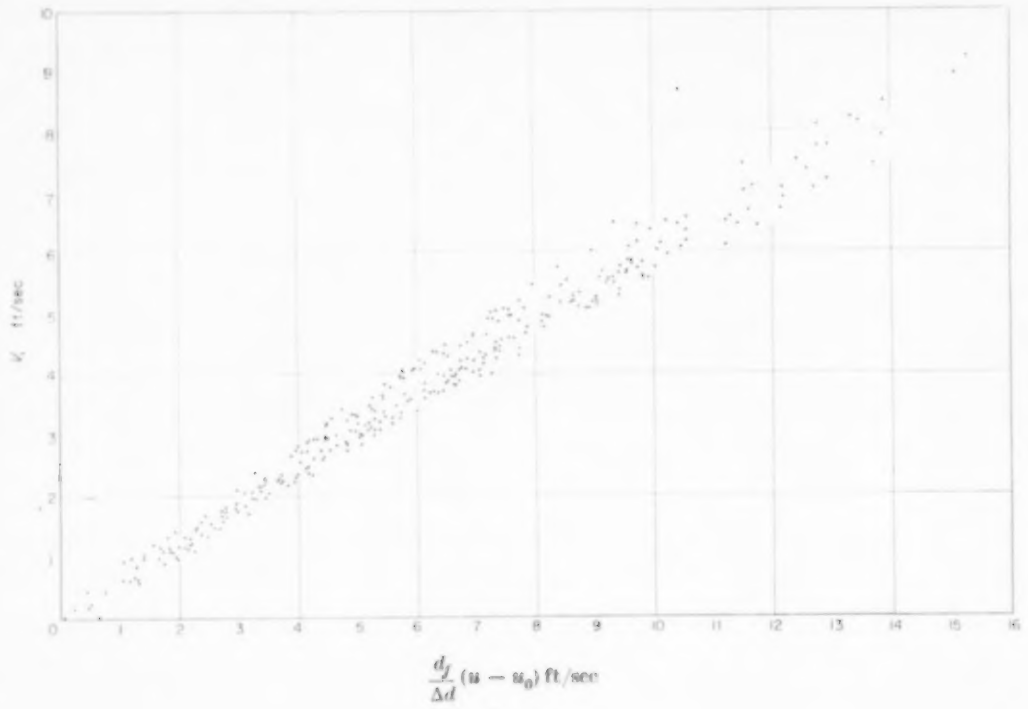

FIG. 1.

In Fig. 1 $(d_f/\Delta d)(u - u_0)$ is plotted against V and it may be seen that for all combinations of float or sphere, tube and liquid B is constant and equal to 1·65.

At the terminal velocity of a body in a liquid, a force balance gives

$$g v (\rho_f - \rho_w) = \phi (V, u) \qquad (5)$$

where ϕ is an unknown function of V and u. ϕ may be assumed to have a form similar to that of F in equations (3) and (4) with a function of V and u replacing V^2, the function being such that it is constant, with varying V and u, for each combination of float, tube and liquid. This condition is satisfied by taking:

$$v (\rho_f - \rho_w) = K_T \left[V - \frac{u}{B} \cdot \frac{d_f}{\Delta d} \right]^2 \qquad (6)$$

Comparing this expression with equation (1) which refers to the operation of a rotameter in turbulent flow $K_T = 1/K_R^2$ if $u = 0$. However K_R has been shown [2] to be a function of the Reynolds Number $\mathrm{Re}_R = V \rho_w \Delta d / \mu$. K_T was calculated for the floats in cylindrical tubes and Fig. 2 shows the relationship between $K_T^{-1/2}$ and Re_R defined as

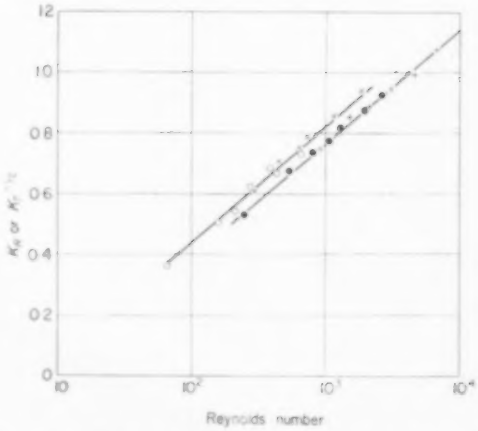

FIG. 2. ● Rotameter with water. ○ Rotameter with glycerol solution. + Cylindrical tube with water. × Cylindrical tube with glycerol solution.

$$\left[V - \frac{u}{B}\frac{d_f}{\Delta d}\right]\frac{\Delta d\,\rho_w}{\mu}$$

The values lie on the same lines as the plot of K_R against Re_R.

Predicting the Frequency Response of a Rotameter

From the work on bodies moving through a cylindrical tube it was possible to derive an expression for the kinetic forces acting on the rotameter float when displaced from its equilibrium position. Substituting the expression from equation (6) into equation (2), the force balance becomes:

$$M\frac{d^2h}{dt^2} = K_T\frac{A_f\rho_w}{2}\left[V - \frac{d_f}{B(d_t - d_f)}\cdot\frac{dh}{dt}\right]^2 - \\ - gv(\rho_f - \rho_w) \qquad (7)$$

but $$V = \frac{Q}{\frac{1}{4}\pi(d_t^2 - d_f^2)}$$

where d_t is the diameter of the rotameter tube in the displaced or transient position of the float.

$$M\frac{d^2h}{dt^2} = \\ K_T\frac{A_f\rho_w}{2}\left[\frac{Q}{\frac{1}{4}\pi(d_t^2 - d_f^2)}\right]^2 - \\ - \frac{2K_TA_f\rho_w\,d_f}{2B(d_t - d_f)}\cdot\frac{Q}{\frac{1}{4}\pi(d_t^2 - d_f^2)}\cdot\frac{dh}{dt} + \\ + \frac{K_TA_f\rho_w\,d_f^2}{2B^2(d_t - d_f)^2}\left(\frac{dh}{dt}\right)^2 - gv(\rho_f - \rho_w) \qquad (8)$$

Q may also be expressed in terms of the equilibrium position of the float in the rotameter tube, using equation (1). Let the diameter of the tube at this point be d_e, then,

$$Q = K_R\cdot\frac{\pi}{4}(d_e^2 - d_f^2)\sqrt{\left[\frac{2gv(\rho_f - \rho_w)}{A_f\rho_w}\right]} \qquad (9)$$

whence equation (8) becomes:

$$\frac{M}{g}\frac{d^2h}{dt^2} = \frac{K_TA_f\rho_w}{2g}\left[\frac{K_R\frac{1}{4}\pi(d_e^2 - d_f^2)}{\frac{1}{4}\pi(d_t^2 - d_f^2)}\right]^2\cdot \\ \frac{2gv(\rho_f - \rho_w)}{A_f\rho_w} - \left[\frac{K_TA_f\rho_w d_f}{gB(d_t - d_f)}\right]^2\cdot \\ \cdot\left[\frac{K_R\frac{1}{4}\pi(d_e^2 - d_f^2)}{\frac{1}{4}\pi(d_t^2 - d_f^2)}\right]\sqrt{\left[\frac{2gv(\rho_f - \rho_w)}{A_f\rho_w}\right]}\cdot \\ \cdot\frac{dh}{dt} + \frac{K_TA_f\rho_w\,d_f^2}{2gB^2(d_t - d_f)^2}\cdot\left(\frac{dh}{dt}\right)^2 - \\ - v(\rho_f - \rho_w) \qquad (10)$$

If 2θ = the angle between the tapered sides of the tube then put

$$d_e = d_f + 2H\tan\theta$$

$$d_t = d_f + 2h\tan\theta$$

Then if θ is small, $H^2\tan^2\theta$ and $h^2\tan^2\theta$ may be neglected compared with $2d_fH\tan\theta$ and $2d_fh\tan\theta$.

Substituting $K_T = 1/K_R^2$, equation (10) becomes:

$$\frac{M}{gv(\rho_f - \rho_w)}\frac{dh^2}{dt^2} + \frac{Hd_f}{2K_RB\tan\theta\,.\,h^2}\cdot \\ \cdot\sqrt{\left[\frac{2A_f\rho_w}{gv(\rho_f - \rho_w)}\right]}\frac{dh}{dt} - \frac{A_f\rho_w}{2gv(\rho_f - \rho_w)}\cdot \\ \cdot\frac{d_f^2}{(2K_RBh\tan\theta)^2}\cdot\left(\frac{dh}{dt}\right)^2 = \frac{H^2 - h^2}{h^2} \qquad (11)$$

Put $H = H_m + H'$ and $h = H_m + h'$, and assume that h' and H' are small; then if $H' = P\sin\omega t$, at long periods of oscillation, i.e. if ω is small, $(dh/dt)^2$ may be neglected and equation (11) becomes:

$$\frac{MH_m}{2gv(\rho_f - \rho_w)}\frac{d^2h'}{dt^2} + \frac{d_f}{2K_RB\tan\theta}\cdot \\ \cdot\sqrt{\left[\frac{A_f\rho_w}{2gv(\rho_f - \rho_w)}\right]}\cdot\frac{dh'}{dt} + h' = P\sin\omega t. \qquad (12)$$

From this equation the frequency response of a rotameter has been calculated.

Experimental

The apparatus for determining the frequency response of a rotameter is shown diagrammatically if Fig. 3. The liquid was pumped from the reservoir A up to the constant head tank B, whilst

VOL 12 1960

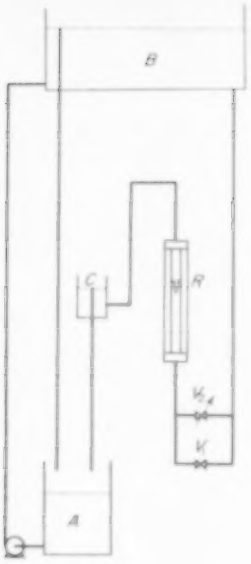

FIG. 3.

the flow to the rotameter was controlled by means of valves V_1 and V_2. Valve V_1 was an ordinary globe valve by means of which the basic flow rate through the apparatus could be adjusted; and V_2 was the valve by means of which a sinusoidal flow was superimposed on the steady flow through V_1. The constant level overflow device C_1 was adjustable to enable the total pressure-drop across the flow system to be controlled.

Attached to the driving shaft of the eccentric, which was used to oscillate valve V_2, was a trip mechanism. This was arranged to close an electric circuit, operating a recording pen whenever the valve was fully open, i.e. when maximum flow was possible through the rotameter. Twin recording drums each with 25 min. capacity were used. The second drum was used to record the instant of making rotameter readings.

The experiment was repeated for several periods of oscillation of from 5 min to 2 sec for each level of flow. Three similar series of runs were carried out using flow-rates which gave rotameter readings near the top, middle and bottom of the scale, while the amplitude was the same in each case. The frequency responses of rotameters with floats made of stainless steel and duralumin (diameter 0·75 in.) were determined using water, and using a 45 per cent solution of glycerol in water as the metered liquid.

Results

From a series of pairs of readings of rotameter float position and time, it was possible to obtain the best sinusoidal wave to fit the points by means of a statistical analysis using the theory of least squares. From this calculation, the phase lag and normalized attenuation were calculated.

In practice, however, this method was found to be very laborious, involving large numbers of arithmetical calculations and a more rapid graphical method was devised. By adjusting the time scale, it was possible to plot all the readings from one experiment on a single set of axes and obtain one cycle of a displaced cosine curve. From this curve, the phase lag was read off directly and the normalized attenuation was calculated from the amplitude of the wave, and the equilibrium flows with the oscillating valve in its two extreme positions. The accuracy of this method was checked in several cases by

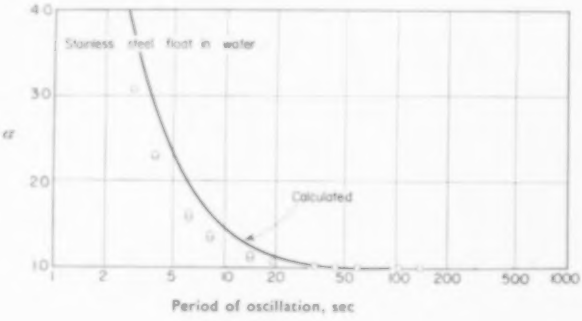

FIG. 4a.

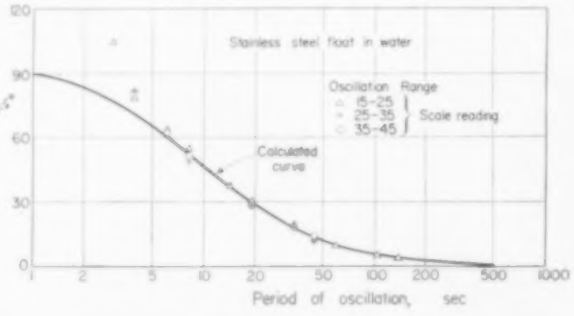

FIG. 4b.

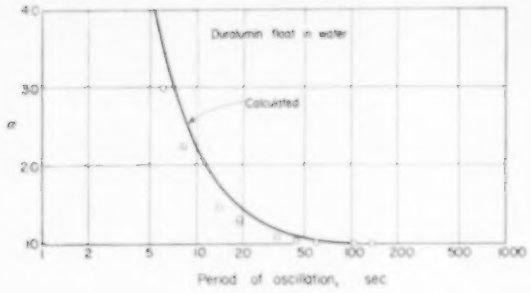

FIG. 4c.

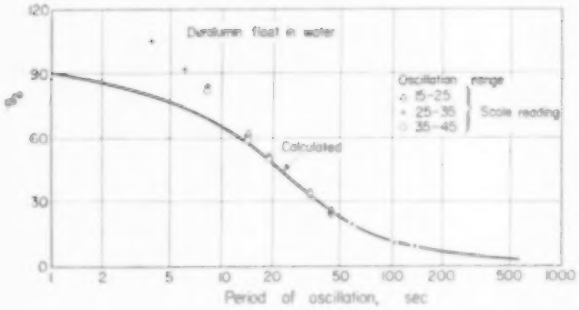

FIG. 4d.

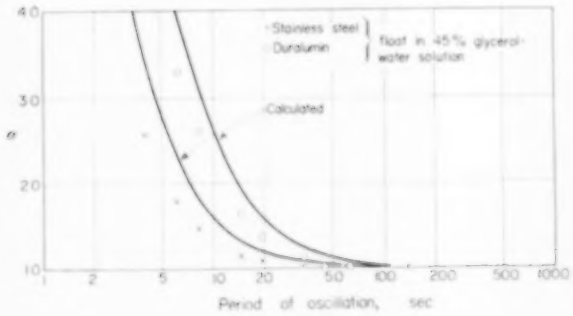

FIG. 5a.

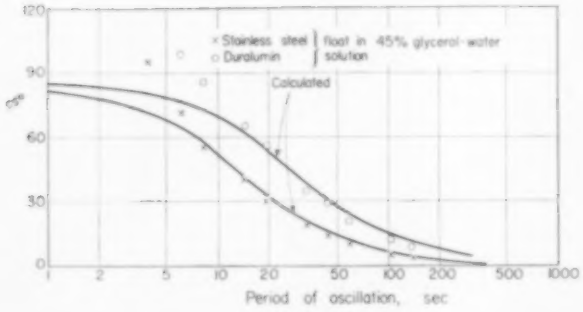

FIG. 5b.

comparison with results obtained from a statistical analysis.

The frequency response curves for rotameters metering water and 45 per cent glycerol solution, using stainless steel and duralumin floats are plotted in Figs. 4 and 5 together with the theoretically predicted values from the solution of equation (12).

DISCUSSION

From Figs. 4 and 5 it may be seen that the response of the rotameter does not change appreciably with the liquid flow-rate; and it was not possible, within the limits of experimental error, to detect any consistent difference in the results at the three flow-rates used in each case. Thus, while all the results are recorded for the frequency response in those cases where water was the metered liquid, only the mean values have been recorded for cases in which the glycerol solution was used.

The curves of phase lag and normalized attenuation show that the simplified differential equation (12) provides a reasonably good approximation to the frequency response of a rotameter at longer periods of oscillation, i.e. at lower values of the angular velocity ω. However, at short periods of oscillation the predicted response deviates increasingly from the experimental values.

This is due to the fact that, in deriving equation (12), the velocity of the rotameter float in the tube was assumed to be small compared with the liquid velocity in the annulus and the square of the float velocity was neglected. This approximation becomes progressively less accurate as ω increases. The deviation of values, calculated using this approximation, from the experimental values would also be expected to be greater, when the coefficient of the $(dh/dt)^2$ term was increased as, for example, by decreasing the density of the float, or by increasing the density and the viscosity of the metered liquid.

Thus the predicted response of the rotameter with glycerol solution begins to deviate appreciably from the experimental results at longer periods of oscillation than with water.

Comparing the corresponding experimental results for the rotameter response with water

and with the 45 per cent glycerol–water solution with a viscosity nearly four times as great, it was observed that the effect of viscosity was relatively small. The response is affected only to the extent by which the viscosity alters the rotameter coefficient K_R, whereas, in the case of laminar flow, the coefficient of dh/dt is proportional to the viscosity [7] and the difference between the two responses is more marked.

Acknowledgements—The authors are indebted to the Royal Dutch Shell Group of Companies for scholarships granted to one of them (G.S.H.) which made possible the research reported in this paper.

Notation

Capital letters

A = cross-sectional area
B = a dimensionless constant
C = a constant
F = force
H = height of float in rotameter tube
K = dimensionless constant
M = mass of float
Q = volumetric flow rate
Re = Reynolds number
V = linear velocity.

Small letters

d = diameter
g = acceleration due to gravity
h = transient height in rotameter tube
t = time
u = float velocity
v = volume of float

Greek letters

α = normalized attenuation
θ = half the angle between the tapered sides of the rotameter
μ = viscosity
ρ = density
ϕ = phase angle

Subscripts

R = appertaining to a rotameter
T = appertaining to a cylindrical tube
e = equilibrium value
f = appertaining to a rotameter float
m = mean value
w = appertaining to the metered liquid

References

[1] Whitwell J. C. and Plumb D. S. *Industr. Engng. Chem.* 1939 **31** 451.
[2] Schoenborn E. M. and Colburn A. P. *Trans. Amer. Inst. Chem. Engrs.* 1939 **35** 359.
[3] Martin J. J. *Chem. Engng. Progr.* 1949 **45** 338.
[4] Fischer K. *et. al. Trans. Amer. Inst. Chem. Engrs.* 1940 **36** 857.
[5] Fritsche R. W. *Petrol. Refin.* 1950 **29** No. 3 123.
[6] Vitovec J. and Rezábek A. *Chem. Listy.* 1957 **51** 159.
[7] MacMillan R. H. *Theory of Control* p. 23. Cambridge University Press 1951.

Chemical Engineering Science, 1960, Vol. 12, pp. 260 to 271. Pergamon Press Ltd., London. Printed in Great Britain

Porosity distributions in a fluidized bed

P. J. Bakker and P. M. Heertjes

(*Received* 5 *October* 1959; *in revised form* 18 *November* 1959)

Abstract—Some theoretical equations, regarding the porosity distribution in a fluidized bed of very large diameter, have been developed. Measurements on this porosity distribution in the centre of a fluidized bed of glass beads and air agreed sufficiently well with the theory. In general three distinct zones in the centre of the fluidized bed could be distinguished. Near the sieve, a sieve effect zone was found, followed by a zone of constant porosity reaching up to the initial bed height at incipient fluidization and above it a zone of increasing porosity for which a probility function has been found. The constants in this function have been correlated with some fluidization variables, such as fluidization velocity, bed weight and particle size.

The bed expansion in all cases showed a linearity with the product of bed weight and fluidization velocity.

Experiments with silica gel and polystyrene pearls instead of glass beads had the same results.

From measurements throughout the whole bed and by connecting points of equal porosity, so called isopores have been obtained, from which streaming patterns in the fluidized bed could be deduced. The influence of the bed weight on such isopores has been presented.

Résumé—Quelques équations théoriques ont étées développées pour la distribution de la porosité dans un lit fluidisé de très grand diamètre.

Des measures de la distribution de la porosité dans le centre d'un lit fluidisé formé des sphères de verre et de l'air étaient sufissamment conforme au théorie.

En général trois zones pourraient être distinguées dans le centre du lit. Près du tamis se trouvait une zone, appellée la zone de l'effit du tamis. Au dessus de cette zone, une zone de porosité constante, ce qui s'étendait jusqu'à la hauteur du lit à l'état préfluidisé. Au dessus de cette zone, la porosité du lit dans la troisième zone, augmentée jusqu'à l'unité. Dans cette zone une fonction de probabilité a été trouvée pours la porosité. Les constantes dans cette fonction ont étées correlées avec quelques variables de fluidisation, comme la vélovité, la masse du lit et le diamétre des particules (sphères).

L'expansion du lit changeait linéairement avec le produit de la masse du lit et la vélocité de fluidisation.

Des expériments avec du silicagel and polystyrene sphères donnaient les mêmes résultats qu'avec les sphères de verre.

Des mesures dans tout le lit et par l'emploi des points de porosité égaux, des isopores ont étés obtenus. La déduction des profiles de vélocité pour l'air et pour les particules était possible. L'influence de la masse du lit sur les isopores a été présentée.

Zusammenfassung—Über die Porositätsverteilung in einem Fliessbett von sehr grossem Durchmesser wurden einige theoretische Gleichunger entwickelt. Messungen über die Porositätsverteilung im Zentrum eines Fliesbetts aus Glaskugeln und Luft stimmten befriedigend mit der Theorie überein. Im allgemeinen kann man drei getrennte Zonen im Zentrum eines Fliessbetts unterscheiden. In der Nähe des Bodens ist eine vom Boden beeinflusste Zone zu finden, auf die dann eine Zone konstanter Porosität folgt, die bis zur anfänhglichen Betthöhe bei beginnender Fluidisierung reicht. Oberhalb liegt eine Zone steigender Porosität, für welche man eine Wahrscheinlichkeitsfunktion angeben kann. Die Konstanten dieser Funktion wurden mit einigen Fliessbettvariablen in Beziehung gebracht, der Fluidisiergeschwindigkeit, dem Bettgewicht und der Teilchengrösse.

Die Bettexpansion hängt in allen Fällen lineal von dem Produkt aus Bettgewicht und Fluidisiergeschwindigkeit ab.

Versuche mit Silicagel und Polystryrolpleren anstelle von Glaskugeln ergaben dieselben Ergebnisse.

Aus Messungen innerhalb des ganzen Bettes und durch Verbinden der Punkte gleicher Porosität erheilt man die sogenannten Isoporen, aus denen das Strömungsbild des Fliessbetts agbeleitet werden könnte. Der Einfluss des Bettgewichts auf diese Isoporen wurde ermittelt.

VOL. 12 1960

Observations on the behaviour of fluidized beds at varying fluidization conditions and the results of porosity measurements in such a bed [1, 2] have lead to a theoretical concept regarding the porosity distribution in a fluidized bed. This concept will be presented in this paper together with the measurements which serve as an illustration of the theory put forward.

The Porosity Distribution in a Fluidized Bed

As can be observed in glass columns, a fluidized bed, under not too extreme fluidization conditions can be divided into at least two layers, a first relatively dense layer from the bed support up to the height of the bed at incipient fluidization and a second relatively dilute layer above this height. The fluidized bed in the first layer consists of two phases, a continuous and a discontinuous phase (see e.g. Toomey and Johnstone [3]). The continuous phase is formed of a bed of a relatively high packing density, the discontinuous dilute phase is formed of gas pockets ascending through the continuous phase. The continuous phase has a density equal to that of the bed in the pre-fluidized state. The ascending gas pockets transport a certain amount of particles to the second layer of the bed. Circulation of the particles takes place, the particles moving downward pass along the wall of the bed.

Instead of the term gas bubbles for the discontinuous phase as used by Toomey and Johnstone, Wicke and Hedden [4] prefer the term cavity, since in fact no phase boundary is present. The cavity is a gas pocket which grows at its top and shrinks at its bottom and thereby moves through the bed. The gas pocket will therefore have an ellipsoid form, with the long axis in the direction of flow. The movement of the gas pockets through the bed is very irregular as has been shown by Matheson, Herbst and Holt [5]. The same authors have found that the increase of the dimension of the gas pocket changes linearly with the height in the pre-fluidized bed.

Interesting work has been done by Yasui and Johanson [6] on the determination of the size characteristics of such gas pockets or cavities. It was found by these authors that the length of the pocket in the direction of flow increased with particle size, with the distance above the bed support and with the gas velocity. This growth with increasing height above the bed support is mainly caused by coalescence of gas pockets, accompanied by a decrease in gas pocket frequency.

In the fluidized bed of the first layer now two gas streams may be distinguished, a gas stream consisting of rising gas pockets and a gas stream through the continuous phase.

From the above, it follows that the point porosity in a certain fixed place in the bed is never constant; at a certain time the porosity is equal to that of the pre-fluidized bed and shows the lowest value possible, some time later a gas pocket passes the point considered; the porosity will then approach its maximum value = 1. Intermediate porosities will occur at other moments. These changing porosities are not easy to handle, therefore in the work to be described an average value has always been taken by integration over the time. Such a time average porosity appeared to be constant under constant fluidization conditions. This measured average porosity is determined by the frequency of the gas pockets at the point chosen, with the restriction that the frequency and/or sizes of the gas pockets is not such that overlapping occurs.

If the time average porosity is assumed to be constant over the diameter of the fluidized bed – an assumption which is close to reality if the influence of the wall can be neglected, for fluidization in which the gas velocity is uniform over the chamber — the question arises as to which porosity distribution can be expected in the direction of flow.

If the superficial gas velocity is V, a gas volume $G_v = A\ V^*$ passes through the bed per unit of time. This gas volume as said consists of two parts, the amount of gas necessary to maintain the continuous phase, G_{mf}, and the amount forming the gas pockets (G_b). The amount G_{mf} is equal to the gas volume necessary for minimum fluidization and equals $V_{mf}\ A'$ in which A' is the cross-sectional area of the tube, not taken up by the gas pockets. This picture shows as

*See nomenclature

a consequence that an amount of particles corresponding to the volume of the gas pockets present in the bed up to the height L_{mf} and of the concentration in the pre-fluidized state, is present in the second layer of the bed above the height L_{mf}.

The density ρ of the continuous phase in the first layer is determined by

$$\rho_c = \rho_s (1 - \epsilon_{mf}) \tag{1}$$

if ρ_f is neglected as compared with ρ_c; ϵ_{mf} in the porosity at minimum fluidization velocity.

Trawinski [7] has derived the same type of equation for the viscosity:

$$\eta_c^* = c' (1 - \epsilon_{mf}) \tag{2}$$

in which c' is a constant with the dimension of a viscosity.

According to Matheson *et al.* [5] the velocity of the gas pocket will increase upon its rise through the bed, due to the growth of the pocket. It will be assumed that the mean gas pocket velocity V_b is proportional to d_b^2, $(\rho_c - \rho_f)$ and η^{-1} [7].

The mean residence time t_b of a gas pocket in the pre-fluidized bed is

$$t_b = \frac{L_{mf}}{V_b} \tag{3}$$

The total volume of gas pockets in the first layer of the fluidized bed (from the bed support to the height L_{mf}) is then given by

$$\mathrm{Vol}_b = G_b \,.\, t_b = G_b \,.\, \frac{L_{mf}}{V_f}$$

Since $G = G_b + G_{mf}$, therefore $VA = G_b + V_{mf} \,.\, A'$ and $A - A' = G_b / V_b$, it follows that:

$$\mathrm{Vol}_b = \frac{A (V - V_{mf}) \,.\, L_{mf}}{V_b - V_{mf}} \tag{4}$$

As said an amount of particles corresponding to this volume must therefore be present above the pre-fluidized bed height L_{mf}.

The porosity of a mixture of solids and gas is defined by

$$\epsilon = \frac{\text{Volume of gas}}{\text{Volume of gas and solids}},$$

therefore: $$\epsilon = 1 - \frac{M}{L.A.\rho_s} \tag{5}$$

in which M = mass of the fluidized bed, L = bed height. Thus for the pre-fluidized bed:

$$\epsilon_{mf} = 1 - \frac{M}{L_{mf} \,.\, A \,.\, \rho_s} \tag{6}$$

The volume of the solid particles in the bed above the height L_{mf}, Vol_{s_1}, according to equation (4) is:

$$\mathrm{Vol}_{s_1} = \frac{(1 - \epsilon_{mf}) \, A \, (V - V_{mf}) \,.\, L_{mf}}{(V_b - V_{mf})}$$

The volume of the particles in the bed from bed support to L_{mf}, Vol_{s_2} is:

$$\mathrm{Vol}_{s_2} = \frac{M}{\rho_s} - \frac{A \,.\, (V \,.\, V_{mf})}{(V_b - V_{mf})} L_{mf} (1 - \epsilon_{mf}).$$

The average porosity ϵ_d of the bed from bed support to L_{mf} will be given by:

$$\epsilon_d = 1 - \frac{M}{L_{mf} \, A \, \rho_s} + \frac{(V - V_{mf})}{(V_b - V_{mf})} (1 - \epsilon_{mf}) \tag{7}$$

or also by substituting (6) into (7):

$$\epsilon_d = \epsilon_{mf} + \frac{(V - V_{mf})}{(V_b - V_{mf})} (1 - \epsilon_{mf}) \tag{8}$$

The variables in this equation are V and V_b, because ϵ_{mf} and V_{mf} are defined by the system and conditions chosen.

For a constant bed weight and particle size, equation (8) simplifies to:

$$\epsilon_d = \epsilon_{mf} + C'' (V - V_{mf}) \tag{9}$$

For a constant fluidization velocity and particle size assuming $V_b :: d_b^2$ (see above) and $d_b :: M$ (according to Matheson [5] and Yasui and Johanson [6]):

$$\epsilon_d = \epsilon_{mf} + \frac{C'''}{C'''' \,.\, M^2 - V_{mf}} \tag{10}$$

The constant porosity ϵ_d from the bed support to the prefluidized bed height L_{mf} only occurs for points in the bed where restoration of the original situation after passing of a gas pocket can take place. Irregular behaviour can therefore be expected near the wall and near the bed support. Near the wall, because of a decreasing gas velocity, a decrease, near the bed support an increase in porosity are to be expected and have indeed been found. The question as to which height in the

bed the influence of the bed support will be felt, cannot be answered in advance.

The particles in the bed above the pre-fluidized bed height L_{mf} have been thrown up by action of the gas pockets. The number of particles thrown up is a function of the number of particles around the gas pocket and of the size of the gas pocket. The height to which a particle will be thrown up depends on three factors:

(1) The velocity of the gas pocket at the height L_{mf}.

(2) The geometrical location of the particles on the gas pocket; a particle on top of the gas pocket will receive a larger impulse than a particle on the side of a gas pocket.

(3) The number and type of collisions between the particles in the region above L_{mf}, relative for example for co-current and counter-current moving particles.

The distribution of the number of particles and therefore the relation between the density $(1 - \epsilon)$ in this region and the height above L_{mf} will be given by a probability function:

$$(1 - \epsilon) = C_1 \exp\left[- C_2 (h - L_{mf})^{C_3}\right] \qquad (11)$$

For $h = L_{mf}$, ϵ should be equal to ϵ_d, therefore:

$$(1 - \epsilon) = (1 - \epsilon_d) \exp\left[- C_2 (h - L_{mf})^{C_3}\right] \qquad (12)$$

In the theoretical considerations as given above no influence of the wall of the bed has been incorporated. In general this will be permitted for columns with large bed diameters. In the experiments to be described a rather small bed has been used, influence of the wall will therefore occur. A number of authors [3, 4, 5, 8, 9, 10, 11, 12, 13] have observed the downward stream of particles along the wall of the fluidized bed, at the bed support these particles are taken by the gas stream and carried upwards in the bed. Porosity differences between wall and centre will therefore undoubtedly exist. Fluidization variables such as fluidization velocity, mass of the bed and particle size will greatly influence the porosity distribution in the dense phase (under L_{mf}) and in the dilute phase (above L_{mf}).

At high velocities no sharp distinction between dilute and dense phase will exist.

Experimental Results

The experiments on the porosity distribution in a fluidized bed have been carried out with glass beads of various sizes and with air as the fluidizing medium in a metal tube of 9 cm diameter; the bed support consisted of an electrolytically made nickel gause with circular openings of approximately 80 μ diameter. To approach a

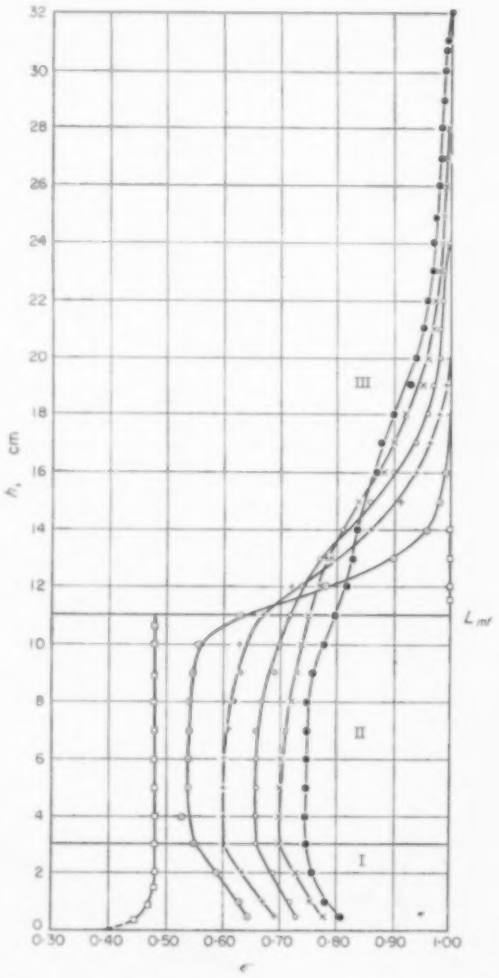

Fig. 1. Porosity as a function of height in the fluidized bed at various velocities (centre of the bed).
$M = 1{,}000$ g
$d_p = 175 - 210\ \mu$
○ 22·7 cm/sec
+ 40·7 cm/sec
○ 59·6 cm/sec
× 78·8 cm/sec
● 98·4 cm/sec
□ incipient fluidization (8·1 cm/sec)

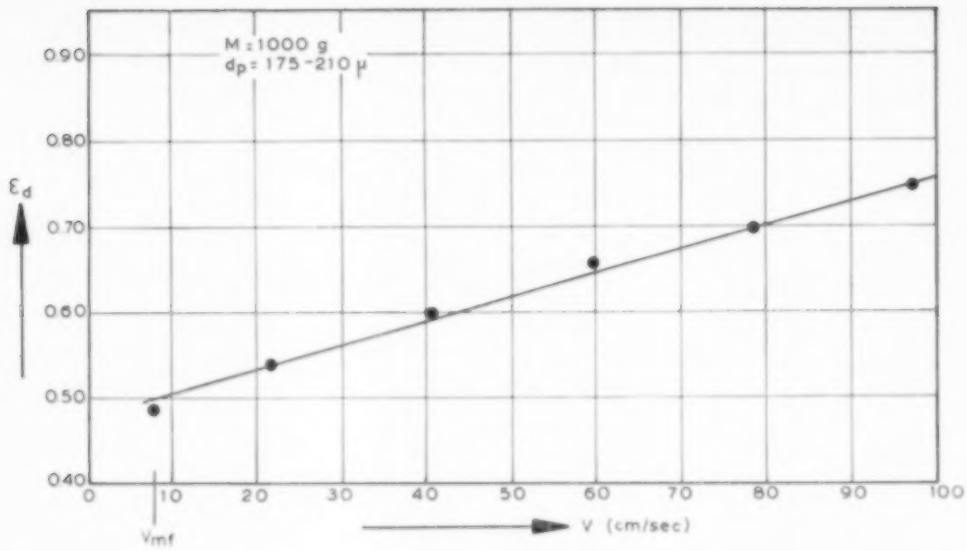

Fig. 2. ϵ_d as a function of fluidization velocity.

good, that is uniform, velocity profile the incoming air passed a layer of Raschig rings under the bed support. A small condenser with a volume of approximately 1 cm³ connected to a rigid nickel tube could be placed in the bed at any place wanted. Full details of the apparatus have been given elsewhere [1, 14]. The capacity of the condenser was measured with a capacitive displacement meter, the resulting variable signal was integrated and by means of a calibration line [2], the mean porosity of the volume of the bed contained in the condenser could be measured.

The method chosen necessitated the introduction of an alien body into the fluidized bed. It is quite conceivable that this would create disturbances in the general flow pattern. It has, however, been found by integrating the $(\epsilon - h)$ curves that the mean porosity value obtained in this way differed in the mean less than ± 4 (maximum 8) per cent from the calculated porosity based on the height of the bed.

The results obtained will be given mainly in graphical form in the next Figures.

For a bed weight of 1000 g porosity measurements in the centre of the column have been carried out with fluidization velocities, varying from the incipient fluidization velocity (8·1 cm/sec for particle size 175–210 μ) to 98·4 cm/sec. The results are given in Fig. 1. The form of the lines obtained indicate the existence in the centre of the bed of three zones. In the first zone, which will be called the sieve effect zone (I) the porosity diminishes with increase of height in the bed. This is probably due to the lifting effect of the air stream entering the bed, as has been said before. Zone II is characterized by a constant porosity (ϵ_d). Between zones II and III a transition zone is found. In zone III the porosity increases gradually to unity. For increasing velocities the $(h - \epsilon)$ line in zone II and in zone I moves to the $\epsilon = 1$ axis. From Fig. 1 it can be seen that the transition of zone II into zone III approximately occurs at the bed height L_{mf}. The $(\epsilon - h)$ line for incipient fluidization for zone I differs from the others in this sense that ϵ decreases near the sieve. This is probably caused by a compression of the pre-fluidized bed near the sieve by the condenser.

The porosity ϵ_d has been plotted in Fig. 2 as a function of the fluidization velocity.

In agreement with the theoretical considerations (equation 9) a linear relationship exists. At incipient fluidization velocity the porosity of the bed should be equal to ϵ_{mf}, the porosity of loosest

packing possible. For a monodisperse system of glass beads, this should be the cubical packing with a porosity $\epsilon_{mf} = 0{\cdot}476$, which is remarkably close to the value of 0·48 as read from Fig. 2. It has to be observed, however, that the system is not monodisperse, which creates a difficulty as to the actual minimum fluidization velocity as well as to the value of ϵ_{mf}. Moreover, vibrations which are almost always present will disturb the type of packing.

Zone I does not allow for much discussion, clearly, the type of sieve used and an entrance effect caused by the change in packing have a large influence on the form of the lines and height of the zone.

A discussion of zone III will follow later on.

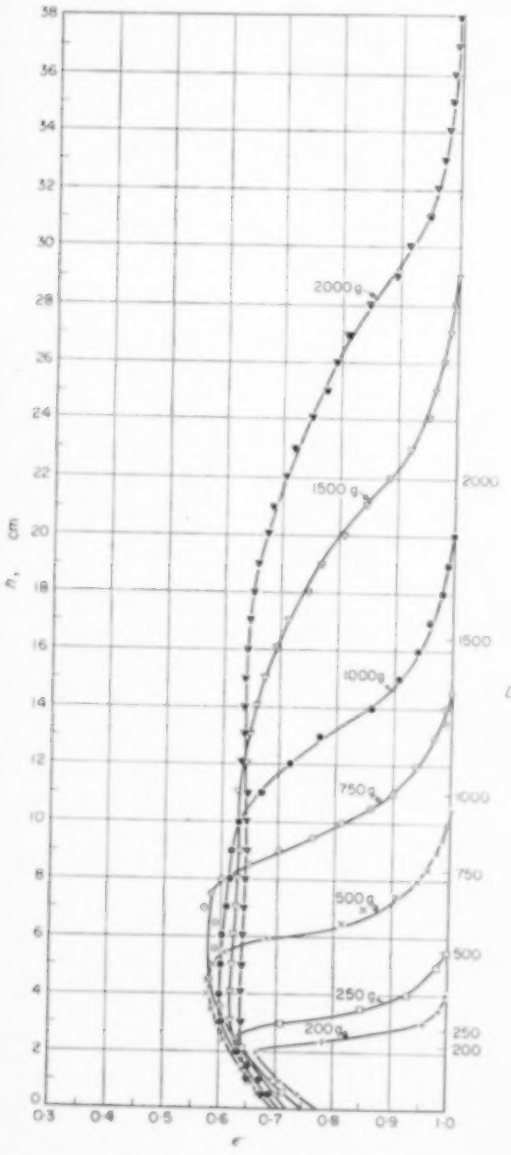

Fig. 3. The influence of the bed mass on the porosity distribution in the centre of a fluidized bed.
$d_p = 175 - 210\ \mu$ $V = 40{\cdot}7$ cm/sec

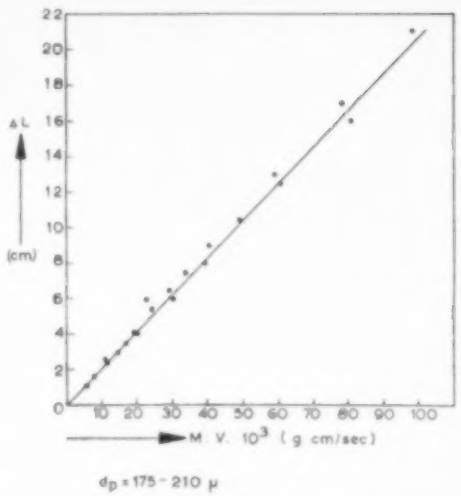

Fig. 4. ΔL as a function of bed weight × fluidization velocity.
$d_p = 175 - 210\ \mu$

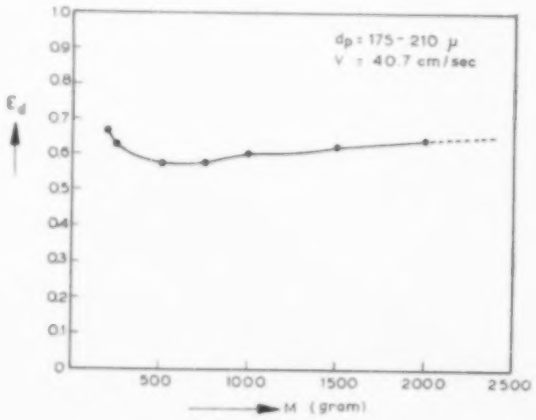

Fig. 5. ϵ_d as a function of bed mass.

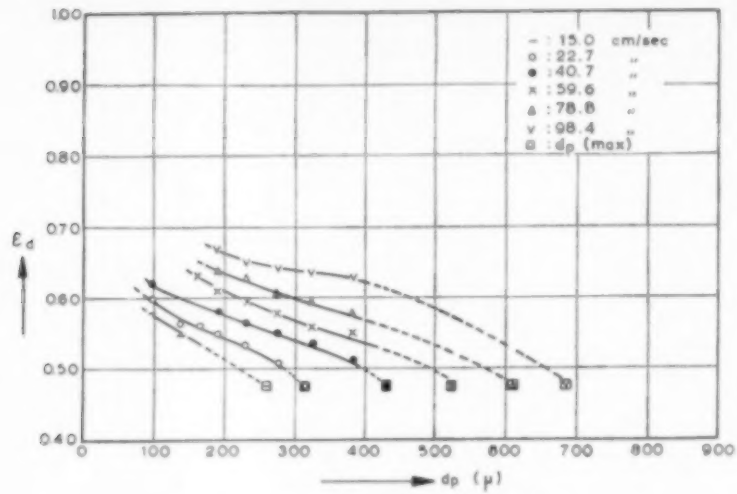

Fig. 6. ϵ_d as a function of particle size.

In another series of experiments the influence of the bed weight on the porosity distribution has been investigated. Results for bed weights varying from 200 and 2000 g at a constant fluidization velocity and again in the centre of the bed have been presented in Fig. 3. It can be concluded that no essential change in form and type of the lines occur at variations of the bed weight. The height of the zone II increases with increasing bed weight. For small bed weights (200 and 250 g) zone II disappears, only a transition point between zone I and III remains. The transition zone of II into III however, increases in importance.

From Fig. 4 it can be seen that the bed expansion $\Delta L = L - L_{mf}$ follows a linear relationship with the product of bed weight times fluidization velocity.

A rather small influence of the bed weight on the porosity ϵ_d (or ϵ of the transition point) exists, as follows from Fig. 5. If the assumptions giving equation (10) are valid the value of ϵ_d for large bed weights should approach $\epsilon_{mf} = 0{\cdot}476$. This, however, is not the case, e.g. due to slugging effects at larger bed weights the curve shows a minimum, whilst the value of $\epsilon = 0{\cdot}476$ is not reached.

A third variable, the particle size d_p, has also been incorporated in the experiments. For a constant bed weight (500 g) experiments with particles of different size have been carried out

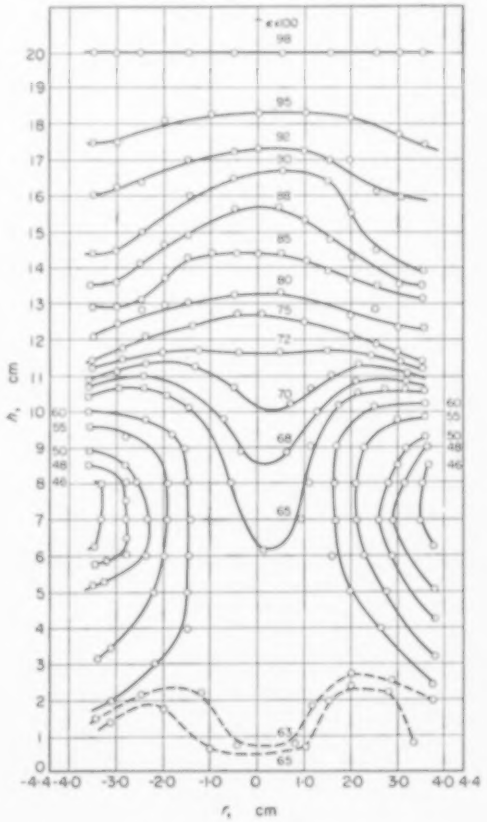

Fig. 7. Isopore-diagram.
$M = 1{,}000$ g $V = 59{\cdot}6$ cm/sec
$d_p = 175 - 210\ \mu$

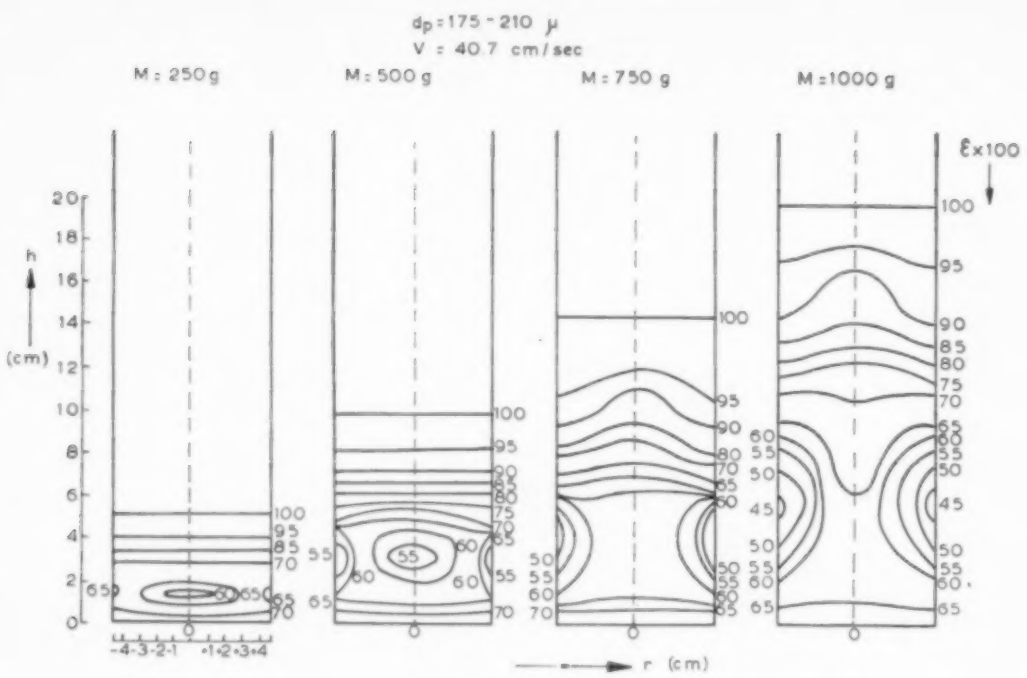

FIG. 8. The influence of the bed mass on the isopore diagrams.

at various fluidization velocities. These are presented in Fig. 6, where ϵ_d is plotted against d_p. The term d_p (max) from Fig. 6 refers to the maximum particle size, for which incipient fluidization exists at the fluidization velocity used.

So far, only measurements in the centre part of the fluidization column have been presented. The porosities out of the centre of the column are different from those in the centre. A radial uniform porosity distribution in the bed has been found. Therefore only the porosity distribution in a plane through the axis of the bed has to be measured. The results will be presented in the form of isopore diagrams, in which, in a plane though the axis, lines are shown connecting points of equal porosities. Such lines have been named *isopores*. An example of such an isopore diagram is presented in Fig. 7. From the isopore diagram streaming patterns in a fluidized bed can be deduced (see [1]). The presence of zones in the bed beneath L_{mf} near the wall of relatively high density indicates the existence of a whirl in the dense part of the bed. Variation of the fluidization velocity does not change the general form of the isopore diagram; the influence of the bed weight, however, is notable. This can be seen in Fig. 8, where for a constant fluidization velocity the schematized isopores are given for bed weights varying from 250 to 1,000 g. It can be concluded that for large bed weights the porosity at the wall decreases. For small bed weights two whirl-like motions occur instead of one at larger bed weights.

Besides with glass pearls some experiments have been carried out with silica gel of 5·5 per cent water content. Fig. 9 shows some measurements for various bed weights; the type of diagram is the same as has been found for glass spheres.

Finally the results as obtained for zone III (see Fig. 1) have been analysed. The values of the constants C_2 and C_3 from equation (12) have been determined by trial and error in such a way that for each line a C_3 value has been established for which the value of C_2 was constant for each point of the line. The values of $C_1 = (1 - \epsilon_d)$ derived from Fig. 2 and of C_2 and C_3 as determined are

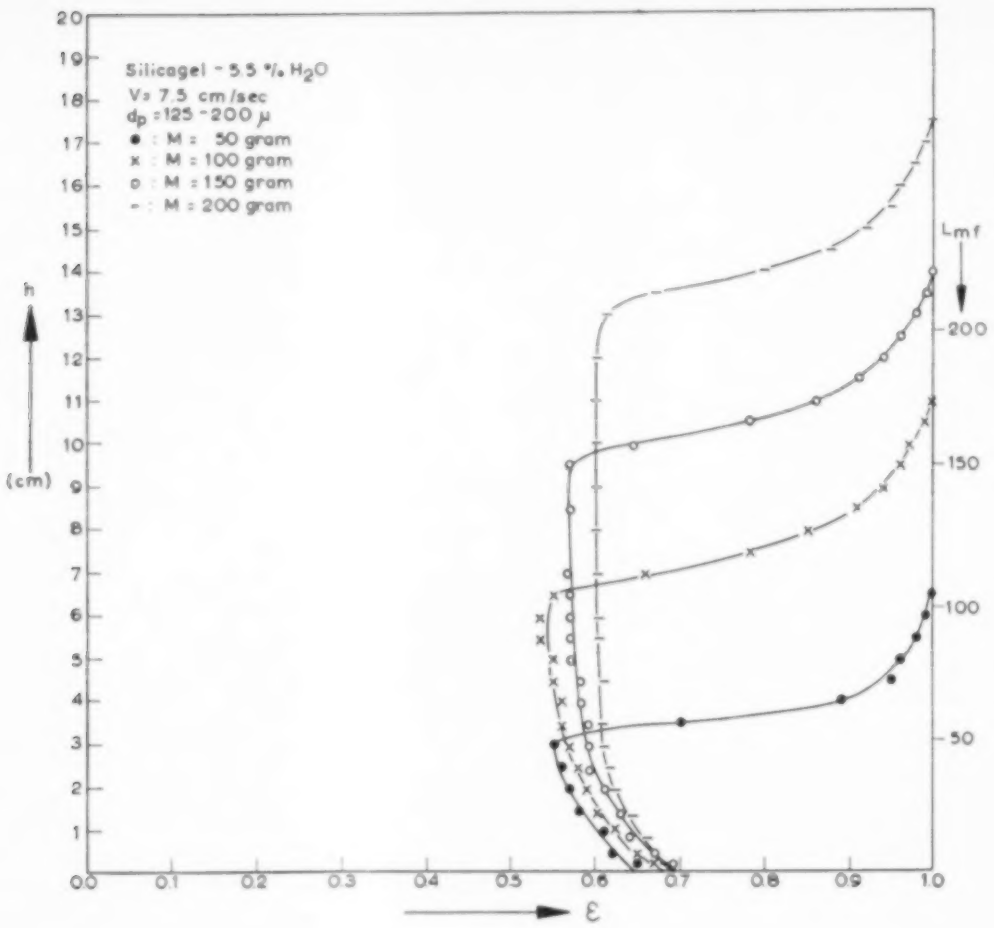

Fig. 9. Experiments with silica.

given in Table 1 for the 6 different velocities of fluidization for a bed of 1,000 g with particles of 175–210 μ.

It can be noted that C_3 is constant and that besides ϵ_d apparently also C_2 is a function of the fluidization velocity V. In the region concerned

Table 1

V (cm/sec)	$C_1 = 1 - \epsilon_d$	C_2	C_3
8·1	0·525	—	—
22·7	0·46	0·59	1·3
40·7	0·40	0·24	1·3
59·6	0·34	0·15	1·3
78·8	0·30	0·11	1·3
98·4	0·25	0·08	1·3

Table 2

M (g)	$C_1 = 1 - \epsilon_d$	C_2	C_3
200	0·33	2·0	1·3
250	0·37	1·4	1·3
500	0·42	0·61	1·3
750	0·42	0·38	1·3
1000	0·40	0·24	1·3
1500	0·37	0·14	1·3
2000	0·36	0·10	1·3

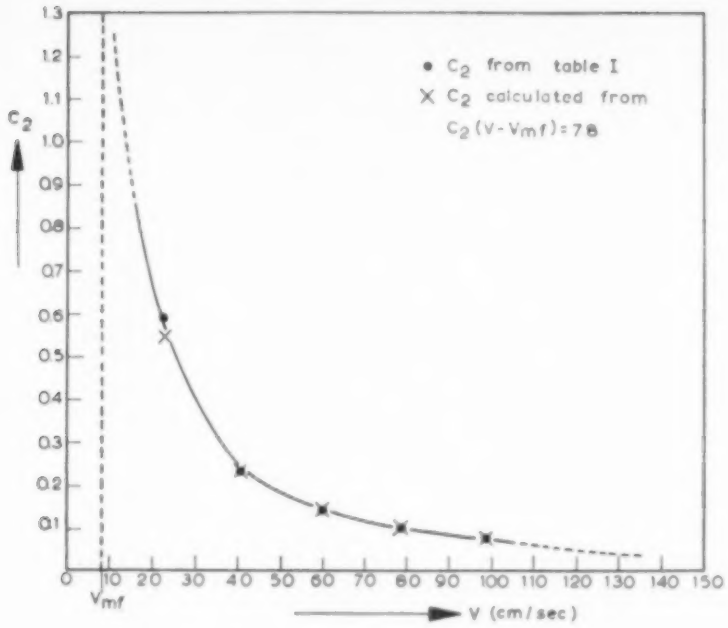

FIG. 10. C_2 as a function of fluidization velocity.

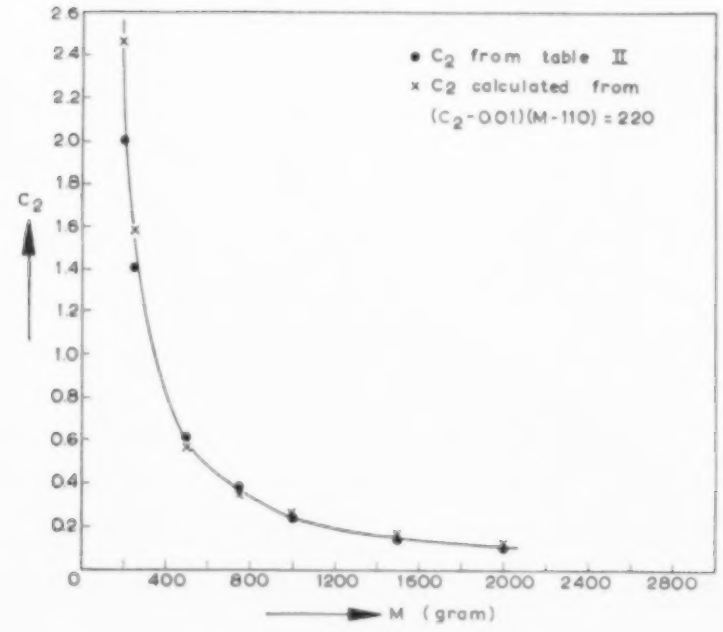

FIG. 11. C_2 as a function of bed mass.

and for a bed weight of 1,000 g of particles of 175–210 μ the relation between C_2 and V can be expressed by the equation $(V - V_{mf}) \times C_2 = 7{\cdot}8$ (see Fig. 10).

In the same way the influence of the bed weight has been analysed, as presented for the same particles and a velocity of 40·7 cm/sec in Fig. 3. Table 2 gives the results.

Again C_3 is a constant and equal to the value found before, C_2 in analogy is a function of M. The relation between C_2 and M in approximation is given by:

$$(C_2 - 0{\cdot}01)\,(M - 110) = 202 \text{ (see Fig. 11).}$$

The same procedure can be applied to the influence of the particle size d_p. The results are given in Table 3. Again C_3 is a constant and C_2 depends on d_p.

Table 3

d_p (μ)	$C_1 = 1 - \epsilon_d$	C_2	C_3
90–105	0·375	0·37	1·3
175–210	0·42	0·61	1·3
210–250	0·44	0·74	1·3
250–300	0·45	0·90	1·3
300–350	0·46	1·28	1·3
350–420	0·48	1·90	1·3

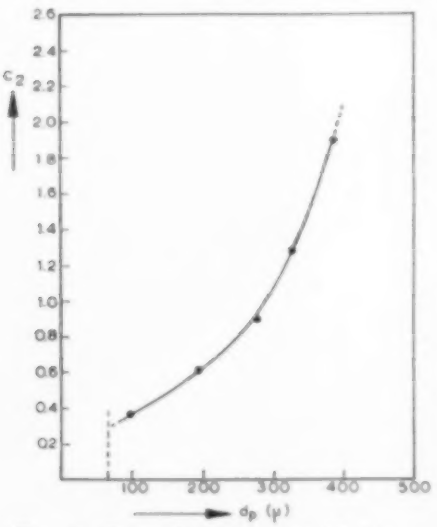

Fig. 12. C_2 as a function of particle size.

The relation between C_2 and d_{p_2} can be represented by the equation $(C_2 - 0{\cdot}3) = 1500\,(d_p - d_{p_{min}})$, which in $d_{p_{min}}$ is the size of the particle just not pneumatically transported under the conditions used (see Fig. 12).

Conclusions

From the experimental results as given it can be concluded that the porosity of a fluidized bed is not constant and the porosity distribution is not simple. However, a remarkably regular behaviour has been found for the time average values of the porosity. The equations as developed are covered rather nicely by the experiments. Rather large variations in fluidization velocity and bed weight do not affect the general pattern of the porosity distribution to a great extent. Even the disappearance of the zone of constant porosity at small bed weights does not influence the validity of the equations developed.

It can be expected that an increase in bed diameter will diminish the influence of the wall on the phenomena as presented. The porosity distributions as given in the centre of the bed will in this case be valid for practically the whole bed.

Notation

A	= cross-sectional area of the fluidized bed	cm^2
A'	= part of cross-sectional area of the fluidized bed	cm^2
c'	= constant	g/cm sec
C'''	= constant	
C''''	= constant	
C'''''	= constant	
C_1	= $(1 - \epsilon_d)$	no dimension
C_2	= constant	
C_3	= constant	no dimension
d_b	= characteristic diameter of gas pocket	cm
d_p	= diameter of particle	cm
G_b	= volume of gas pockets per unit time	cm^3/sec
G_{mf}	= volume of gas for minimum fluidization, per unit time	cm^3/sec
G_v	= total volume of gas passing the fluidized bed, per unit time	cm^3/sec
h	= height in the fluidization column	cm
L	= total height of the fluidized bed	cm
L_{mf}	= total height of the fluidized bed at incipient fluidization	cm
M	= bed weight	g
t_b	= mean residence time of gas pocket in the bed	sec
V	= fluidization velocity	cm/sec

V_b = mean velocity of gas pocket in the fluidized bed — cm/sec
V_{mf} = minimum fluidization velocity — cm/sec
Vol_b = total volume of gas pockets in the fluidized bed — cm^3
Vol_{s1} = volume of solid particles in the bed above the height L_{mf} — cm^3
Vol_{s2} = volume of solid particles in the bed from bed support to L_{mf} — cm^3
ϵ = porosity of the fluidized bed — no dimension
ϵ_d = porosity of the fluidized bed in zone II — no dimension
ϵ_{mf} = porosity of the fluidized bed at incipient fluidization — no dimension
ρ_c = density of the continuous phase — $\mathrm{g/cm}^3$
ρ_f = density of the fluidizing gas — $\mathrm{g/cm}^3$
ρ_s = density of the particles — $\mathrm{g/cm}^3$
η_c = viscosity of the continuous phase — g/cm sec
η_f = viscosity of the fluidizing gas — g/cm sec
ΔL = bed expansion — cm

References

[1] Bakker P. J. and Heertjes P. M. *Brit. Chem. Engng.* 1958 **3** 240.

[2] Bakker P. J. and Heertjes P. M. *Brit. Chem. Engng.* 1959 **4** 524.

[3] Toomey R. D. and Johnstone H. F. *Chem. Engng. Progr.* 1952 **48** 220.

[4] Wicke E. and Hedden K. *Chem.-Ing.-Tech.* 1952 **24** 82.

[5] Matheson G. L., Herbst W. A. and Holt P. H. *Industr. Engng. Chem.* 1949 **41** 1099.

[6] Yasui G. and Johanson L. N. *Amer. Inst. Chem. Engrs. J.* 1958 **4** 445.

[7] Trawinski H. *Chem.-Ing.-Tech.* 1953 **25** 229.

[8] Kettenring K. N., Manderfield E. L. and Smith J. M. *Chem. Engng. Progr.* 1950 **46** 139.

[9] Gilliland, E. R. and Mason E. A. *Industr. Engng. Chem.* 1953 **45** 1177.

[10] van Heerden C. *J. Appl. Chem.* (*Lond.*) 1952 **2** 87.

[11] Miller C. O. and Logwinuk A. K. *Industr. Engng. Chem.* 1951 **43** 1220.

[12] Parent J. D., Yagol N. and Steiner C. S. *Chem. Engng. Progr.* 1947 **43** 429.

[13] Dow W. M. and Jakob M. *Chem. Engng. Progr.* 1951 **47** 637.

[14] Bakker P. J. Thesis, Delft 1958.

VOL. 12 1960

Chemical Engineering Science, 1960, Vol. 12, pp. 272 to 278. Pergamon Press Ltd., London. Printed in Great Britain

The transient response of a distillation column to changes in feed composition

R. M. Wood* and W. D. Armstrong

Department of Chemical Engineering,
Pembroke Street, Cambridge

(*Received* 1 *January* 1960; *in revised form* 18 *January* 1960)

Abstract—Wilkinson and Armstrong [1] have derived an expression which predicts the response of plate compositions in a distillation column to step changes in feed composition. This theory is valid up to moderate values of time but cannot be used to predict the changes in composition when the column approaches the new state of equilibrium. Following the same approach it is possible to derive considerably simpler expressions which are valid for the initial part of the response. These solutions can then be extended so as to give the way in which the column approaches equilibrium. The theory is compared with experimental results obtained from a pilot distillation column [6].

Résumé—Wilkinson et Armstrong [1] ont établi une expression qui prévoit la réponse des compositions du plateau dans une colonne à distiller pour une variation par stades dans la compositions du plateau dans une colonne à distiller pour une variation par stades dans la composition de l'alimentation. Cette théorie est valable jusqu'aux valeurs modérées du temps mais ne peut être utilisée pour prévoir les variations dans la composition quand la colonne tend vers le nouvel état d'équilibre. En attaquant le problème de la même façon il est possible d'établir des expressions excessivement simples qui sont valables pour la partie initiale de la réponse. Ces solutions peuvent être étendues de façon à indiquer la manière dont la colonne tend vers l'équilibre. La théorie est comparée avec les résultats expérimentaux obtenus à partir d'une colonne de distillation pilote.

Zusammenfassung—Wilkinson und Armstrong [1] haben einen Ausdruck abgeleitet, der die Antwortfunktion der Flüssigkeitszusammensetzung auf dem Boedn einer Destillationskolonne angibt für eine sprunghafte Aenderung der Zulaufzusammensetzung. Diese Theorie ist bis zu nicht zu grossen Werten der Zeit gültig, sie kann aber nicht benutzt werden, um die Aenderung der Zusammensetzung vorauszusagen, wenn die Kolonne sich dem neuen Gleichgewichtszustand nähert. Nach derselben Methode kann man einfachere Ausdrücke ableiten,die für den Anfangsteil der Antwort gültig sind. Diese Lösungen können entsprechend dem Weg der Annäherung der Kolonne an den Gleichgewichtszustand erweitert werden. Die Theorie wurde mit experimentellen Ergebnissen aus einer Technikums-Destillationskolonne verglichen.

Introduction

This paper is an extension of the work of Wilkinson and Armstrong [1] for predicting the transient behaviour of a plate type distillation column to changes in feed composition. The same theoretical model is considered and the theoretical basis of some of the steps taken in the present work may be found in their paper.

Theoretical Treatment

A material balance over plate n in the enriching section of the column shown in Fig. 1, following a step change in feed composition Δx_F gives

$$L_E(\delta x_{n-1} - \delta x_n) + V(\delta y_{n+1} - \delta y_n) = H\frac{\partial \delta x_n}{\partial t} \quad (1)$$

where H is the molar plate hold-up, and δx_n is the displacement of the composition of the liquid on plate n from equilibrium conditions.

From the definition of the Murphree plate efficiency based on liquid phase compositions $E = (x_n - x_{n-1})/(x_n^* - x_{n-1})$ and assuming that

*Present address: Department of Chemical Engineering, University College, Swansea.

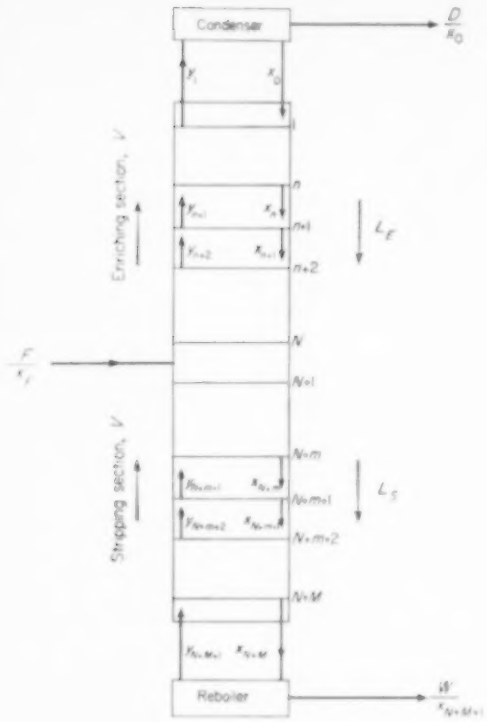

FIG. 1. The column.

the equilibrium data for the enriching section may be represented by $y_n = \alpha_E x_n^* + \beta_E$ it may be shown that

$$\delta y_n = \frac{\alpha_E}{E}\left[\delta x_n - (1 - E)\,\delta x_{n-1}\right] \qquad (2)$$

Substituting (2) into (1) and transforming the equation by the Laplace transform gives

$$X_{n-1} - (1 + S_E + p)\,X_n + S_E X_{n+1} = 0 \qquad (3)$$

where

$$S_E = \frac{\alpha_E V}{E L_E + \alpha_E V (1 - E)}$$

and the non-dimensional time

$$T = \frac{\alpha_E V (1 - E) + E L_E}{EH}\, t\,.$$

Following WILKINSON and ARMSTRONG [1] and reducing the finite difference equation (3) to a differential equation by Taylor's theorem, the general solution of X_n is

$$X_n = A \exp nu_1 + B \exp nu_2 \quad 0 \leqslant n \leqslant N \qquad (4)$$

where

$$u_{1,2} = -\frac{(S_E - 1)}{S_E + 1} \pm \pm \sqrt{\left[\left(\frac{S_E - 1}{S_E + 1}\right)^2 + \frac{2p}{1 + S_E}\right]} \qquad (5)$$

Similarly by considering a material balance over plate $(N + m)$ in the stripping section of the column it may be shown that

$$X_{N+m} = C \exp\left[(N + m)v_1\right] + D \exp\left[(N + m)v_2\right] \quad 1 \leqslant m \leqslant M + 1 \qquad (6)$$

where

$$v_{1,2} = -\frac{(S_S - 1)}{S_S + 1} \pm \pm \sqrt{\left[\left(\frac{S_S - 1}{S_S + 1}\right)^2 + \frac{2\alpha_E S_S p}{\alpha_S S_E (1 + S_S)}\right]} \qquad (7)$$

$$S_S = \frac{\alpha_S V}{E L_S + \alpha_S V (1 - E)}$$

and α_S is the slope of the equilibrium line for the stripping section.

The boundary conditions requred to determine the functions A, B, C and D are:

(*i*) *Condenser*

Neglecting the condenser hold-up the boundary condition at the top of the column is

$$X_0 = \alpha_E' X_1 \quad \text{where} \quad \alpha_E' = \frac{\alpha_E}{E + \alpha_E (1 - E)}.$$

Taking the first two terms of the Taylor expansion for X_1 gives

$$\left(\frac{dX_n}{dn}\right)_{n=0} = \frac{(1 - \alpha_E')}{\alpha_E'} X_0 \qquad (8)$$

Substituting (4) into (8)

$$A = B\,\frac{\{-u_2 - [(\alpha_E' - 1)/\alpha_E']\}}{u_1 + [(\alpha_E' - 1)/\alpha_E']} \qquad (9)$$

From (5) and (9) it may be seen that A and B are of the same order of magnitude, for the special case $S_E = \alpha_E' = 1$, $A = B$.

(*ii*) *Reboiler*

Similarly by taking material balance over the reboiler, the boundary condition at the base of the column may be shown to be

$$\left(\frac{dX_{N+m}}{d(N+m)}\right)_{m=M+1} = \frac{E(1-\alpha_S)S_S}{\alpha_S} \cdot X_{N+M+1} - \frac{pw\,\alpha_E S_S}{\alpha_S S_E} \cdot X_{N+M+1} \quad (10)$$

where w is the ratio of the reboiler hold-up to the plate hold-up. Substituting (6) into (10)

$$D\exp(N+M+1)(v_2-v_1) = -C\frac{(pw\alpha_E S_S/\alpha_S S_E)+E[(\alpha_S-1)S_S/\alpha_S]+v_1}{(pw\alpha_E S_S/\alpha_S S_E)+E[(\alpha_S-1)S_S/\alpha_S]+v_2} \quad (11)$$

From the definition of v_1 and v_2 in (7) it may be seen that

$$C < \left| D\exp -2(N+M+1)\sqrt{\left[\left(\frac{1-S_S}{1+S_S}\right)^2 + \frac{2\alpha_E S_S p}{\alpha_S S_E(1+S_S)}\right]}\right| \quad (12)$$

(*iii*) *Plate N*

From a material balance over plate N in the unsteady state

$$L_E\,\delta x_{N-1} + V\delta y_{N+1} - L_E\delta x_N - V\delta y_N = H\frac{\partial\delta x_N}{\partial t} \quad (13)$$

putting $n = N$ in 1 and subtracting this equation from (13) gives

$$\delta y_{N+1} = \delta y^+_{N+1} \quad (14)$$

The superscript denotes that δy^+_{N+1} is the change in vapour composition which would occur if plate $(N+1)$ were in the enriching section of the column.

Substituting for δy^+_{N+1} from (2) and for δy_{N+1} from the corresponding equation for the stripping section into (14)

$$\alpha_S[\delta x_{N+1} - (1-E)\delta x^+_N] = \alpha_E[\delta x^+_{N+1} - (1-E)\,\delta x_N] \quad (15)$$

Transforming (15) and substituting (4) and (6) into the resulting equation

$$\begin{aligned}\alpha_S\{&C\exp[(N+1)v_1] + D\exp[(N+1)v_2] - (1-E)[C\exp(Nv_1) + D\exp(Nv_2)]\} = \\ \alpha_E\{&A\exp[(N+1)u_1] + B\exp[(N+1)u_2] - (1-E)[A\exp(Nu_1) + B\exp(Nu_2)]\}\end{aligned} \quad (16)$$

From the definition of $v_{1,2}$ (7) and (12), it may be seen that the left hand side of (16) consists of terms proportional to

$$\exp -(N+1)\sqrt{\left[\left(\frac{1-S_S}{1+S_S}\right)^2 + \frac{2\alpha_E S_S p}{\alpha_S S_E(1+S_S)}\right]} \quad \text{and to}$$

$$\exp -(N+2M+1)\sqrt{\left[\left(\frac{1-S_S}{1+S_S}\right)^2 + \frac{2\alpha_E S_S p}{\alpha_S S_E(1+S_S)}\right]}.$$

In expressions of this type the Laplace operator p appears to have the same effect as an ordinary variable which lies along the range $\infty \leqslant p \geqslant 0$ as $0 \leqslant T \leqslant \infty$. Thus it may be seen that for the initial part of the response, i.e. p apparently large, the C terms in (16) are small compared with those containing D and may be neglected. Similarly from (9) it can be shown that the B terms in (16) are also negligible and the equation simplifies to

$$\alpha_S D\{\exp[(N+1)v_2] - (1-E)\exp(Nv_2)\} = \alpha_E A\{\exp[(N+1)u_1] - (1-E)\exp(Nu_1)\} \quad (17)$$

(*iv*) *Plate* $(N+1)$

Similarly by considering a material balance over plate $(N+1)$ in the unsteady state

$$L_E A\exp(Nu_1) - L_S D\exp(Nv_2) + F\Delta x_F/p = 0 \quad (18)$$

Solving for A and D from (17) and (18) and hence determining B and C from (9) and (11) and substituting these values into equations (4) and (6) gives

VOL. 12 1960

$$\frac{\alpha_E L_S X_n}{\alpha_S F \Delta x_F} = \frac{[\exp(v_2) - (1-E)]\exp[-(N+1)u_1]}{p\{1-(1-E)[1-(\alpha_S L_E/\alpha_E L_S)]\exp(-u_1) - (\alpha_S L_E/\alpha_E L_S)\exp(v_2-u_1)\}} \times$$

$$\times \left\{\exp(nu_1) - \frac{[u_1 + (\alpha_E' - 1)/\alpha_E']\exp nu_2}{u_2 + (\alpha_E' - 1)/\alpha_E'}\right\} \qquad (19)$$

$$\frac{L_S X_{N+m}}{F \Delta x_F} = \frac{1-(1-E)\exp(-u_1)}{p\{1-(1-E)[1-(\alpha_S L_E/\alpha_E L_S)]\exp(-u_1) - (\alpha_S L_E/\alpha_E L_S)\exp(v_2-u_1)\}} \times$$

$$\times \left\{\exp(mv_2) - \frac{(p w \alpha_E S_S/\alpha_S S_E) + [E(\alpha_S - 1)S_S/\alpha_S] + v_2}{(p w \alpha_E S_S/\alpha_S S_E) + [E(\alpha_S - 1)S_S/\alpha_S] + v_1} \times \exp[(M+1)v_2 - (M+1-m)v_1]\right\} \qquad (20)$$

Following WILKINSON and ARMSTRONG and using the pseudo-equilibrium line [2] the corresponding equations are

$$\frac{'\alpha_E L_S X_n}{'\alpha_S F \Delta x_F} = \frac{\exp[-(N+1)u_1 + v_2]}{p[1-('\alpha_S L_E/'\alpha_E L_S)\exp(v_2-u_1)]}\left\{\exp(nu_1) - \frac{u_1 + [('\alpha_E - 1)/'\alpha_E]}{u_2 + [('\alpha_E - 1)/'\alpha_E]}\exp(nu_2)\right\} \qquad (21)$$

and

$$\frac{L_S X_{N+m}}{F \Delta x_F} = \frac{1}{p[1-('\alpha_S L_E/'\alpha_E L_S)\exp(v_2-u_1)]} \times$$

$$\left\{\exp(mv_2) - \frac{(p w L_E/L_S) + [('\alpha_S - 1)V/L_S] + v_2}{(p w L_E/L_S) + [('\alpha_S - 1)V/L_S] + v_1}\exp[(M+1)v_2 - (M+1-m)v_1]\right\} \qquad (22)$$

where

$$'\alpha_E = \frac{\alpha_E}{E + (\alpha_E V/L_E)(1-E)}$$

and

$$'\alpha_S = \frac{\alpha_S}{E + (\alpha_S V/L_S)(1-E)}$$

are the slopes of the pseudo-equilibrium lines and the non-dimensional time $= L_E t/H$. The expressions for $u_{1,2}$ are identical for both cases, but using the pseudo-equilibrium lines

$$v_{1,2} = \frac{-(S_S - 1)}{(S_S + 1)} \pm \pm\sqrt{\left[\left(\frac{S_S - 1}{S_S + 1}\right)^2 + \frac{2L_E p}{L_S(1+S_S)}\right]}$$

(contrast equation 7)

when the plate efficiency is unity the two pairs of expressions are identical.

In order to transform X_n and X_{N+m} back into the time domain it is necessary to invert functions of the form

$$\frac{1}{p}\exp - \left\{r\sqrt{\left[p + \frac{(S_E-1)^2}{2(1+S_E)}\right]} + s\sqrt{\left[p + \frac{(S_E-1)^2 \alpha_S S_E}{2(1+S_S)\alpha_E S_S}\right]}\right\}.$$

In order to simplify the inversion of X_n and X_{N+m} it was assumed that for the initial part of the response $p \gg (1-S_E)^2/2(1+S_E)$. This would appear to be valid for columns operating at fairly high reflux ratios and has been justified elsewhere [3]. Hence $u_{1,2}$ and $v_{1,2}$ simplify to

$$u_{1,2} = \frac{-(S_E - 1)}{S_E + 1} \pm \sqrt{\left(\frac{2p}{1+S_E}\right)}$$

and

$$v_{1,2} = \frac{-(S_S - 1)}{S_S + 1} \pm \sqrt{\left[\frac{2\alpha_E S_S p}{\alpha_S S_E (1+S_S)}\right]}$$

With this approximation the inversion of (19) and (20) becomes fairly straightforward and is effected by expanding

$$\frac{1}{1-(1-E)[1-(\alpha_S L_E/\alpha_E L_S)]\exp(-u_1) - (\alpha_S L_E/\alpha_E L_S)\exp(v_2-u_1)}$$

by the binomial theorem and inverting the expression term by term. (All the relevant Laplace transforms may be found in Carslaw and Jaeger [4]).

Extension of the theory to bigger values of time

For the transient response of a single enriching section to a step change in feed composition, it has been shown [5] that the solution is

$$\delta x_n(T) = \delta x_n(T = \infty) + \sum_{i=1}^{I} J_{ni} \exp p_i T \qquad (23)$$

It is thought that for the complete column the response would have a similar form. For the approach to equilibrium (23) may be written as

$$1 - \frac{\delta x_n(T)}{\delta x_n(T = \infty)} = \frac{-J_{n1}}{\delta x_n(T = \infty)} \exp p_1 T$$

or $$\log_e\left[1 - F_n(T)\right] = \log_e\left[\frac{-J_{n1}}{\delta x_n(T = \infty)}\right] + p_1 T$$

$F_n(T)$ is the fractional approach to equilibrium. Hence from the calculated steady state change in plate composition the response may be extended to larger values of time.

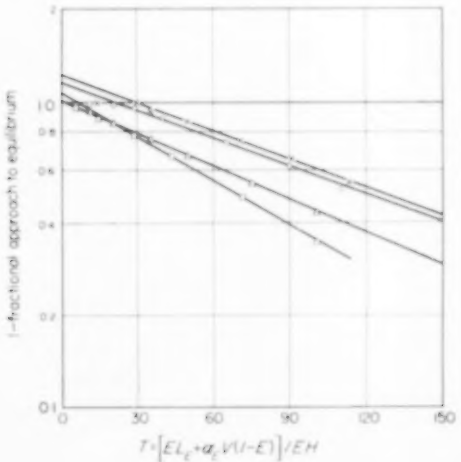

Fig. 2. Theoretical response of the top product and plate 8 to a step change in feed composition.
× □ Using pseudo-equilibrium line for plates 0 and 8
○ △ Using E directly for plates 0 and 8

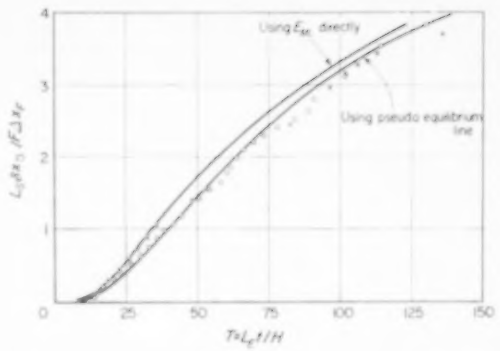

Fig. 3. Response of the top product composition to a step change in feed composition.
—— Theoretical Wilkinson ○ run F.T.P.1.
× run F.T.P. 2.

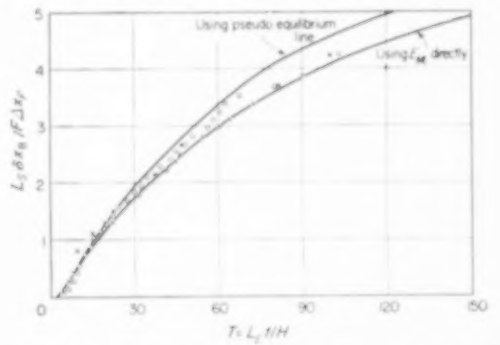

Fig. 4. Response of the composition of plate 8 to a step change in feed composition.
—— Theoretical Wilkinson × run F14·1
○ run F14·2.

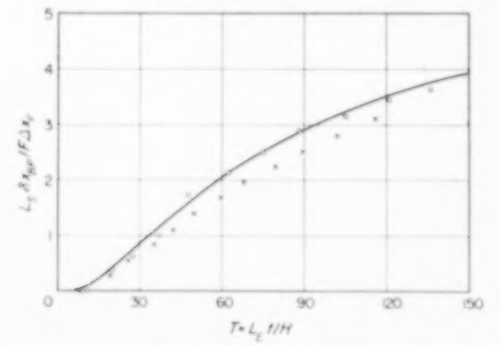

Fig. 5. Response of the bottom product composition to a step change in feed composition.
—— Theoretical Wilkinson ○ run F.B.P.1
× run F.B.P.2.

Comparison of theory and experiment

The experimental results of Wilkinson [6] were obtained at conditions which approximate closely to those required for comparison with the present theory.

For the top product and plate 8, (19) was evaluated up to $T = 100$. The theoretical results were then plotted as $[1 - F_n(T)]$ against T on semilog paper (Fig. 2). Good straight lines could be drawn through the points and therefore it was possible to extend the curves to larger values of time. The theoretical curves are plotted with the results of Wilkinson on Figs. 3 and 4. Similarly (21) derived using the pseudo-equilibrium lines was evaluated for the top product and plate 8, and is also plotted on Figs. 3 and 4.

As an example of the use of the equations for a plate in the lower half of the column, (20) was evaluated for the initial part of the response and may be compared with the experimental results in Fig. 5.

Discussion

The agreement between theory and experiment is within 20 per cent, which is thought to be reasonable when account is taken of the many approximations made in the theoretical derivation. The agreement between the curves obtained using the pseudo-equilibrium lines and plate efficiency directly is also within 20 per cent and thus perhaps the increased labour required to evaluate (19) compared with (21) is hardly justified under these operating conditions. At lower values of the plate efficiency the divergence is likely to be greater and the more accurate solution might then be warranted.

The values obtained for the first decay constant p_1 for the top and bottom products and for plate 8 are $-0{\cdot}0071$, $-0{\cdot}0083$ and $-0{\cdot}0083$ reciprocal units of non-dimensional time. These values are quite close and give added justification for the method used to extend the solution as the column approaches equilibrium.

Conclusions

Theoretical expressions have been derived for the response of a distillation column to changes in feed composition. These expressions have been derived both by using the pseudo-equilibrium lines and by using the plate efficiency directly. The theory agreed with the experimental results of Wilkinson to within 20 per cent which is also the maximum divergence between the two theoretical expressions.

Notation

α = slope of equilibrium line

$'\alpha$ = slope of pseudo-equilibrium line

$$\alpha_E' = \frac{\alpha_E}{\alpha_E(1 - E) + E}$$

$$\alpha_S' = \frac{\alpha_S V + E(L_S - V)}{EL_S + \alpha_S V(1 - E)}$$

β = constant in the equation of the vapour–liquid equilibrium line $y = \alpha x^* + \beta$

m = plate number stripping section

n = plate number enriching section

p = Laplace operator

r = a constant

s = a constant

t = time following a disturbance — min

$u_{1,2}$ = defined by (5)

$v_{1,2}$ = defined by (7)

w = ratio of the reboiler hold-up to plate hold-up

x = mole fraction of the more volatile component in the liquid

y = mole fraction of the more volatile component in the vapour

A, B, C, D = functions in equations (4) and (6)

E = Murphree plate efficiency (liquid)

F = molar feed rate — mole/min

$F(T)$ = fractional approach to equilibrium

H = plate liquid hold-up — mole

I = number of roots

J = exponential multipliers

L = liquid flow rate — mole/min

M = number of plates in the stripping section

N = number of plates in the enriching section

$$S = \frac{\alpha V}{\alpha V(1 - E) + EL}$$

T = non-dimensional time $\dfrac{EL_E + \alpha_E V(1 - E)}{EH} \cdot t$

V = vapour flow rate — mole/min

X = Laplace transform of δx

Subscripts

i = general term

m = plate number stripping section

n = plate number enriching section

E = enriching section

F = feed

S = stripping section

References

[1] Wilkinson W. L. and Armstrong W. D. *Chem. Engng. Sci.* 1957 **7** 1.

[2] Wilkinson W. L. and Armstrong W. D. *Plant and process Dynamic Characteristics* p. 56. Butterworths, London 1957.

[3] Wood R. M., Ph.D. Thesis p. 98. University of Cambridge 1959.

[4] Carslaw H. S. and Jaeger J. C. *Conduction of Heat in Solids* (2nd Ed.) p. 494. Oxford University Press 1959.

[5] Marshall W. R. and Pigford R. L. *The Application of Differential Equations to Chemical Engineering Problems* (2nd printing) p. 152. University, of Delaware 1948.

[6] Wilkinson W. L., Ph.D. Thesis, p. 124. University of Cambridge 1956.

VOL.
12
1960

Chemical Engineering Science, 1960, Vol. 12, pp. 279 to 287. Pergamon Press Ltd., London. Printed in Great Britain

On the response of stagewise processes to stationary randomly-fluctuating inputs

A. Acrivos
Department of Chemical Engineering, University of California, Berkeley

(*Received* 27 *December* 1959 ; *in revised form* 20 *January* 1960)

Abstract—This theoretical paper deals with the response of stagewise processes to stationary randomly-fluctuating inputs with Gaussian probability distributions. It is shown how the problem may be formulated mathematically and solved in a manner believed to be more straightforward than the techniques presently used in control theory. Exact solutions are obtained for linear systems and two asymptotic series are developed for cases where the fluctuations are either slow or rapid. By means of these expressions, which involve only simple algebraic operations, it is possible to calculate without too much difficulty the probability that certain critical variables in the system will exceed a prespecified range of values.

Résumé—Cet article de la réponse des systèmes étagés à des signaux stationnaires présentant des variations aléatoires suivant une loi de distribution gaussienne de la probabilité. Il montre comment le problème peut être exprimé sous forme mathématique et résolu de façon à obtenir une estimation de la réponse de manière plus directe que par les méthodes actuellement utilisées en théorie du contrôle. Il indique les solutions exactes obtenues pour des systèmes linéaires et donne deux développements en séries asymtotique pour le cas de variations lentes ou rapides respectivement. Au moyen de ces expressions, qui ne comportent que de simples opérations algébriques, il est possible de calculer sans grande difficulté la probabilité pour que certaines variables critiques du système dépassent des valeurs fixées à l'avance.

Zusammenfassung—Diese theoretische Arbeit behandelt die Antwortfunktion von stufenweisen Prozessen auf stationäre, zufällig schwankende Eingangsfunktionen mit Gaus'schen Wahrscheinlichkeitsverteilungen. Es wird gezeigt, wie man das Problem mathematisch formulieren und wie man es zielstrebiger lösen kann, als mit den gegenwärtig benutzten Mitteln der Theorie der Regeltechnik. Für lineare Systeme werden exakte Lösungen erhalten und für Fälle, bei denen die Schwankungen entweder langsam oder schnell sind, werden zwei asymptotische Reihen entwickelt. Mit Hilfe dieser Ausdrücke, die nur einfache algebraische Operationen erfordern, ist es möglich, ohne zu grosse Schwierigkeiten die Wahrscheinlichkeit zu berechnen, mit der bestimmte kritische Variable im System einen vorgegebenen Bereich überschreiten.

Introduction

The response of stagewise processes to changes in the input variables has received an increasing amount of attention in the last few years, for it is being realized that systems designed solely on the basis of their steady state performance may possess undesirable transient characteristics and may therefore be difficult to control. In particular, since it is usually highly advantageous for the product of a given process to be of essentially uniform quality, the operating system including the controller must be so designed that the characteristic properties of the products should not be allowed to vary outside prespecified, and sometimes quite narrow, band limits. Thus, for example, it is known that in many polymerization reactions the reaction temperature may have a profound influence not only on the quality but sometimes even on the nature of the product, and it is for this reason that in such processes the the temperature cannot be permitted to vary more than a few degrees from its desired value.

Such problems are of course quite common in many of the more important stagewise processes in chemical engineering – stirred tank reactors, distillation columns, extraction units, etc. to mention but a few – and it is clear therefore that before one can attach a suitable control system to an operating unit one must be in a position to predict how the process will respond

to input disturbances which are known or expected to occur. Such upsets are of two rather general types: they either take place in some orderly fashion and may therefore be represented by well-behaved mathematical functions of time, or they occur in a purely random manner which is describable only in a statistical sense. So far, the majority of papers on this subject which have appeared in chemical engineering literature [1, 2, 3] have studied transient phenomena of the first type with sinusoidal or step functions as input disturbances. In many practical situations, however, the input fluctuations are of a completely different nature, for they occur in an unpredictable and random manner.

The theoretical analysis to be presented below will deal precisely with this problem of how a stagewise system will be expected to respond to such randomly fluctuating input conditions. Mathematically, the problem is by no means new. Its importance was recognized some time ago by electrical engineers, and a commonly employed method of solution can be found in many of the standard texts on control theory [4, 5, 6]. On the other hand, the applicability of these established tools of analysis to stagewise systems of particular interest to chemical engineers was not demonstrated until quite recently by Katz [7] and by Aris and Amundson [8]. It turns out, however, that due to the considerable complexity of the typical chemical engineering stagewise process and therefore of the mathematical model which describes its behaviour, the usual procedure for attacking this rather involved problem becomes quite cumbersome.

The present study was therefore motivated by the desire to devise a formal mathematical development which would be somewhat more straightforward and easy to manipulate than the techniques presently used in control theory and, as a consequence, suitable for handling stagewise systems with a large number of components.

The Mathematical Model for Linear Systems and Its Formal Solution

It has already been established [1, 8, 9] that, for small perturbations about the steady state, the transient behaviour of any stagewise system is governed mathematically by the matrix equation

$$\frac{dx}{dt} + Az = z \tag{1}$$

where the column vector $x = \{x_i\}$ has as its components the characteristic variables of the stagewise process measured from their corresponding steady state values. In a system of stirred-tank reactors, for example, these variables would represent in general the temperatures, concentrations and flow-rate variations in the different interconnected units. On the other hand, the elements z_i of the column with $z = \{z_i\}$ are directly related to the different input fluctuations which cause the system to depart from the desired steady state, while the components a_{ij} of the constant matrix $A = \{a_{ij}\}$ may as a rule be calculated without difficulty from the steady state solution of the appropriate algebraic equations which characterize the process [9].

If now z were a known function of time, then the response of the system to such a disturbance could easily be obtained from the general solution of equation (1). If, however, as we shall suppose from now on, the elements of z_i are all stationary random functions which may be described in a statistical sense only, then the problem at hand is indeed quite different in nature from the usual transient phenomenon of control theory. This follows from the fact that what a theoretical analysis is supposed to yield in such a case is not the instantaneous value of each component x_i in the system (which is clearly impossible since z cannot be completely specified in the usual sense) but the probability that one or more of the variables x_i will lie outside predetermined critical limits. Thus, for example, if it were known that the reaction temperature in a given process should not be permitted to exceed a certain upper limit or fall below a specified value lest undesirable side products be formed, then it would indeed be of considerable interest to the control engineer to be able to predict the probability of such an event occurring.

To simplify the development we shall suppose next that all the elements z_i of the column vector z are normally distributed with zero mean, as is

usually the case to a first approximation at least. It then follows [5] that the elements of x are also Guassian. Therefore, the probability distribution of all the elements x_i, and in particular the probability that they would lie outside set limits, could readily be calculated by the standard techniques of statistics if the variance of each x_i were determined. Thus the main objective of our analysis will be to show how these variances may be derived from equation (1).

Before proceeding with our solution however we find it advantageous to introduce here the square correlation matrix $\boldsymbol{Z} = \{z_{ij}(h)\}$ the elements of which are defined by

$$z_{ij}(h) \equiv \overline{z_i(t)\, z_j(t+h)} \tag{2}$$

where the average may be taken either with respect to time, or, in view of the ergodic hypothesis, in the probability space. We see then that $z_{ij}(h)$ is the familiar cross-correlation function [4, 5] between the two random variables z_i and z_j which, in the absence of any periodicity in the fluctuations, vanishes as $h \to \pm \infty$ [4]. This correlation matrix is a function of h only and not of time, if, as we shall suppose, we are dealing only with stationary random disturbances, the mean properties of which in a statistical sense are time independent. We shall further suppose that $\boldsymbol{Z}(h)$ is already known since it is related to the uncontrolled input upsets which cause the system to fluctuate.

Let us next postmultiply each term in equation (1), which is evaluated at time t, by the *row* vector $z_T = \{z_i(t+h)\}$. Upon averaging we can show that the modified equation (1), may be transformed into

$$-\frac{d\boldsymbol{\Phi}}{dh} + \boldsymbol{A}\boldsymbol{\Phi} = \boldsymbol{Z}(h) \tag{3}$$

where:

$$\left.\begin{aligned} &\boldsymbol{\Phi} = \{\phi_{ij}\}, \\ &\phi_{ij}(h) = \overline{x_i(t)\, z_j(t+h)}, \text{ and} \\ &\overline{z_j(t+h)\frac{dx_i}{dt}} = \lim_{\Delta t \to 0} \frac{\overline{z_j(t+h)\, x_i(t+\Delta t) - z_j(t+h)\, x_i(t)}}{\Delta t} = -\frac{d\phi_{ij}}{dh} \end{aligned}\right\} \tag{4}$$

The solution to equation (3) subject to the boundary conditions

$$\boldsymbol{\Phi} = 0 \text{ for } h \to \pm \infty \tag{5}$$

is

$$\boldsymbol{\Phi} = \exp \boldsymbol{A}h \int_h^\infty \exp(-\boldsymbol{A}\tau)\, \boldsymbol{Z}(\tau)\, d\tau \tag{6}$$

This may be verified by direct substitution. Furthermore, since the process is assumed to be stable about its average steady state, the characteristic roots of $\boldsymbol{A}$ must have positive real parts [9] and thus, as required by equation (5), it is indeed true that

$$\lim_{h \to -\infty} \exp \boldsymbol{A}h = 0$$

On the other hand, if the *transpose* of equation (1)

$$\frac{dx_T}{dt} + x_T \boldsymbol{A}_T = z_T \tag{7}$$

which is evaluated at time $(t+h)$ is *premultiplied* through by $x(t)$, and then averaged, it may be reduced into

$$\frac{d\boldsymbol{X}}{dh} + \boldsymbol{X}\boldsymbol{A}_T = \boldsymbol{\Phi} \tag{8}$$

where

$$\boldsymbol{X} \equiv \{\overline{x_i(t)\, x_j(t+h)}\} \tag{9}$$

will be recognized as the correlation matrix of the process output variables. Therefore, if again $\boldsymbol{X} = 0$ as $h \to \infty$,

$$\boldsymbol{X} = \left[\int_{-\infty}^{h} \boldsymbol{\Phi}(\tau) \exp(\boldsymbol{A}_T \tau)\, d\tau\right] \exp(-\boldsymbol{A}_T h) \tag{10}$$

and, in view of equation (6),

$$X = \left\{ \int_{-\infty}^{0} \exp(A\tau) \left[\int_{\tau}^{\infty} \exp(-Ay)\, Z(y)\, dy \right] \exp(A_T \tau)\, d\tau \right\} \exp(-A_T h) \tag{11}$$

Finally, if, as is usually the case, one is interested only in the variance of the individual fluctuations x_i, then one need only to compute the diagonal elements of the matrix X_0, which is obtained from equation (11) by setting $h = 0$. Thus

$$\boxed{X_0 = \int_{-\infty}^{0} \exp - A\tau \left[\int_{\tau}^{\infty} \exp(-Ay)\, Z(y)\, dy \right] \exp(A_T \tau)\, d\tau} \tag{12}$$

Mathematical Simplifications of the Formal Solution

It has been established in the preceding section that the formal solution of our linear problem may be given by the rather impressive looking equation (12). It can be shown of course that, as expected, equation (12) is equivalent to the result that is obtained by the more standard techniques, yet it is felt that not only is our derivation more straightforward but that the form of the solution is more suitable for numerical computations especially for complicated systems with large order matrices. The reason for this is that equation (12), which involves products of matrices only, is in general quite amenable to mathematical manipulations especially under those conditions where, as we shall show, useful simplifications may be carried out.

In general, the exact numerical evaluation of equation (12) is a rather formidable task. We shall therefore devote a considerable portion of the remaining part of this paper to examining ways in which we could simplify the rather involved mathematical expressions and thereby lighten any numerical work. To accomplish this in a straightforward manner we must first examine the integral

$$\int_{\tau}^{\infty} \exp(-Ay)\, Z(y)\, dy \tag{13}$$

which appears in equation (12). We note first of all that according to Sylvester's theorem [10], the matrix exponential function may be expanded in the form

$$\exp(-Ay) = \sum_{k=1}^{n} \exp(-\lambda_k y)\, U_k \tag{14}$$

where n is the order of the matrix, λ_k its characteristic roots, assumed distinct and, in view of the postulated stability of our system, with positive real parts, and U_k are the idempotent matrices of A [10]. Therefore,

$$\int_{\tau}^{\infty} \exp(-Ay)\, Z(y)\, dy = \sum_{k=1}^{n} U_k \int_{\tau}^{\infty} \exp(-\lambda_k y)\, Z(y)\, dy \tag{15}$$

This equation is clearly of very limited usefulness for computational purposes, since it is well known how difficult it is in general to evaluate numerically the characteristic roots and the idempotent matrices of A. It will become apparent, however, that equation (15) is indeed quite valuable, from a theoretical standpoint, since it will allow us to derive and to justify the approximations which follow.

Let us then consider the typical element z_{ij} of the square matrix Z. Since $z_{ij}(h)$ is the cross-correlation function of the two random variables z_i and z_j, it has the general shape shown in Fig. 1. In particular, we define the two positive characteristic parameters h_{ij} and θ_{ij} by the following two relations:

$$|z_{ij}(h)| \leqslant \epsilon \text{ for all } |h| > h_{ij} \tag{16}$$

and

$$|z_{ij}(h) - z_{ij}(0)| \leqslant \epsilon \text{ for all } |h| \leqslant \theta_{ij} \tag{17}$$

where ϵ is an arbitrary small number (ϵ, for example, may be set equal to 0·1). Furthermore, if λ_1 and λ_n are the characteristic roots of A with, respectively, the minimum and maximum real parts so that

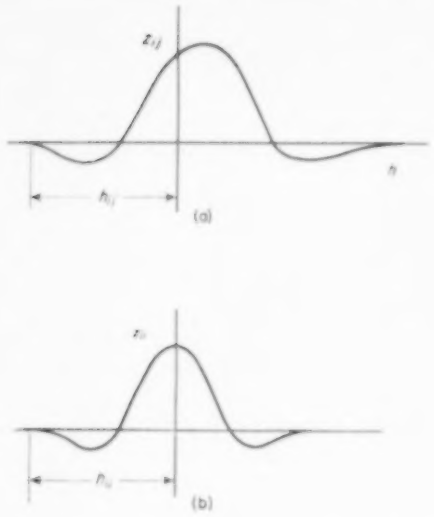

FIG. 1. A plot of (a) typical cross-correlation function and (b) typical auto-correlation function of two random variables.

$$\left.\begin{aligned} R(\lambda_1) &= \min_j R(\lambda_j) \\ \text{and} \qquad R(\lambda_n) &= \max_j R(\lambda_j) \end{aligned}\right\} \tag{18}$$

where the symbol R denotes the real part of a number, then we may segregate the random disturbances into two broad categories according to whether:

$$R(\lambda_1) > \frac{1}{\theta_{ij}} \tag{19}$$

or

$$R(\lambda_n) < \frac{1}{h_{ij}} \tag{19a}$$

We shall show now how equations (12) or (15) may be simplified if either of the above two asymptotic conditions is met.

Case I

If the input fluctuations are such that equation (19) is obeyed approximately by all the elements of the square matrix $\mathbf{Z}$, then the integral given by equation (18) may be calculated conveniently as follows: We first expand $\mathbf{Z}(h)$ into a power series, so that

$$\mathbf{Z}(h) = \mathbf{Z}_0 + h\mathbf{Z}_1 + \frac{h^2}{2'}\mathbf{Z}_2 + \cdots\cdots$$

where the representative kth term of the expansion is given by

$$\mathbf{Z}_k = \left\{\left(\frac{d^k z_{ij}}{dh^k}\right)_{h=0}\right\}$$

It is then easy to verify that

$$\begin{aligned} X_0 = {} & A^{-1}\mathbf{Z}_0 A_T^{-1} + \\ & + \left[A^{-2}\mathbf{Z}_1 A_T^{-1} - A^{-1}\mathbf{Z}_1 A_T^{-2}\right] + \\ & + \left[A^{-3}\mathbf{Z}_2 A_T^{-1} - A^{-2}\mathbf{Z}_2 A_T^{-2} + \right. \\ & \left. + A^{-1}\mathbf{Z}_2 A_T^{-3}\right] + \cdots \end{aligned} \tag{20}$$

an expression which is indeed most convenient for numerical computations on a high speed computer, since it involves only products of matrices. Interestingly enough, though, equation (20) may also be derived by an iterative scheme based on our two fundamental equations (3) and (8). Thus, if to a first approximation we neglect both derivatives in these two equations, we find that

$$\Phi \simeq A^{-1}\mathbf{Z}(h); \quad X \simeq A^{-1}\mathbf{Z}(h)A_T^{-1} \tag{21}$$

and therefore

$$X_0 = A^{-1}\mathbf{Z}_0 A_T^{-1}$$

which is identical to the first term of equation (20). If now the two derivatives are approximated by making use of equation (21), and if the resulting expressions are solved once more one can verify that indeed the first two terms of equation (20) are obtained. This iterative procedure may then be repeated successively to yield equation (20) in its entirety.

We see, therefore, that since the derivative terms in equations (3) and (8) represent in a sense the capacity of the stagewise system and are, as a consequence, related to its ability to dampen out the input fluctuations, the solution given by equation (20) is nothing more than an expansion about the so-called "quasi steady state." That is we first assume that the system can respond instantaneously to the applied disturbance and then correct our mathematical solution by an iterative procedure of successive approximations. Thus we would expect that this series expansion given by equation (20) would converge rapidly,

from a computational standpoint, if the dominant of the input fluctuations were small compared to the equivalent residence time of the stagewise system. It can be shown that this is mathematically equivalent to the inequality given by equation (19), and we shall refer to such disturbances as "slow."

Case II

On the other hand, if the dominant frequencies of the input fluctuations are large compared to the equivalent residence time of the system, and if in particular the input disturbances approach a mathematical idealization known as "white noise" [4, 8], then the "quasi steady state" approximation is clearly unsatisfactory. The series expansion for X_0 given by equation (20) will, therefore, either converge very slowly or will even diverge, so that a different asymptotic solution is needed.

We can now simplify equation (12) by noting that when all the fluctuations are of the above type, the various cross-correlation functions $z_{ij}(h)$ approach zero even for small values of h. Consequently, since $h_{ij} \to 0$ (see Fig. 1), equation (19a) must be satisfied. This then suggests the following expansion of our solution. If we first rearrange equation (12) into

$$X_0 = \int_{-\infty}^{0} \exp(A\tau)\, L \exp(A_T\, \tau)\, d\tau - \int_{-\infty}^{0} \exp(A\tau) \left[\int_{-\infty}^{\tau} \exp(-Ay)\, Z(y)\, dy \right] \exp(A_T\, \tau)\, d\tau$$

we can show that by expanding the exponential functions in the second term,

$$X_0 = \int_{-\infty}^{0} \exp(A\tau)\, L \exp(A_T\, \tau)\, d\tau + \int_{-\infty}^{0} \tau Z(\tau)\, d\tau + \tfrac{1}{2} \left\{ \left(\int_{-\infty}^{0} \tau^2 Z\, d\tau \right) A_T - A \int_{-\infty}^{0} \tau^2 Z\, d\tau \right\} + \ldots \quad (21)$$

where the matrix L is given by

$$L \equiv \int_{-\infty}^{\infty} \exp(-A\tau)\, Z(\tau)\, d\tau \equiv \{l_{ij}\} \quad (22)$$

It is easy to verify now that indeed the convergence of equation (21) is very rapid if $h_{ij} \to 0$ for all the elements $z_{ij}(h)$ of the matrix Z. Furthermore, L itself may be conveniently calculated by the series

$$L = \int_{-\infty}^{\infty} Z(\tau)\, d\tau - A \int_{-\infty}^{\infty} \tau Z(\tau)\, d\tau + \frac{A^2}{2!} \int_{-\infty}^{\infty} \tau^2 Z(\tau)\, d\tau + \ldots . \quad (23)$$

which again will converge quickly if all $h_{ij} \to 0$.

Unfortunately, however, the evaluation of the first term in equation (21) is somewhat involved and must be carried out by an indirect method. It is clear first of all that if the input disturbances belong truly to the type known as "white noise" so that

$$z_{ij}(h) \equiv l_{ij}\, \delta(h)$$

where $\delta(h)$ is the familiar delta function of mathematical physics, the equation (21) would reduce to

$$X_0 = \int_{-\infty}^{0} \exp(A\tau)\, L \exp(A_T\, \tau)\, d\tau$$

We see, therefore, that the first term in equation (21) represents nothing more than the "white noise" approximation to the input fluctuations. In that case, equation (6) may be simplified into

$$\Phi = \exp(Ah)\, L \text{ for } h \leqq 0$$

and as can be verified by direct substitution into equation (8),

$$X = \exp(Ah)\, X^*_0 \text{ for } h \leqq 0$$

where the constant matrix X^*_0 satisfies the algebraic expression

$$\boxed{AX^*_0 + X^*_0 A_T = L} \quad (24)$$

The following is a rather straightforward scheme for obtaining X^*_0: If the transpose of equation (24) is added to equation (24) one can show that

$$A\left[X^*_0 + (X^*_0)_T\right] + \left[X^*_0 + (X^*_0)_T\right] A_T = L + L_T \quad (26)$$

VOL 12 196

We next let

$$A\left[X^*_0 + (X^*_0)_T\right] = (L + L_T) + F \qquad (27)$$

where F is an unknown skew-symmetric matrix of the form

$$F = \begin{pmatrix} 0 & f_{12} & f_{13} & \cdots \\ -f_{12} & 0 & f_{23} & \cdots \\ -f_{13} & -f_{23} & 0 & \cdots \\ \vdots & \vdots & \vdots & \end{pmatrix} \qquad (28)$$

Therefore,

$$X^*_0 + (X^*_0)_T = A^{-1}(L + L_T) + A^{-1}F \qquad (29)$$

The elements of F are finally computed by taking into account the fact that $X^*_0 + (X^*_0)_T$ is symmetric. Thus, by equating the approximate terms in equation (29) we can obtain $\left[n(n-1)/2\right]$ algebraic equations for the unknowns f_{ij}. It should also be noted carefully that since, for reasons explained earlier, one will in general be interested only in the diagonal elements of X^*_0, which are identical to the variances of the output variables, one need not proceed any further once equation (26) has been solved.

It is clear then that equation (21) may be written in the form

$$X_0 = X^*_0 + \int_{-\infty}^{0} \tau Z(\tau)\, d\tau + \\ + \tfrac{1}{2}\left[\left(\int_{-\infty}^{0} \tau^2 Z\, d\tau\right) A_T - A\int_{-\infty}^{0} \tau^2 Z\, d\tau\right] + \cdots . \qquad (30)$$

where X^*_0 is given by equation (24). The computation of this expression is quite straightforward once X^*_0 has been evaluated, for the remaining terms in the series involved only products of matrices. Furthermore, since Z may usually be approximated by a linear combination of simple matrix functions, the integrations in equations (22) and (30) may as a rule be carried out analytically without much difficulty.

The general case

In any actual situation, the input fluctuations will naturally be of both kinds: "slow" and "rapid." In view of the linearity of our basic equations, however, the solution of this more realistic problem may easily be derived. Thus if we let

$$Z \equiv Z_1 + Z_2$$

where all the elements of Z_1 and Z_2 satisfy, approximately, equations (19) and (19a) respectively, then

$$X_0 = X_1 + X_2$$

where X_1 is given by equation (20) with $Z = Z_1$ and X_2 is given by equation (30) with $Z = Z_2$.

Conclusions

In this theoretical analysis we have studied the response of linear stagewise systems to stationary randomly fluctuating inputs with Gaussian probability distributions. A formal mathematical development of the problem was presented which is somewhat more straightforward and easy to manipulate than the techniques presently used in control theory, since it leads to a solution which may be drastically simplified under asymptotic conditions. Thus an expansion about the "quasi steady state" results in equation (20), whereas for "rapid" fluctuations equation (30) is preferable. In general, the essential features of such a transient problem may be clearly brought out by segregating the disturbances into two broad classes, "slow" and "rapid." Then, using the appropriate asymptotic expansion, which were derived in this paper for these two types of fluctuations, the computation of the variances of the critical output variables may be caried out without much difficulty, for it involves only simple algebraic operations suitable for a high speed digital computer.

Appendix

A numerical example

A simple numerical example will serve to illustrate the essence of our theoretical analysis. We shall consider a system which may be represented mathematically by matrix equations which involve only second order matrices, for, as already shown by Aris and Amundson [8], the transient response of a single stirred-tank reactor may be adequately described by precisely such a mathematical model.

Let

$$A = \begin{pmatrix} 2 & 1/3 \\ 1 & 1/2 \end{pmatrix} \text{ and } Z = \exp(-\alpha|h|)\begin{pmatrix} 1 & 0 \\ 0 & 0 \end{pmatrix}$$

where α is a positive parameter. By performing the appropriate calculations we can show that

$$\lambda_1 = 0{\cdot}3035 \qquad \lambda_2 = 2{\cdot}1965$$

$$U_1 = \begin{pmatrix} 0{\cdot}1038 & -0{\cdot}1761 \\ 0{\cdot}5283 & 0{\cdot}8963 \end{pmatrix} \qquad U_2 = \begin{pmatrix} 0{\cdot}8963 & 0{\cdot}1761 \\ 0{\cdot}5283 & 0{\cdot}1038 \end{pmatrix}$$

Equation (12) can now be integrated without difficulty by the use of Sylvester's theorem. One finds that

$$X_0 = \frac{1}{\lambda_1(\lambda_1+\alpha)}\begin{pmatrix} 0{\cdot}01077 & -0{\cdot}05484 \\ -0{\cdot}05484 & 0{\cdot}2791 \end{pmatrix} + \frac{1}{\lambda_1+\lambda_2}\frac{2\alpha+\lambda_1+\lambda_2}{(\lambda_1+\alpha)(\lambda_2+\alpha)}\begin{pmatrix} 0{\cdot}1861 & -0{\cdot}4187 \\ -0{\cdot}4187 & -0{\cdot}5582 \end{pmatrix} + \frac{1}{\lambda_2(\lambda_2+\alpha)}\begin{pmatrix} 0{\cdot}8034 & 0{\cdot}4735 \\ 0{\cdot}4735 & 0{\cdot}2791 \end{pmatrix} \qquad (a)$$

This exact solution has two asymptotic forms depending on whether $\alpha \to 0$ or $\alpha \to \infty$.

Case I. The "quasi steady state" approximation, equation (20), is applicable when $\alpha \to 0$. Thus by neglecting all but the first term in equation (20), we can show that

$$X_0 = \begin{pmatrix} 9/16 & -9/8 \\ -9/8 & 9/4 \end{pmatrix} + O(\alpha) \qquad (b)$$

Case II. Equation (30) must be considered when $\alpha \to \infty$. In particular if only the first term of equations (23) and (30) are taken into account, then

$$X_0 = \frac{1}{\alpha}\begin{pmatrix} 0{\cdot}550 & -0{\cdot}300 \\ -0{\cdot}300 & 0{\cdot}60 \end{pmatrix} + O(1/\alpha^2) \qquad (c)$$

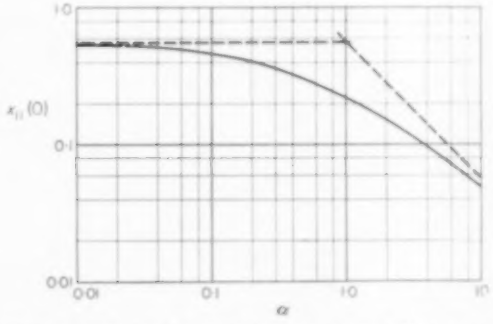

FIG. 2. The variance of the output variable x_1 as a function of α for the numerical example.

$x_{11}(0)$ and $x_{22}(0)$, respectively the variances of the two random output variables x_1 and x_2, are shown in Figs. 2 and 3 as functions of the parameter α, together with their asymptotic forms as given by equations (b) and (c). It is clearly seen that both $x_{11}(0)$ and $x_{22}(0)$ may be adequately described by the leading terms of their asymptotic expansions about $\alpha = 0$ and $\alpha \to \infty$. It is felt, therefore,

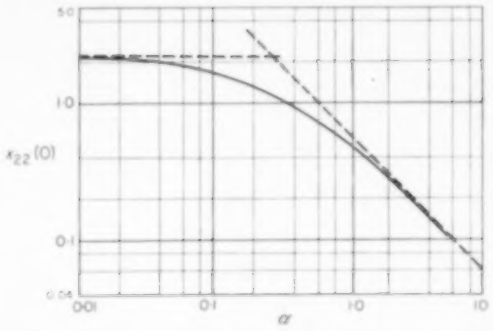

FIG. 3. The variance of the output variable x_2 as a function of α for the numerical example.

that this simple numerical example has served to illustrate our main point of view, namely that for those high order processes for which an exact solution cannot be conveniently obtained, the two asymptotic expansions given by equations (20) and (30) will indeed provide in general an acceptable representation for the main characteristic features of the system.

NOTATION

h = the independent variable in the cross-correlation functions (see equation 2)

$A = \{a_{ij}\}$, a constant square matrix, characteristic of the system (see equation 1)

$x = \{x_i\}$, a column matrix the components of which are the characteristic variables of the system

$z = \{z_i\}$, a column matrix with the fluctuating input variables as its elements

$\overline{z_{ij}(h)} = \overline{z_i(t+h)\,z_j(t)}$, the cross-correlation function of the two random variables z_i and z_j

$Z = \{\overline{z_i(t+h)\,z_j(t)}\}$, the correlation matrix of the inputs

$X = \{\overline{x_i(t)\,x_j(t+h)}\}$, the correlation matrix of the variables of the system

$\Phi = \{\phi_{ij}(h)\}$ where $\phi_{ij} = \overline{x_i(t)\,z_j(t+h)}$

$L = \{l_{ij}\}$, a square matrix defined by equation (22)

λ_k = the characteristic roots of A [10]

U_k = the idempotent matrices of A [10]

n = the order of the matrix A

$\left.\begin{matrix} \theta_{ij} \\ h_{ij} \end{matrix}\right|$ = characteristic parameters of the cross-correlation function $z_{ij}(h)$ (see Fig. 1)

Subscripts

0 = denotes the matrix evaluated at $h = 0$

T = the transpose of a matrix or a column vector

References

[1] Bilous O., Block H. D. and Piret E. L. *Amer. Inst. Chem. Engrs. J.* 1957 **3** 248.

[2] Rose A., Johnson C. L. and Williams T. J. *Industr. Engng. Chem.* 1956 **48** 622.

[3] Williams T. J., Harnett R. A. and Rose A. *Industr. Engng. Chem.* 1956 **48** 1008.

[4] James H. M., Nichols N. B. and Phillips R. S. *Theory of Servomechanisms.* Chap. 6. McGraw-Hill, New York 1947.

[5] Laning J. H. and Battin R. H. *Random Processes in Automatic Control.* Chap. 5. McGraw-Hill, New York 1956.

[6] Truxal J. G. *Automatic Feedback Control System Synthesis.* Chap. 7 and 8. McGraw-Hill, New York 1955.

[7] Katz S., *Chem. Engng. Sci.* 1958 **9** 61.

[8] Aris R. and Amundson N. R. *Chem. Engng. Sci.* 1959 **9** 250.

[9] Acrivos A. *J. Soc. Industr. Appl. Math.* 1956 **4** 1.

[10] Frazer R. A., Duncan W. J. and Collar A. R. *Elementary Matrices.* Cambridge University Press 1952.

VOL.
12
1960

Influence of mass transfer on coalescence of drops

(*Received* 29 *January* 1960)

In recent years increasing interest has been shown in interfacial phemonena during mass transfer between phases. Lewis [1] found that at liquid-liquid interfaces solute transfer may cause severe disturbances. The explanation offered by Sigwart and Nassenstein [2] that these phenomena occur as a result of gradients in the interfacial tension caused by non-uniform mass transfer along the interface seems to be satisfactory.

The above studies have been made by observations of flat interfaces or single drops suspended in a continuous liquid phase. Less attention has been paid to the industrially more important case of the behaviour of swarms of droplets under the influence of mass transfer. Johnson and Bliss [3] as early as 1946 found that in a spray extraction column mass transfer was highest when the solute was transferred from the continuous phase to the droplets. When solute was extracted from the drops much larger drop sizes were observed, a phenomenon that was ascribed to increased coalescing of drops. Pratt and co-workers [4] found that in different types of extraction equipment, droplets were considerably larger if the solute was transferred from the droplets than if transfer was in the opposite direction. As a result, maximum allowable flow rates in these cases were very high. For example, with toluene as the dispersed phase the flooding rate of a rotating disk contactor column is 100–200 per cent higher when acetone is transferred from the droplets to the continuous water phase than when the direction of transfer is reversed or when no solute is present at all [4].

The increased coalescence rate has sometimes been ascribed to droplet oscillation as found in the single drop studies mentioned earlier. It has however been shown in a previous communication that the actual cause of droplet oscillation, viz. the development of interfacial tension gradients is also responsible for the differences in stability of foams in the related field of gas–liquid contacting [5]. The explanation given may be repeated here shortly: when during a mass transfer operation two gas bubbles in a liquid approach each other, the small amount of liquid between the bubbles tends to come into equilibrium with the gas phase very quickly, while along the rest of the bubble area mass transfer is still going on. The compound diffusing from the bubble phase will therefore be present at the highest concentration in the liquid film between the bubbles. When this higher concentration is accompanied by a lower surface tension, liquid is drawn away from the interfacial film (Maragnoni effect) and coalescence is promoted. In the opposite case coalescence is retarded and the gas bubbles are very stable (foaming).

It appears that this explanation also holds for the occurrence of coalescence in liquid–liquid systems. This may be illustrated by considering the system benzene–acetic acid–water. Approximate interfacial tensions for this system are shown in Fig. 1. We assume for example that the benzene phase is dispersed, and that it originally contains 1 per cent of acetic acid. According to Fig. 1,

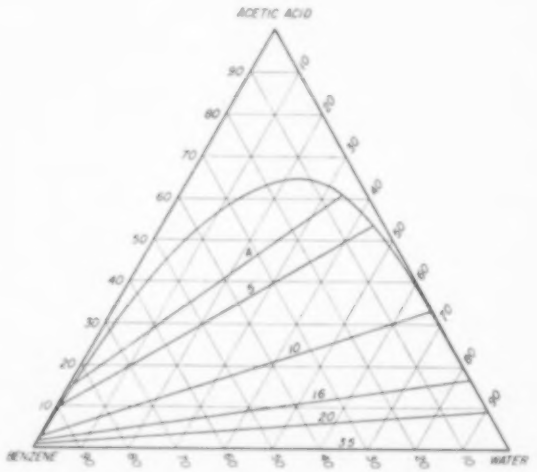

Fig. 1. Approximate interfacial tensions at 20 °C for equilibrium compositions (% vol.) in the system: benzene–acetic acid–water (dyn/cm.)

the interfacial tension with respect to the small amount of equilibrated water phase in the contact area between adjacent drops will rapidly approach a value of about 20 dyn/cm. Along the rest of the drop, mass transfer continues, the relatively small amount of liquid in the drop now tending to come into equilibrium with the large amount of surrounding water phase, which is solute-free. Interfacial tension will therefore continuously increase and finally approach the value of 35 dyn/cm. for the solute-free system. Under the influence of the different surface forces, water will be withdrawn from the contact area, thus promoting coalescence.

It is easily shown with the aid of Fig. 1 that when water is the dispersed phase and acetic acid is transferred from the drops to a continuous benzene phase, the interfacial tension gradients developing around the drops have the

VOL.
12
1960

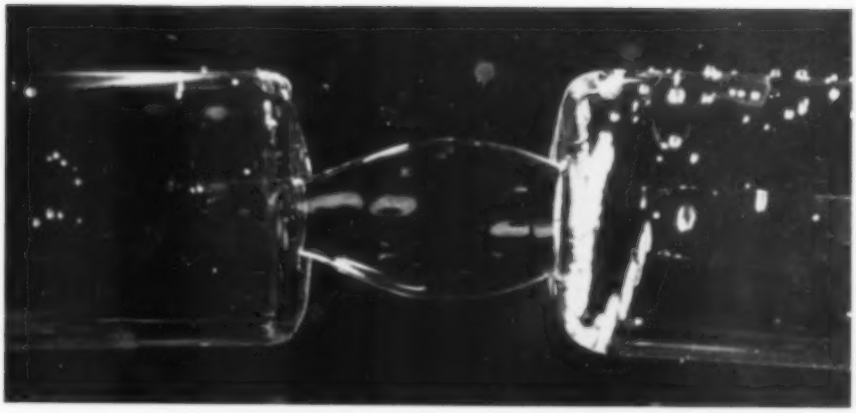

FIG. 2 (a). Benzene/CCl_4 acetic acid–water system. Acetic acid transfer from drops to continuous water phase–immediate coalescence.

FIG. 2(b). Benzene/CCl_4 acetic acid–water system. Acetic acid transfer from continuous water phase to drops, strong retardation of coalescence.

VOL
12
196

same sign and coalescence is also promoted. Upon the addition to two immiscible liquids of increasing amounts of a third liquid, miscible with both, miscibility will in general be increased. Therefore the tendency of interfacial tension change with solute concentration is generally the same as that shown in Fig. 1. The statement [4] that coalescence occurs whenever there is mass transfer from the drops into the continuous phase is therefore in accordance with the explanation offered here.

When, on the other hand, solute is transferred to the droplet phase, the above reasoning predicts that coalescence will be retarded and the emulsion will become relatively stable. This is again illustrated by reference to Fig. 1. When the aqueous solution around the benzene drops contains e.g. 5 per cent acetic acid, the interfacial tension in the whole system will eventually approach about 24 dyn/cm (equilibration of a relatively small droplet with an excess of continuous phase), but the first thing to happen will be an advanced extraction of the water film in the contact area between drops (equilibration of a relatively small volume of continuous phase with an excess of droplet phase); this will increase the interfacial tension locally to about 35 dyn/cm. Therefore, continuous phase liquid will be drawn towards the contact area, stabilizing the drops.

Since little evidence of retardation of drop coalescence can be found in literature, experiments were carried out to confirm the above point of view. In these experiments, drops were caused to form at the ends of two capillary tubes. These tube ends were facing each other in a beaker filled with the liquid which served as the continuous phase. During their growth the drops approached each other. The time passing between the moment of first contact and the occurrence of coalescence was observed.

The following ternary systems were used:

benzene–acetic acid–water;

carbon tetrachloride–acetic acid–water;

carbon tetrachloride/benzene–acetic acid–water;

methyl *iso*butyl ketone–acetic acid–water;

chloroform–acetone–water.

In all systems the liquid mentioned secondly was used as the solute.

Without a solute the time needed for coalescence varied widely within each of the systems investigated. The mean values for the various systems were found to show marked differences as well. With a solute, however, the behaviour was quite different. When the solute was dissolved in the drops, coalescence invariably occurred almost at once after the first visible contact, irrespective of whether the organic solvent or the water was the dispersed phase. With the solute dissolved in the continuous phase, however, coalescence was strongly retarded and in some cases did not occur at all, not even if big drops had a large area of contact (see the photographs in Fig. 2). The same behaviour was observed when both phases contained a solute, with an excess (above the equilibrium value) in one of them. The experiments thus completely confirm the analogy between the effect of mass transfer on dispersed-phase interaction in gas–liquid systems and that in liquid–liquid systems. The authors hope to report on more quantitative aspects of the latter case in a future paper.

Koninklijke/Shell-Laboratorium, Amsterdam

H. Groothuis
F. J. Zuiderweg

References

[1] Lewis J. B. *Chem. Engng. Sci.* 1954 **3** 248.

[2] Sigwart K. and Nassenstein H. *Ver. dtsch. Ing. Z.* 1956 **98** 453.

[3] Johnson H. F. and Bliss H. *Trans. Amer. Inst. Chem. Engrs.* 1946 **42** 331.

[4] Pratt H. R. C. *et al.*, *Trans. Inst. Chem. Engrs. (Lond).* 1957 **35** 301.

[5] Zuiderweg F. J. and Harmens A. *Chem. Engng. Sci.* 1958 **9** 89.

Book Reviews

Techniques of Polymer Characterization. Edited by P. W. Allen. Butterworths, London 1959. 256 pp. 50s.

This book presents a survey of eight major laboratory techniques used in polymer science in as many chapters written by academic and industrial experts. P. W. Allen writes briefly about choice of solvents and preparation of solutions ; R. W. Hall on fractionation ; H. T. Hookway on osmometry ; D. F. Rushman on other " colligative " molecular weight measurements ; F. W. Peaker on light-scattering ; P. F. Onyon on viscometry ; G. F. Price on end-group analysis ; and R. J. Ceresa on characterization of graft and block polymers. The general standard of the book is acceptable and occasionally comes near to perfection, especially in its presentation of the theory and practice of light scattering by Dr. Peaker, who has incorporated much of his own unrivalled experience in a well-balanced historical account. Several hundred recent literature references make the book as a whole a valuable source of technical information.

Some rather minor sources of irritation must be mentioned. In a book of this kind there must be many references to materials, their trade-names and suppliers. Here they are given with a disconcerting lack of uniform clarity and completeness. Araldite resin, for instance, is recommended without any such details, while a Bakelite varnish is merely referred to as V9700. Membranfilter Gesellschaft (Gottingen) (sic) on p. 101 is amplified to Membranfilter Gesellschaft (Gottingen, German Federal Republic) on p. 103. The address of the Shirley Institute is not given, though equally relevant, in connexion with " Test Leaflet No. Chem. 6 " (mentioned on p. 230). The fullest possible documentation on anything that is worth recommending or quoting would surely be appreciated by readers of any book concerned with techniques. Incidentally, the purification of reagent-grade benzene (p. 125) can now be avoided by buying the grade suitable for molecular weight measurements (m.p. $\geq$ 5·4 °C ; from British Drug Houses, Poole, Dorset).

The description of transport of solvent through a semi-permeable membrane as ' liquid flow ' (p. 91) is to be deprecated ; so is reference to the term c^3 as the cubic term (p. 109). The reader is warned (p. 82) that even precision-bore glass tubing may vary in diameter by 0·1 mm along a single length of capillary. The reviewer has never found variations nearly as large as this, though the manufacturers, in their commendable caution, limit their guarantee to such tolerances. In practice one finds that such tubing is often as good as that described by F. S. Dainton *et al.* (*Trans. Faraday Soc.* 1957 **53** 1269) which varied only by $\pm$ 0·0005 mm over a length of 30 cm.

One effect of reading this book is to feel one's appetite whetted for more. Some disappointment must be felt that a more comprehensive and ambitious book has not emerged. Over 10 years ago, Weissberger's Volume I of " *Physical Methods of Organic Chemistry*," though not restricted to polymer science, did not only include admirable chapters (now out of date) on viscometry and osmotic pressure, but besides devoted 110 pages to ultracentrifuge techniques. Surely Dr. Allen's pleas of lack of space, and of lack of general use of the ultracentrifuge will be widely regretted and challenged. Let us be grateful that eight experts can be found within 100 miles of Oxford to bring up to date the exciting story of polymer characterization in the fields included. " *Techniques of Polymer Characterization*," even in its present form, will save many man-hours at the polymer scientist's bench. But let us hope for a much fuller second edition in due course.

N. Gordon.

Book Received

Proceedings of the 1960 Heat Transfer and Fluid Mechanics Institute. Edited by D. M. Mason, W. C. Reynolds and W. G. Vincenti. Stanford University Press 1960.

SELECTION OF CURRENT PAPERS OF INTEREST TO CHEMICAL ENGINEERS

W. R. Mickelson: Measurements of the effect of molecular diffusivity in turbulent diffusion. *J. Fluid. Mech.* 1960 **7** 397–400.

C. C. Leiby and C. L. Chen: Diffusion coefficients, solubilities and permeabilities for He, Ne, H_2 and N_2 in Vycor glass (used as a semi-permeable membrane). *J. Appl. Phys.* 1960 **31** 268–274.

W. K. Kim, N. Haria, T. Ree and H. Eyring: Theory of non-Newtonian flow—III A method for analysing non-Newtonian flow curves (See also *J. Appl. Phys.* 1955 **26** 793 and 800) *J. Appl. Phys.* 1960 **33** 358–361.

D. A. Haydon and F. H. Taylor: On adsorption at the oil/water interface and the calculation of electrical potential in the aqueous surface phase—1. Neutral molecules and a simplified treatment for ions. *Phil. Trans. Roy. Soc.* 1960 **252** A1009 225–248.

P. H. Thomas and P. G. Smith: Simple dosage meter for high density thermal radiation. *J. Sci. Instrum.* 1960 **37** 73–76.

D. F. Leach and J. M. M. Neilson: Design of a single electrode capacitor for use with moisture meters and similar apparatus. *J. Sci. Instrum.* 1960 **37** 77–80.

J. T. Bevans and R. V. Dunkle: Radiant interchange within an enclosure—I. Absorption and emmision behaviour of gases. *J. Heat Transfer* (*Trans. Amer. Soc. Mech. Eng.* Series C) 1960 **82** 1–7. II. General interchange equations. *ibid.* 1960 **82** 8–13. III. A method for solving multinode networks and a comparison of the band energy and gray radiation approximations. *ibid.* 1960 **82** 14–19.

G. Stolz: Numerical solutions to an inverse problem of heat conduction for simple shapes (i.e. given temperature distribution, find surface flux) *J. Heat Transfer* (*Trans. Amer. Soc. Mech. Eng.* Series C) 1960 **82** 20–26.

R. G. Vines: Measurement of the thermal conductivities of gases at high temperatures. *J. Heat Transfer* (*Trans. Amer. Soc. Mech. Eng.* Series C) 1960 **82** 48–52.

H. Sogin: Laminar transfer from isothermal spanwise strips on a flat plate. *J. Heat Transfer* (*Trans. Amer. Soc. Mech. Eng.* Series C) 1960 **82** 53–63.

E. M. Sparrow and J. L. Gregg: The effect of vapour drag on rotating condensation. *J. Heat Transfer* (*Trans. Amer. Soc. Mech. Eng.* Series C) 1960 **82** 71–72.

J. G. Barton and W. H. Sellers: Radiation fin effectiveness *J. Heat Transfer* (*Trans. Amer. Soc. Mech. Eng.* Series C) 1960 **82** 73–75.

S. L. Soo and C. L. Tien: Effect of the wall on two-phase (solid particles in gas) turbulent motion. *J. Appl. Mech.* (*Trans. Amer. Soc. Mech. Eng.* Series E) 1960 **27** 5–15.

K. A. Gardner: Heat exchanger tube sheet design—3. U-tube and bayonet tube-sheets (See also *J. Appl. Mech.* 1948 **15** A 377 and 1952 **19** 159). *J. Appl. Mech.* (*Trans. Amer. Soc. Mech. Eng.* Series E) 1960 **27** 25–33.

H. Schlichting: Some developments in boundary layer research in the past thirty years. *J. Roy. Aeronaut. Soc.* 1960 **64** 64–80.

P. G. Morgan: High speed flow through perforated plates. *J. Roy. Aeronaut. Soc.* 1960 **64** 103–105.

G. V. Jeffreys: Phase equilibrium for the system cyclohexane, normal heptane and aniline. *J. Inst. Petrol.* 1960 **64** 26–30.

S. R. M. Ellis and R. J. Bennett: Effects of composition and vapour velocity upon the efficiency of an Oldershaw column. *J. Inst. Petrol.* 1960 **46** 19–25.

SELECTION OF CURRENT SOVIET PAPERS OF INTEREST TO CHEMICAL ENGINEERS*

B. A. Chertkov and D. L. Puklina: Effect of temperature on rate of absorption of SO_2 from gases. *Zh. prikl. Khim.* 1960 **33** 9–13.

M. L. Varlamov, E. L. Kricheskaya, G. A. Manakin, L. M. Kozakova and A. N. Gospodinov: Sonic coagulation of sulphuric acid mist. *Zh. prikl. Khim.* 1960 **33** 14–20.

V. P. Postnikov: Heat transfer in packed scrubbers at higher gas velocities. *Zh. prikl. Khim.* 1960 **33** 117–127.

I. N. Bushmakin: Effect of reflux ratio on performance of rectification columns. *Zh. prikl. Khim.* 1960 **33** 127–133.

I. A. Gildenblat, A. S. Furmanov and N. M. Zhavoronkov: Vapour pressure of crystalline naphthalene. *Zh. prikl. Khim.* 1960 **33** 246–248.

B. G. Bergo, V. M. Platonov, M. E. Aerov and V. A. Evtuchenko: Calculation of rectification processes on analogue computers. *Khim. Prom.* 1959 (7) 555–560.

B. I. Vainshtein, A. Kh. Breger and N. P. Sirkus: Calculation of radio-chemical plant with powerful source of gamma radiation for oxidation of benzene to phenol. *Khim. Prom.* 1959 (7) 560–565.

V. A. Nikashina, M. M. Senyabin and A. V. Gordienski: Radiochemical stability of some ion-exchange resins towards X-ray and gamma radiation. *Khim. Prom.* 1959 (7) 573–575.

B. A. Chertkov: Effect of concentration of SO_2 in gas on its rate of absorption by various solvents. *Khim. Prom.* 1959 (7) 586–591.

M. T. Rusov: Empirical rate equation for the process of ammonia synthesis and its application. *Khim. Prom.* 1959 (7) 594–596.

Ya. G. Vinokur and V. V. Dilman: Study of bubbling liquid beds by means of gamma rays. *Khim Prom.* 1959 (7) 619–621.

A. G. Kasatkin, D. M. Popov and Yu. V. Akselrod: Heat transfer through walls of cooling coil under bubbling conditions. *Khim. Prom.* 1959 (7) 622–624. Cooling of liquid on plates during absorption of SO_2 and SO_3.

V. V. Streltsov and A. A. Komarovski: Calculation of continuous apparatus for the dissolution of salt in a fixed bed. *Khim. Prom.* 1959 (7) 624–627.

A. M. Rozen, S. M. Karpacheva, S. F. Medvedev, E. P. Rodionov and L. F. Kiseleva: Study of mass transfer in packed columns in extraction by tributylphosphate. (Extraction and re-extraction of nitric acid). *Khim. Prom.* 1959 (7) 627–630.

P. I. Sanin, A. D. Petrov, N. V. Melenteva, A. P. Meshcheryakov, E. P. Kaplan, E. S. Pokrovskaya and D. N. Andreev: Viscosity of hydrocarbons at low temperatures. *Khim. Tekh. Topl. Masel* 1960 **3** (2) 11–19.

S. V. Pvov and V. B. Falkovski: Method of calculation of chemical reactors of bubbling type. *Khim. Tekh. Topl. Masel* 1960 **5** (2) 52–54.

S. P. Detkov: On radiant transfer between grey surfaces. *Zh. tekh. Fiz.* 1960 **30** 96–104.

S. I. Mochan and O. G. Revzina: Calculation of aerodynamic resistance of surface heating elements. *Teploenergetika* 1960 **6** (2) 34–40.

*To assist readers, translations of any article appearing in the above list can be obtained at a reasonable charge. All orders should be addressed to the Administrative Secretary of the Pergamon Institute at either Headington Hill Hall, Oxford or 122 East 55th Street, New York 22 whichever is more convenient.

VOL 12 1960

0974-27-4

VOL.
12
960

END